Circadian and homeostatic modulation of sleep spindles in the human electroencephalogram

Inauguraldissertation

zur
Erlangung der Würde eines Doktors der Philosophie
vorgelegt der
Philosophisch-Naturwissenschaftlichen Fakultät
der Universität Basel

von

Vera Knoblauch
aus Oberentfelden (AG)

Ausgeführt unter der Leitung von

Prof. Dr. Anna Wirz-Justice
Dr. Christian Cajochen
Abteilung Chronobiologie
Psychiatrische Universitätsklinik Basel

Basel, 2004

Genehmigt von der Philosophisch-Naturwissenschaftlichen Fakultät auf Antrag von

Dissertationsleiterin:	Prof. Dr. Anna Wirz-Justice
Fakultätsverantwortlicher:	Prof. Dr. Heinrich Reichert
Korreferent:	PD Dr. Hanspeter Landolt

Basel, den 10. Februar 2004

Prof. Dr. Marcel Tanner
Dekan

Table of contents

Summary

Sleep spindles are transient EEG oscillations of about 12-16 Hz. Together with slow waves, they hallmark the human non-REM sleep EEG. Sleep spindles originate in the thalamus and are suggested to have a sleep protective function by reducing sensory transmission to the cortex. Other evidence points to an involvement of sleep spindles in brain plasticity processes during sleep. Previous studies have shown that sleep spindles are both under homeostatic (sleep-wake dependent) and circadian (time of day-dependent) control. Furthermore, frequency-specific topographical distribution of power density within the spindle frequency range has been reported. The aim of this thesis was to assess homeostatic and circadian influences on spectral spindle frequency activity (SFA) and spindle parameters in different brain regions.

Healthy young volunteers participated in both a 40-h sleep deprivation (SD) and a 40-h multiple nap paradigm. The recovery nights after the SD and the nap protocol served to assess the effect of enhanced and reduced homeostatic sleep pressure, respectively. The multiple nap paradigm revealed the modulation of sleep spindles across the circadian cycle. Two different methodological approaches were used to analyze the EEGs: classical spectral analysis (Fast Fourier Transform, FFT) and a new method for instantaneous spectral analysis (Fast Time Frequency Transform, FTFT), developed as a part of this thesis project in collaboration with Wim Martens from TEMEC, The Netherlands.

Slow wave activity (SWA, spectral power density in the 0.75-4.5 Hz range) and spindle frequency activity (SFA, spectral power density in the spindle frequency range) in the high frequency range (13.75-16.5 Hz) were oppositely affected by the differential levels of sleep pressure (Chapter 2). These effects strongly depended on brain location. After SD, the SWA increase compared to the baseline night was most pronounced in the beginning of the night and in the fronto-central region. Power density in the high spindle frequency range was reduced in the centro-parietal brain region. After the nap protocol, when sleep pressure was reduced, power density in the SWA range was decreased at the beginning of the night. SFA was generally increased after the nap protocol. The data indicate that the balance between SWA

and high-frequency spindle activity may represent a sensitive marker for the level of homeostatic sleep pressure.

The new method of FTFT revealed that spindle density was reduced after SD (Chapter 3). This reduction was particularly apparent in the frontal derivation, and most pronounced in the first half of the night. The reduction of spindle density with its temporal and local specificity confirms the inverse homeostatic regulation of slow waves and sleep spindles. Sleep spindles had a lower frequency and a higher amplitude after SD. Within an individual spindle, frequency variability was reduced, which indicates that sleep spindles were more stable and homogenous after SD. The increase in spindle amplitude and the reduced intra-spindle frequency variability suggests a higher degree of synchronization in thalamocortical neurons under high homeostatic sleep pressure.

EEGs during the nap paradigm were analyzed to compare SFA and sleep spindle characteristics during and outside the circadian phase of melatonin secretion (the “biological night” and “biological day”, respectively) (Chapter 4). In naps occurring during the phase of melatonin secretion, lower spindle frequencies were promoted, indexed as a reduction in mean spindle frequency (i.e. slowing of sleep spindles) and an increase in spindle amplitude and SFA in the low-frequency range (up to ~14.25 Hz) paralleled by a reduction in the high-frequency range (~ 14.5-16 Hz). Furthermore, spindle density was increased, and intra-spindle frequency variability reduced during the night. Thus, the circadian pacemaker is likely to promote low-frequency, high amplitude and homogenous sleep spindles during the biological night. The circadian modulation of sleep spindles may be a way by which the circadian system modulates and times sleep consolidation. This circadian modulation clearly depended on brain location such that it was maximal in the parietal and minimal in the frontal derivation.

Taken together, the segregated analysis of different spindle parameters by the new high-time and high-frequency resolution spindle analysis provides new insights into sleep spindles and their regulation. Both homeostatic and circadian processes affected sleep spindles characteristics in a topography-specific manner. These state-dependent local aspects provide further evidence that sleep is a dynamic phenomenon which reflects use-dependent recovery or reactivation processes.

Chapter 1

Introduction

Sleep, sleep electroencephalography (EEG), and analysis of the sleep EEG

Sleep occupies one third of our lives, but many of its secrets have not yet been revealed. On the behavioral level, sleep in mammals is mainly characterized by a typical body posture, muscle relaxation, reduced responsiveness to external stimuli, and rapid reversibility (Campbell and Tobler, 1984). Taken together, these characteristics permit one to distinguish between sleep and quiet wakefulness or between sleep and vegetative states such as hibernation or coma. On the level of brain activity, neuronal activity patterns fundamentally differ between sleep and wakefulness, and undergo substantial changes also within sleep itself. Much of what is known today about brain activity during human sleep is due to the discovery (Berger, 1929) and development of electroencephalography (EEG), a method by which electrical activity in the cortex can be recorded by scalp electrodes. The electroencephalogram displays the summated synaptic potentials at the cortical surface, recorded by scalp electrodes (Lopes da Silva et al., 1986; Niedermeyer and Lopes da Silva, 1987). The patterns in this voltage-vs.-time graph are commonly called brain waves, whose frequency, amplitude and waveform can be quantified. In addition to the electrophysiological potentials measured from the cortex (EEG), sleep researchers also rely on electrophysiological muscle and eye potentials to determine sleep stages (i.e. polysomnography).

A systematic method for visually scoring human EEG sleep was developed more than 30 years ago to ensure standardised terminology (Rechtschaffen and Kales, 1968). It differentiates between 3 major vigilance states: waking, rapid-eye-movement (REM) sleep, and non-rapid-eye-movement (NREM) sleep. NREM sleep is further subdivided into 4 stages: 1 to 4. Stage 3 and 4 together are referred to as slow wave sleep (SWS). The scoring rules for wakefulness and NREM sleep are mainly based on the frequency, amplitude and waveform of the EEG waves.

Wakefulness is characterized by low-amplitude, high-frequency activity, while during NREM sleep, high-amplitude, low-frequency waves predominate (Figure 1a). The EEG during REM sleep is similar to the waking EEG, but the definition for REM sleep additionally demands low muscle tone in the submental electromyogram (EMG) and rapid movements in the electrooculogram (EOG).

Continuous recording of the sleep EEG reveals that the cortex alternates between NREM and REM sleep in a cyclic manner. During normal nocturnal sleep, NREM-REM sleep cycles with a duration of about 90-100 minutes. These 'sleep cycles' are repeated 4-5 times during a normal 8-h sleep episode. The proportion of different sleep stages in a sleep cycle changes across the sleep episode such that the percentage of SWS is highest in the first sleep cycle and diminishes over subsequent cycles, whereas the percentage of REM sleep and stage 2 sleep increases from the first to the last cycle.

Quantification of the EEG on the basis of visual scoring is limited. The difference between sleep stages is based on arbitrary, discrete criteria and therefore does not properly reflect the continuous physiological mechanisms that underlie changes in the EEG. Thus, other methods have been developed by which the EEG signal can be analyzed. One of the most common methods to quantify EEG activity is spectral analysis by means of the fast Fourier transform (FFT) (Dietsch, 1932). The FFT, in essence, decomposes a waveform (e.g. EEG waves) into sinusoids of different frequency and phase which sum to the original waveform. It identifies or distinguishes the different frequency sinusoids and their respective amplitudes. Thereby, the EEG signal is transformed from a time into a frequency domain. This requires a stationary signal. EEG waves during sleep are not stationary, but by analyzing short time windows (e.g. 4 s), a quasi-stationary signal can be obtained for these short intervals. The length of the time window determines the slowest detectable wave, and thereby frequency resolution. For the short time window, spectral analysis calculates overall power density per frequency bin (i.e. $\mu V^2/Hz$) by combining incidence and amplitude. The resulting power spectrum depicts this power as a function of frequency bin and thus expresses the contribution of each frequency bin to the power of the total signal (Figure 1b).

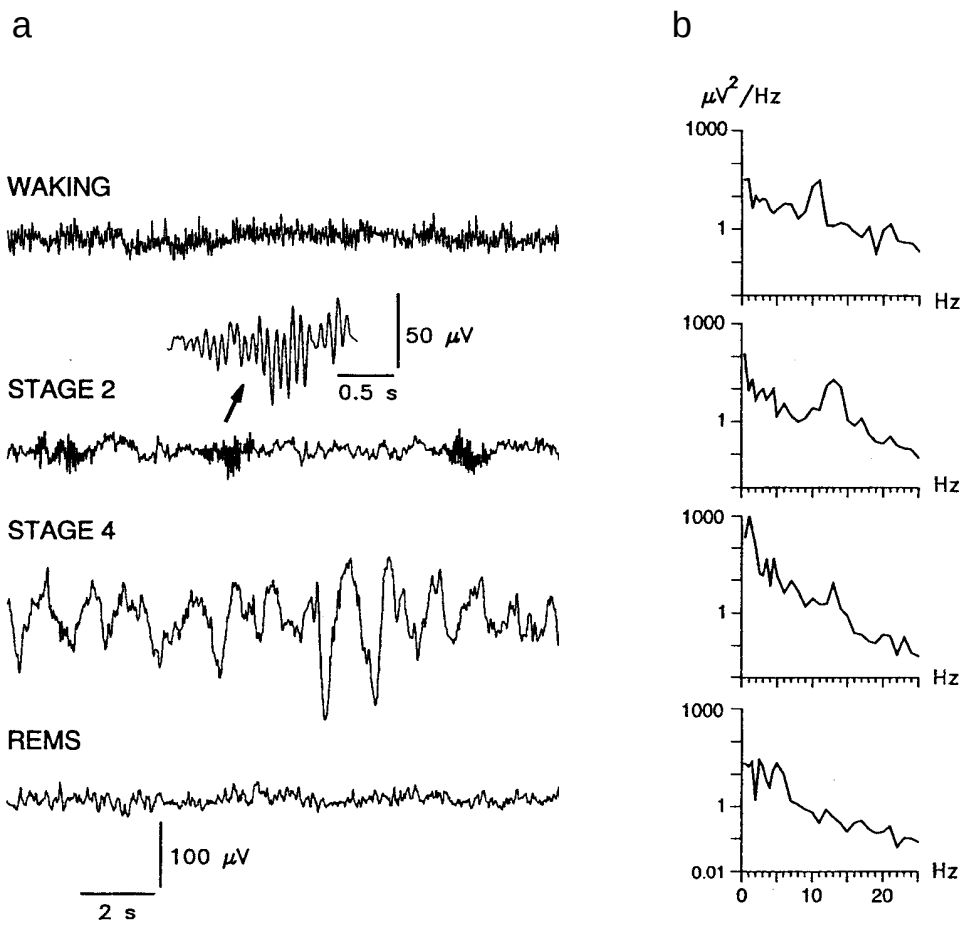

Figure 1. EEG signals (a) and corresponding power spectra (b) during wakefulness, stage 2, stage 4 and REM sleep in a young healthy adult. Power spectra represent the average of four 4-s epochs and are plotted on a logarithmic scale. During wakefulness (eyes closed), the alpha rhythm (8-13 Hz) in the EEG gives rise to a peak around 11 Hz in the power spectrum. Sleep spindles (see inset for a expanded segment) occur preferentially during stage 2 are reflected in a peak in the spindle frequency band (11-15 Hz). High amounts of slow waves during stage 4 give rise to high power density in the slow wave range (< 4 Hz). REM sleep is dominated by activity in the theta frequency band (4-8 Hz) (Adopted with permission from Aeschbach, 1995)

NREM sleep oscillations: sleep spindles and slow waves

Synchronization of brain activity, i.e. the simultaneous activation of large population of neurons, is a fundamental feature that discriminates NREM sleep from REM sleep and wakefulness. Although wakefulness and REM sleep differ substantially at the behavioral level (motor output is markedly suppressed during REM sleep), the EEG during these two vigilance states is similar, and exhibits low spatio-temporal coherence in the cerebral cortex. In contrast, the high-amplitude, low-frequency activity during NREM sleep is synchronized over large cortical areas (Destexhe et al., 1999).

Two essential types of synchronized oscillations that hallmark the EEG during NREM sleep are slow waves and sleep spindles. Slow waves, or delta waves, are low-frequency (0.75-4.5 Hz), high-amplitude (>75 μV) oscillations. The differentiation between NREM stages 2-4 in human sleep scoring is mainly based on the abundance of slow waves, and their increase is considered to represent increasing sleep depth. Sleep spindles are transient (0.5-2 s) oscillations of about 12-15 Hz that recur approximately every 3-10 s (Figure 1a, see also Figure 2 in Chapter 4). The name “spindle” refers to their characteristic shape with progressively increasing, then decreasing amplitude. Sleep spindles are more abundant in stage 2 than in SWS (De Gennaro et al., 2000b; Dijk et al., 1993; Zeitlhofer et al., 1997).

Sleep spindles and their circadian and homeostatic regulation is the main topic of this thesis. The following sections outline cellular mechanisms, regulation, topographical distribution and putative functional significance of sleep spindles.

Homeostatic and circadian regulation of sleep

Sleep and wakefulness are regulated by the interaction of two processes, a homeostatic and a circadian process (Borbély, 1982; Daan et al., 1984) (Figure 2). The homeostatic process represents the sleep-wake-dependent need for sleep which gradually increases the longer we stay awake. Homeostatic sleep regulation implies that manipulations that increase sleep drive or sleep need (e.g. sleep deprivation) ought to increase subsequent sleep intensity and/or duration. The circadian process defines the influence of time of day on sleep, independent of the prior history of sleep

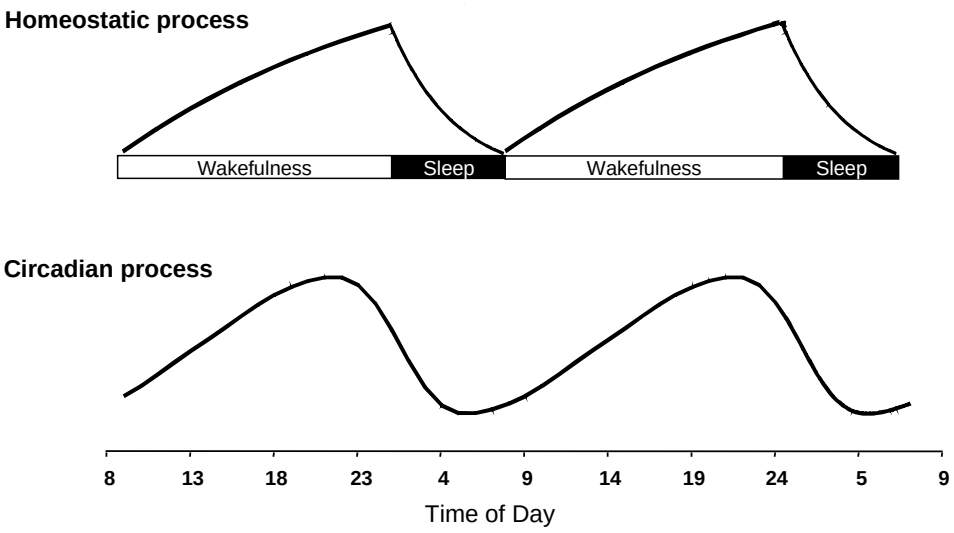

Figure 2. Schematic representation of the 2 major processes underlying sleep regulation. A homeostatic pressure for sleep builds up during wakefulness and dissipates during sleep. The circadian process modulates sleep timing, sleep propensity and structure in dependence of the time of day. Modified from Borbély, 1982.

or wakefulness. The homeostatic and the circadian process develop independently, but their interaction determines the timing, duration, and quality of both sleep and wakefulness.

Homeostatic process

A homeostatic pressure for sleep progressively builds up during waking and dissipates during the following sleep episode. The level of homeostatic sleep pressure at sleep onset directly depends on the duration of prior wakefulness. A reliable marker for homeostatic sleep pressure is slow wave activity (SWA, spectral power density in the 0.75-4.5 Hz range) during NREM sleep. It decreases throughout the course of the sleep episode, independent of time of day (Weitzman et al., 1980), and is augmented at the beginning of the night when wakefulness prior to sleep has been extended (Borbély et al., 1981; Dijk et al., 1993). Conversely, reduction of sleep pressure by an early evening nap results in reduced SWA in the beginning of the subsequent night sleep (Werth et al., 1996b). This homeostatic regulation suggests that slow-wave activity may be linked to some restorative aspect of sleep. However, the mechanisms and functions of slow-waves homeostasis are still unclear.

Circadian process

Circadian rhythms, i.e. endogenous rhythms with a periodicity of about 24 hours, can be observed in a variety of physiological and behavioral variables in humans, such as core body temperature, heart rate, plasma hormone levels, performance, subjective alertness, or sleep-wake behavior. Under normal conditions, circadian rhythms are synchronized to the 24-h cycle of the environment. The most important synchronizer, or ‘zeitgeber’, is the daily light-dark cycle. In the absence of external zeitgebers, circadian rhythms ‘free run’, that is, they oscillate with their endogenous period, which in humans is usually slightly longer than 24 hours (Aschoff and Wever, 1962; Czeisler et al., 1999). In mammals, circadian rhythms are generated by a circadian pacemaker located in the suprachiasmatic nuclei (SCN) of the hypothalamus (for a review see Van Esseveldt et al., 2000). SCN lesions result in disruption of the

circadian rest-activity / sleep-wake cycle and other circadian rhythms in rats (Stephan and Zucker, 1972; Tobler et al., 1983; Eastman et al., 1984). Recently, enormous progress in understanding the cellular and molecular basis of circadian rhythms has been achieved. Genes driving molecular circadian oscillations, so called 'clock genes' have been identified, first in *Drosophila* (Stanewsky, 2002), and later in mammalian SCN cells. Many of these genes are expressed in an oscillating manner on the transcriptional or translational level via autoregulatory feedback loops (see Albrecht, 2002 and Reppert and Weaver, 2002 for reviews). In the last few years, the detection of clock gene expression in extra-SCN tissues has expanded the original view of a unique circadian pacemaker in mammals (for a review see Schibler and Sassone-Corsi, 2002; Balsalobre, 2002; Schibler et al., 2003). According to current concepts, the master clock in the mammalian SCN synchronizes a variety of oscillators in peripheral tissues, such as liver, heart, and kidney. These peripheral clocks, in contrast to the master clock, are not sensitive to light, but to different non-photic entraining cues appropriate to their function, for example feeding for the liver or activity for muscle.

The timing of human sleep strongly depends on circadian phase (Dijk and Czeisler, 1995; Dijk et al., 1997). Circadian phase in humans can be measured by the rhythm of core body temperature or pineal melatonin secretion. During entrainment to the 24-h day, sleep is usually initiated approximately 6 hours before and terminated approximately 2 hours after the nadir of the core body temperature rhythm (Czeisler et al., 1992; Duffy et al., 1998). The circadian drive for sleep (assessed by latency to sleep onset, sleep efficiency, subjective alertness) is highest close to the minimum of the circadian rhythm of core body temperature, i.e. few hours before to the usual time of awakening under entrained conditions, and is lowest some hours before normal bedtime (Weitzman et al., 1974; Strogatz et al., 1987; Dijk and Czeisler, 1994). This paradoxical circadian timing of sleep propensity makes sense if one interprets its function to counteract both the increasing homeostatic drive for sleep during towards the end of the normal 16-h waking day, as well as the decrease in homeostatic drive for sleep towards the end of the nocturnal sleep episode. This suggests that the interaction of the homeostatic and circadian processes in sleep regulation helps to consolidate sleep and wakefulness in the normal 8:16-h sleep-wake cycle (Dijk and Czeisler, 1994).

Not only sleep timing, but also internal sleep structure depends on circadian phase. REM sleep undergoes a strong circadian modulation with a maximal REM sleep propensity in the morning hours, shortly after the core body temperature minimum (Czeisler et al., 1980; Endo et al., 1981). Within NREM sleep, circadian phase affects EEG activity in distinct frequency bands (Dijk and Czeisler, 1995; Dijk et al., 1997; see below)

Experimental segregation of the circadian and homeostatic component

In the course of a sleep episode, elapsed time since sleep onset changes simultaneously with circadian phase. Therefore, sleep is influenced by both the homeostatic and circadian process at any given time. In order to segregate sleep-wake dependent and circadian influences on sleep, sleep needs to be distributed evenly across the 24-h cycle. In forced desynchrony protocols, study participants live under an artificial non-24-h (typically 28 h) sleep-wake schedule for several weeks (Dijk and Czeisler, 1995). A period of 28 hours is beyond the range of entrainment of the human circadian pacemaker. The sleep-wake cycle is desynchronized from the circadian pacemaker as followed by the circadian rhythms of plasma melatonin or core body temperature. Thus, in the course of the experiment, sleep is initiated at many different circadian phases with an almost constant prior wake time. Thus, for each time point during sleep, circadian phase and time elapsed since sleep onset can be computed. The circadian and sleep dependent component can then be educed by averaging the data with respect to circadian phase and time elapsed since sleep onset, respectively.

The homeostatic component of sleep regulation is often studied by experimentally manipulating sleep pressure. In sleep deprivation protocols, homeostatic sleep pressure is enhanced by an extension of the waking episode prior to sleep. Comparison of the following recovery night with a baseline night reveals the effect of homeostatic sleep pressure, provided that baseline and recovery night are scheduled to begin at the same circadian phase. Most findings cited in the following section about homeostatic and circadian regulation of sleep and sleep spindles come from forced desynchrony or sleep deprivation studies.

Homeostatic and circadian regulation of sleep spindles

After sleep deprivation, spindle density and spindle frequency activity (SFA, spectral power density in the spindle frequency range) were reduced in the following recovery night (Borbély et al., 1981; Dijk et al., 1993; De Gennaro et al., 2000b; Landolt et al., 2000). Forced desynchrony experiments revealed that SFA as well as spindle incidence, amplitude, frequency and duration all increase with the progression of sleep at all circadian phases (Dijk and Czeisler, 1995; Dijk et al., 1997; Wei et al., 1999). These findings indicate an inverse homeostatic relationship between slow waves and sleep spindles. However, a more detailed inspection revealed that this inverse relationship does not hold for the entire spindle frequency range: only high-frequency-, but not low-frequency spindle activity was reduced after SD (15-Hz bin, Borbély et al., 1981; 13.75-14 Hz, Dijk et al., 1993; 14.25-15 Hz, Landolt et al., 2000). From EEG power spectra, it cannot be concluded whether this frequency-specific effect is caused by a general slowing in the spindle frequency range, which would decrease the incidence of high-frequency spindles, or if it represents a frequency-specific change in the amplitude, i.e. a decrease in the amplitude of high-frequency spindles, or both.

The strength of the circadian modulation is very different for slow waves and sleep spindles. Forced desynchrony experiments reveal that SWA is only minimally affected by circadian phase, whereas spindle frequency activity exhibits a high-amplitude circadian rhythm (Dijk et al., 1997). This circadian rhythm is frequency-specific: SFA between 12.25-13 Hz is highest at the peak of the circadian rhythm of melatonin secretion, while SFA between 14.25-15.5 Hz reaches a minimum at this circadian phase (Dijk et al., 1997) (Figure 3). Furthermore, a significant circadian modulation has been found for spindle incidence, amplitude, frequency and duration (Wei et al., 1999). This modulation is such that highest spindle incidence, longest spindle duration and lowest spindle frequency coincide with the circadian phase at which sleep normally occurs (Wei et al., 1999).

The mechanism by which the circadian pacemaker in the SCN influences sleep spindles has not yet been revealed. Direct neuronal pathways from the SCN to the thalamus may exist. Alternatively, the circadian signal could be mediated indirectly, via other neuronal pathways and/or other outputs of the circadian system, such as melatonin or core body temperature. Exogenous melatonin administered

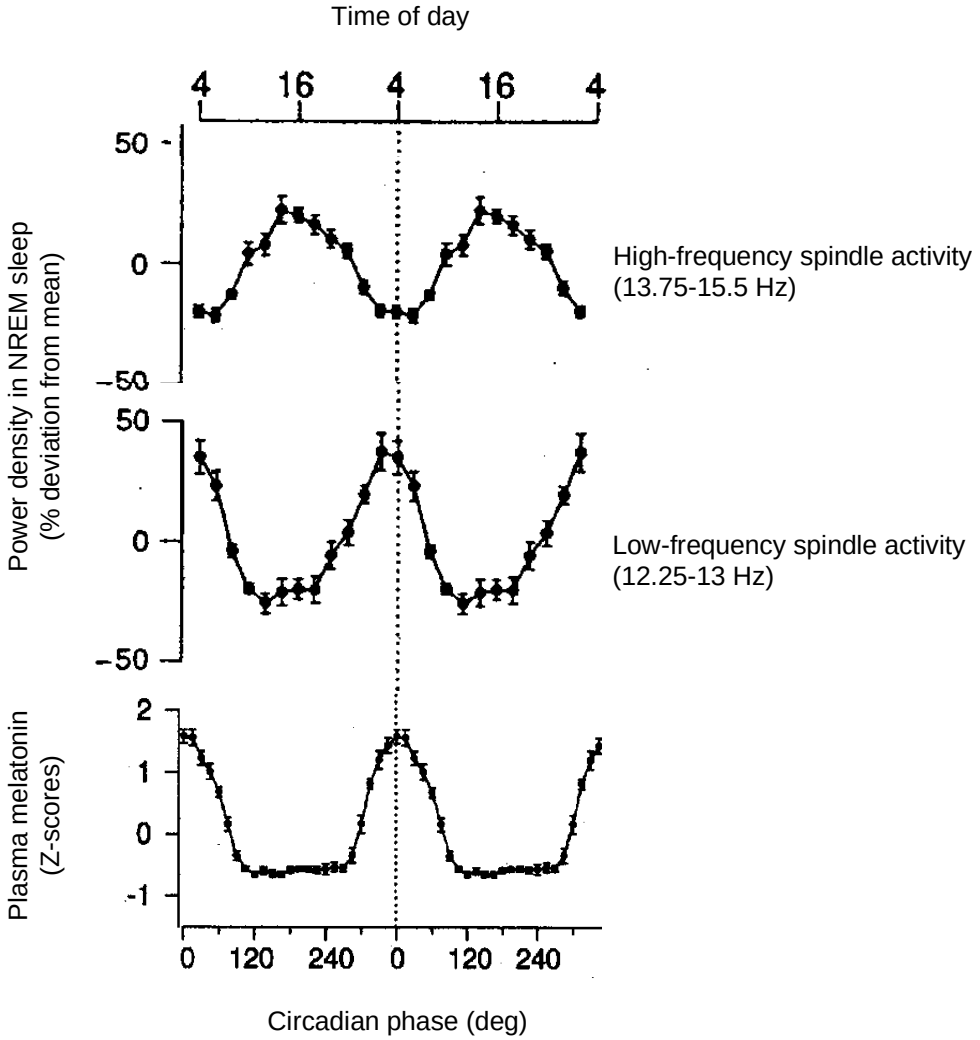

Figure 3. Phase relationships between the circadian rhythms of low- and high-frequency spindle activity during NREM sleep and plasma melatonin. Modified from Dijk, 1997.

during the day when no endogenous secretion occurs, enhances SFA during daytime sleep, thus mimicking a nocturnal profile in the power spectra. (Dijk et al., 1995). This suggests that the circadian rhythm of melatonin secretion could be the signal by which the pacemaker influences sleep spindles. A more detailed discussion of putative pathways is given in Chapter 4.

Neurophysiology of sleep spindles

In vitro and *in vivo* studies carried out mainly in cats by the group of Steriade, have revealed the cellular mechanisms underlying sleep spindles in mammals (for a review see Steriade et al., 1993b). Sleep spindles are generated by a thalamo-cortical network, which comprises the interplay between reticular thalamic, thalamocortical, and cortical pyramidal cells. Studies in cats have located the site of origin for spindle oscillations in the reticular nucleus of the thalamus (for references see Steriade et al., 1993b). Isolation of the reticular nucleus from the rest of the thalamus and cerebral cortex abolishes spindle oscillations in the thalamus and the cortex, whereas neurons within the isolated reticular nucleus are still capable of generating spindle oscillations. This capacity depends on the level of membrane hyperpolarization. During wakefulness, the thalamus and cortex receive ascending activation from brainstem nuclei. The removal of this activation at the transition from wakefulness to sleep allows thalamocortical and thalamic reticular cells to undergo a progressive hyperpolarization, which changes the firing pattern of these neurons from the single spike mode to a rhythmic burst mode. When a certain hyperpolarization level is achieved (between –55 and –65 mV in cats), rhythmic bursts with a frequency of 7-14 Hz are generated in reticular neurons. Via GABA (γ-aminobuturic acid)-containing inhibitory axons, these oscillations are imposed on other nuclei within the thalamus and lead to the appearance of rhythmic inhibitory postsynaptic potentials (IPSP) in thalamocortical neurons. These neurons fire rebound bursts of action potentials at the offset of IPSPs; reticular and thalamocortical cells thus show an inverse pattern during these oscillations. The bursts of action potentials in thalamocortical cells converge onto reticular thalamic nuclei, thereby closing the loop for rhythmic oscillation. From thalamic neurons, the bursts are also transferred via thalamocortical projections to the cortex, where they induce excitatory postsynaptic

potentials in cortical pyramidal cells. The sum of these potentials at the cortical surface is represented as sleep spindles in the EEG (for a review see Steriade et al., 1993b).

As for sleep spindles, the generation of slow wave oscillations depends on the degree of hyperpolarization of thalamocortical cells. They occur at more negative membrane potentials (between -68 and -90 mV in cats) by the interplay of several cation currents. In this way, the progressive hyperpolarization after sleep onset first leads to the appearance of spindle oscillations, which become replaced by slow wave oscillations when deepening of sleep proceeds and thalamocortical neurons reach a voltage range at which slow wave oscillations are triggered (for a review see Amzica and Steriade, 1998).

For thalamic oscillations to be reflected in the EEG, a large number of neurons has to oscillate synchronously in these frequency modes. In the absence of a synchronizing mechanism, thalamic neurons would send incongruent signals to the cortex. Such a mechanism is represented by cortically generated slow (< 1 Hz) oscillations (Steriade et al., 1993a; Steriade et al., 1994; Contreras et al., 1996; Mölle et al., 2002). They arise from a rhythmic alternation of the membrane potential between a depolarized and a hyperpolarized voltage level and are widely synchronized over various cortical areas. These oscillations are transmitted via corticothalamic projections to the thalamus, where they govern the grouping and synchronization of spindles and slow waves, leading to their simultaneous appearance over widespread areas.

Functional significance of sleep spindles

The function of sleep spindles is still poorly understood. It is suggested that sleep spindles may have a sleep-protecting function by gating synaptic transmission to the cortex. The thalamus, where sleep spindles are generated, plays a key role in the modulation and transmission of sensory stimuli from the periphery to the cortex. During wakefulness, when the EEG is desynchronized, sensory information is transferred through thalamic relay nuclei to cortical areas (Steriade et al., 1993b). During sleep, oscillations in the thalamus are associated with synaptic inhibition and reduced sensory transmission; the cortex is protected from arousing stimuli (Steriade

et al., 1993b; Amzica and Steriade, 1998). Two studies in humans have investigated event-related potentials elicited by auditory stimuli during spindle episodes and non-spindle episodes in stage 2 and found stronger inhibition of information processing in the presence of sleep spindles (Elton et al., 1997; Cote et al., 2000). Administration of classical hypnotics, such as benzodiazepines, increases spindle frequency activity and reduces SWA (Johnson et al., 1976; Borbély et al., 1985; Trachsel et al., 1990; Brunner et al., 1991). This has led to the assumption that the sleep-facilitating action of these drugs may be based on their ability to increase sleep spindles, and thereby increase arousal threshold (Johnson et al., 1976).

Other studies point to an involvement of sleep spindles in synaptic plasticity and memory processes. Memory consolidation is one of the proposed functions of sleep, for which there is growing evidence from animal and human studies (for reviews see Sejnowski and Destexhe, 2000; Peigneux et al., 2001). Sleep may provide a state during which recently acquired information is reactivated and consolidated in the absence of interfering external stimuli. The relationship between sleep and memory is highly complex, since it varies both with different types of memory (i.e. declarative and procedural) and different sleep states (REM sleep, SWS, stage 2; reviewed by Peigneux et al., 2001). For declarative memory it is suggested that new information is temporarily stored in the hippocampus, and transferred during sleep to a more permanent store in the neocortex (Buzsàki, 1998; Wilson and Mc Naughton, 1994). In rats, hippocampal and anatomically connected cortical neurons, which have been activated during wakefulness, are reactivated during NREM sleep, which supports this concept (Sutherland and Mc Naughton, 2000). There is evidence that sleep spindles are involved in the consolidation of declarative memory. Spindle density increases in the night after a declarative learning task, but not after a non-learning control task of equal cognitive demands (Gais et al., 2002). Furthermore, recall performance is correlated with spindle density. (Gais et al., 2002). Another study reported an increase in spindle density and in the duration of stage 2 sleep after intensive maze learning (Meier-Koll et al., 1999). Siapas et al. found a temporal correlation between hippocampal ripples (100-200 Hz oscillations) and cortical spindles (Siapas and Wilson, 1998). The co-activation of hippocampus and neocortex may be important for the hippocampal-neocortical information transfer during memory consolidation. The underlying cellular mechanisms are still largely unknown. A model has been proposed, according to

which spindle oscillations facilitate permanent synaptic changes by triggering Ca^{2+} entry into cortical pyramidal cells. This massive and repeated (at a frequency of 7-14 Hz) Ca^{2+} entry would induce long-term synaptic changes (Sejnowski and Destexhe, 2000).

Local aspects of sleep

It is now generally accepted that sleep is not a unitary process over the whole brain, but comprises local features. The most spectacular example in mammals is the alternating unihemispheric sleep in dolphins (Oleksenko et al., 1992). In humans, functional neuroimaging techniques, such as positron emission tomography (PET), have revealed distinct regional patterns of neuronal activity during different vigilance states stages, i.e. wakefulness, SWS and REM sleep (Maquet et al., 1997; Schwartz and Maquet, 2002; for reviews see Maquet and Phillips, 1998; Maquet, 2000). SWS is associated with a global decrease in cerebral blood flow, glucose metabolism, and oxygen metabolism. A decrease in glucose metabolism that exceeds the global decrease was found in the thalamus (Maquet et al., 1990; Maquet et al., 1992). Studies in which EEG and neuroimaging techniques were combined revealed a negative correlation between regional cerebral blood flow (rCBF) in the thalamus and EEG slow wave- and spindle frequency activity (Hofle et al., 1997). The decrease in rCBF in the thalamus may reflect the reduced excitatory input from the brainstem activating system to thalamic neurons, as well as the GABAergic inhibition by thalamic reticular neurons, associated with NREM sleep. Within the cortex, distinct areas exhibit particularly low rCBF. These are probably the areas where a high proportion of neurons is engaged in the synchronous sleep oscillations (Maquet, 2000). Topographical analysis of the human sleep EEG shows that power density in distinct frequency bands exhibits specific regional distribution during NREM sleep. Power density in the 1-4 Hz band (SWA) and in the 9-12 Hz band (alpha activity) exhibit a frontal maximum, power density in the 5-8 Hz band (theta activity) is maximal at the occipital area (Finelli et al., 2001). Spindle frequency activity and spindle density are highest in the centro-parietal region (Zeitlhofer et al., 1997; De Gennaro et al., 2000b; De Gennaro et al., 2000a; Finelli et al., 2001). However, when analyzed with a higher frequency resolution, slow and fast spindles exhibit a clearly

different topographical distribution (Gibbs and Gibbs, 1950; Scheuler et al., 1990; Jobert et al., 1992; Zeitlhofer et al., 1997; Werth et al., 1997b; Anderer et al., 2001). Sleep spindles with a frequency around 12 Hz are most abundant in the frontal brain region, whereas sleep spindles with a frequency around 14 Hz have a centro-parietal maximum. It is not yet clear whether this frequency-specific distribution reflects a topography-dependent modulation of spindle frequency, or if it represents two (functionally) different types of sleep spindles originating from distinct thalamic sources, as suggested by some authors (Zeitlhofer et al., 1997; Anderer et al., 2001)

The above mentioned studies addressed topographical aspects of sleep during normal baseline sleep. Previous studies have also shown that variations in the level of sleep pressure do not affect EEG activity equally in brain regions (Werth et al., 1996a; Cajochen et al., 1999; Finelli et al., 2001). Local aspects in the regulation of SWA have recently gained attention. Power density in the 2-Hz bin is highest in the frontal derivation at the beginning of the night; this frontal dominance declines over consecutive NREM sleep episodes (Werth et al., 1997a). After sleep deprivation, the largest increase in SWA occurs in the frontal EEG derivations (Cajochen et al., 1999; Finelli et al., 2001). Thus, both indices of homeostatic sleep pressure, the decline of SWA in the course of a baseline night, and the increase of SWA after extended wakefulness, exhibit a frontal predominance. High-level cognitive functions, such as self-observation, planning, prioritising and decision-making, depend predominantly on the frontal lobes (see Muzur et al., 2002 and Horne, 1993), and it is tempting to speculate that frontal brain areas accumulate a higher need for sleep as a consequence of their intensive use during the daytime (see Horne, 1992). Indeed, skills assigned to the prefrontal cortex have been shown to be particularly impaired by a sleep deficit (for references see Muzur et al., 2002 and Horne, 1993). Studies in humans and rats have directly demonstrated that activation of specific brain areas during wakefulness influences the neuronal activity in these areas during subsequent sleep. Unilateral activation of the left sensory cortex by vibratory stimuli administered to the right hand in humans induced a shift in low-frequency EEG power density to the left hemisphere in the central derivation overlying the somatosensory cortex in the first hour of sleep (Kattler et al., 1994). In rats, cutting the vibrissae on one side, and thereby producing a unilateral sensory input via intact vibrissae, resulted in a shift in low-frequency EEG power density towards the hemisphere contralateral to the intact vibrissae during subsequent sleep

(Vyazovskiy et al., 2000). Thus, in both studies, there was a shift of low-frequency EEG power density to the regions that have been particularly activated during preceding wakefulness. A recent study of 6-h continuos auditory stimulation during wakefulness reported an increase in power density in the alpha and spindle frequency range, as well as changes in the cortical coherence between the auditory cortex and other cortical regions over a broad frequency range during subsequent SWS (Cantero et al., 2002). The authors interpreted these changes in cortical activity patterns during SWS as homeostatic mechanisms in response to an excessive use of specific synapses associated to auditory processing.

But how do events during wakefulness influence brain activity during sleep? This question is still not fully answered. It is assumed that activity within neuronal groups during wakefulness leads to the production and accumulation of sleep promoting substances, which thereafter modulate sleep propensity (Obal and Krueger, 2003). Different candidates for such putative endogenous 'sleep factors' have been proposed, such as adenosine, interleukin-1 and growth hormones (Borbély and Tobler, 1989; Krueger and Obal, 1993; Benington and Heller, 1995; Krueger et al., 1999; Obal and Krueger, 2003). In a recent paper, Tononi and Cirelli proposed a hypothesis that links sleep with synaptic homeostasis. According to this hypothesis, local synaptic potentiation leads to an increase of SWA, and thus an intensification of sleep, in these brain areas. SWA, in turn, is associated with synaptic downscaling important for the maintenance of synaptic balance (Tononi and Cirelli, 2003).

Taken together, although the exact mechanisms remain to be established, a considerable number of reports indicate that local activation of brain regions during wakefulness results in sleep EEG changes in these regions. This supports the hypothesis that local aspects of sleep regulation may reflect recovery or reactivation processes in brain areas that have been particularly active during wakefulness (Benington and Heller, 1995; Horne, 1993).

Most of these studies were concerned with local use-dependent aspects of SWA topography. The significance of state-dependent changes in the topography of sleep spindles is much less known.

Methods used for the analysis of sleep spindles

FFT was applied to the EEG soon after its introduction, and spectral analysis remains the most widespread signal processing method in sleep research. However, it has its limits (for discussions see Geering et al., 1993; Ktonas and Gosalia, 1981). Since spectral analysis quantifies overall power by combining incidence and amplitude for a particular frequency band, it cannot differentiate between low-amplitude, high-incidence EEG activity and high-amplitude, low-incidence EEG activity of a particular frequency within the short time window (Ktonas and Gosalia, 1981). In particular, transient EEG phenomena, such as sleep spindles, are not well characterized by spectral analysis. Also, it does not discriminate synchronized spindle activity from ongoing de-synchronized activity in the same frequency band. In Chapter 3 and 4, a new method for spindle analysis is described in detail. The method, based on the fast time frequency transform (FTFT), discriminates synchronized activity from background noise and calculates amplitude and incidence of synchronized spindle frequency activity with a high frequency (0.25 Hz)- and temporal (0.125 s)-resolution, as well as yielding a series of different spindle parameters.

Objective and structure of the thesis

The general purpose of the present thesis was to gain a more comprehensive understanding of the regulation of sleep spindles during human NREM sleep. It was aimed to quantify the contribution of the homeostatic and circadian process with a special focus on topographical aspects. For this, EEGs from 4 midline electrodes along the antero-posterio axis were compared. A further main aim was to segregate different spindle characteristics, such as incidence, density, frequency or amplitude, in order to quantify the effect of circadian phase and sleep homeostasis for these parameters. This extends conventional analysis of EEG spectral power density in the spindle frequency range to give a more detailed and comprehensive description of circadian and sleep-wake dependent modulation of sleep spindles. For these purposes, in collaboration with Wim Martens from TEMEC, The Netherlands, a method for the detection and analysis of sleep spindles has been developed, validated and finally incorporated.

To assess homeostatic and circadian influences on sleep, a study protocol was designed that comprised a 40-h sleep deprivation (SD) and a 40-h multiple nap schedule in a balanced crossover design (see Figure 1 in Chapter 2). With the SD protocol, the effect of enhanced homeostatic sleep pressure on sleep parameters in the subsequent recovery night could be assessed. The nap protocol served to distribute sleep over the whole circadian cycle by simultaneously keeping homeostatic sleep pressure low and relatively constant throughout the 40-h period. Thereby, the influence of circadian phase on sleep could be quantified virtually free from confounding homeostatic influences.

All data presented in this thesis were collected in the above described experiment. Two chapters deal with the effect of differential levels of homeostatic sleep pressure on sleep spindles: the comparison of the effects of enhanced and reduced homeostatic sleep pressure on spectral SWA and SFA are reported in Chapter 2, whereas in Chapter 3, the relative contribution of different spindle characteristics to the observed changes in the EEG power spectra are quantified. The circadian modulation of SFA and spindle characteristics analyzed during the nap protocol are described in Chapter 4.

References

Aeschbach D. Dynamics of the human sleep electroencephalogram: effects of hypnotics, sleep deprivation, and habitual sleep length. Dissertation ETH No 11177, 1995.

Albrecht U. Functional genomics of sleep and circadian rhythm invited review: regulation of mammalian circadian clock genes. J Appl Physiol 2002; 92: 1348-1355.

Amzica F, Steriade M. Electrophysiological correlates of sleep delta waves. Electroencephalogr Clin Neurophysiol 1998; 107: 69-83.

Anderer P, Klösch G, Gruber G, Trenker E, Pascual-Marqui RD, Zeitlhofer J, et al. Low-resolution brain electromagnetic tomography revealed simultaneously active frontal and parietal sleep spindle sources in the human cortex. Neuroscience 2001; 103: 581-592.

Aschoff J, Wever R. Spontanperiodik des Menschen bei Auschluss aller Zeitgeber. Die Naturwissenschaften 1962; 49: 337-342.

Balsalobre A. Clock genes in mammalian peripheral tissues. Cell Tissue Res 2002; 309: 193-199.

Benington JH, Heller HG. Restoration of brain energy metabolism as the function of sleep. Prog Neurobiol 1995; 45: 347-360.

Berger H. Über das Elektroenzephalogramm beim Menschen. Archiv für Psychiatrie und Nervenkrankheiten 1929; 87: 527-570.

Borbély AA, Baumann F, Brandeis D, Strauch I, Lehmann D. Sleep deprivation: effect on sleep stages and EEG power density in man. Electroencephalogr Clin Neurophysiol 1981; 51: 483-495.

Borbély AA. A two process model of sleep regulation. Human Neurobiol 1982; 1: 195-204.

Borbély AA, Mattmann P, Loepfe M, Strauch I, Lehmann D. Effect of benzodiazepine hypnotics on all-night sleep EEG spectra. Human Neurobiol 1985; 4: 189-194.

Borbély AA, Tobler I. Endogenous sleep-promoting substances and sleep regulation. Physiol Rev 1989; 69: 605-670.

Brunner DP, Dijk DJ, Münch M, Borbèly AA. Effect of zolpidem on sleep and sleep EEG spectra in healthy young men. Psychopharmacology 1991; 104: 1-5.

Buzsàki G. Memory consolidation during sleep: neurophysiological perspective. J Sleep Res 1998; 7(Suppl 1): 17-23.

Cajochen C, Foy R, Dijk DJ. Frontal predominance of a relative increase in sleep delta and theta EEG activity after sleep loss in humans. Sleep Res Online 1999; 2: 65-69.

Campbell SS, Tobler I. Animal sleep: a review of sleep duration across phylogeny. Neurosci Biobehav Rev 1984; 8: 269-300.

Cantero JL, Atienza M, Salas RM, Dominguez-Marin E. Effects of prolonged waking-auditory stimulation on electroencephalogram synchronization and cortical coherence during subsequent slow-wave sleep. J Neurosci 2002; 22: 4702-4708.

Contreras D, Destexhe A, Sejnowksi T, Steriade M. Control of spatiotemporal coherence of a thalamic oscillation by corticothalamic feedback. Science 1996; 274: 771-774.

Cote KA, Epps T, Campbell KB. The role of the spindle in human information processing of high-intensity stimuli during sleep. J Sleep Res 2000; 9: 19-26.

Czeisler CA, Zimmerman JC, Ronda JM, Moore-Ede MC, Weitzman ED. Timing of REM sleep is coupled to the circadian rhythm of body temperature in man. Sleep 1980; 2: 329-346.

Czeisler CA, Dumont M, Duffy JF, Steinberg JD, Richardson GS, Brown EN, et al. Association sleep-wake habits in older people with changes in output of circadian pacemaker. Lancet 1992; 340: 933-936.

Czeisler CA, Duffy JF, Shanahan TL, Brown EN, Mitchell JF, Rimmer DW, et al. Stability, precision, and near-24-hour period of the human circadian pacemaker. Science 1999; 284: 2177-2181.

Daan S, Beersma DGM, Borbély AA. Timing of human sleep: recovery process gated by a circadian pacemaker. Am J Physiol Regulatory Integrative Comp Physiol 1984; 246: R161-R183.

De Gennaro L, Ferrara M, Bertini M. Topographical distribution of spindles: variations between and within NREM sleep cycles. Sleep Res Online 2000a; 3: 155-160.

De Gennaro L, Ferrara M, Bertini M. Effect of slow-wave sleep deprivation on topographical distribution of spindles. Behav Brain Res 2000b; 116: 55-59.

Destexhe A, Contreras D, Steriade M. Spatiotemporal analysis of local field potentials and unit discharges in cat cerebral cortex during natural wake and sleep states. J Neurosci 1999; 19: 4595-4608.

Dietsch G. Fourier-Analyse von Elektroenkephalogrammen des Menschen. Pflüger's Arch Ges Physiol 1932; 230: 106-112.

Dijk DJ, Hayes B, Czeisler CA. Dynamics of electroencephalographic sleep spindles and slow wave activity in men: effect of sleep deprivation. Brain Res 1993; 626: 190-199.

Dijk DJ, Czeisler CA. Paradoxical timing of the circadian rhythm of sleep propensity serves to consolidate sleep and wakefulness in humans. Neurosci Lett 1994; 166: 63-68.

Dijk DJ, Czeisler CA. Contribution of the circadian pacemaker and the sleep homeostat to sleep propensity, sleep structure, electroencephalographic slow waves, and sleep spindle activity in humans. J Neurosci 1995; 15: 3526-3538.

Dijk DJ, Roth C, Landolt HP, Werth E, Aeppli M, Achermann P, et al. Melatonin effect on daytime sleep in men: suppression of EEG low frequency activity and enhancement of spindle frequency activity. Neurosci Lett 1995; 201: 13-16.

Dijk DJ, Shanahan TL, Duffy JF, Ronda JM, Czeisler CA. Variation of electroencephalographic activity during non-rapid eye movement and rapid eye movement sleep with phase of circadian melatonin rhythm in humans. J Physiol 1997; 505: 851-858.

Duffy JF, Dijk DJ, B KE, Czeisler CA. Later endogenous circadian temperature nadir relative to an earlier wake time in older people. Am J Physiol Regulatory Integrative Comp Physiol 1998; 275: R1478-R1487.

Eastman CI, Mistlberger RE, Rechtschaffen A. Suprachiasmatic nuclei lesions eliminate circadian temperature and sleep rhythms in the rat. Physiol Behav 1984; 32: 357-368.

Elton M, Winter O, Heslenfeld D, Loewy D, Campbell K, Kok A. Event-related potentials to tones in the absence and presence of sleep spindles. J Sleep Res 1997; 6: 78-83.

Endo S, Kobayashi T, Yamamoto T, Fukuda H, Sasaki M, Ohta T. Persistence of the circadian rhythm of REM sleep: a variety of experimental manipulations of the sleep-wake cycle. Sleep 1981; 4: 319-328.

Finelli LA, Borbély AA, Achermann P. Functional topography of the human nonREM sleep electroencephalogram. Eur J Neurosci 2001; 13: 2282-2290.

Gais S, Mölle M, Helms K, Born J. Learning-dependent increases in sleep spindle density. J Neurosci 2002; 22: 6830-6834.

Geering BA, Achermann P, Eggimann F, Borbély AA. Period - amplitude analysis and power spectral analysis: a comparison based on all - night sleep EEG recordings. J Sleep Res 1993; 2: 121-129.

Gibbs FA, Gibbs EL. Atlas of Electroencephalography. Cambridge: Addison-Wesley Press, 1950.

Hofle N, Paus T, Reutens D, Fiset P, Gotman J, Evans AC, et al. Regional cerebral blood flow changes as a function of delta and spindle activity during slow wave sleep in humans. J Neurosci 1997; 17: 4800-4808.

Horne J. Human slow-wave sleep and the cerebral cortex. J Sleep Res 1992; 1: 122-124.

Horne JA. Human sleep, sleep loss and behaviour: implications for the prefrontal cortex and psychiatric disorder. Br J Psychiatry 1993; 162: 413-419.

Jobert M, Poiseau E, Jähnig P, Schulz H, Kubicki S. Topographical analysis of sleep spindle activity. Neuropsychobiology 1992; 26: 210-217.

Johnson LC, Hanson K, Bickford RG. Effect of flurazepam on sleep spindles and K-complexes. Electroencephalogr Clin Neurophysiol 1976; 40: 67-77.

Kattler H, Dijk DJ, Borbély AA. Effect of unilateral somatosensory stimulation prior to sleep on the sleep EEG in humans. J Sleep Res 1994; 3: 159-164.

Krueger JM, Obal F. A neuronal group theory of sleep function. J Sleep Res 1993; 2: 63-69.

Krueger JM, Obal F, Fang J. Why we sleep: a theoretical view of sleep function. Sleep Med Rev 1999; 3: 119-129.

Ktonas PY, Gosalia AP. Spectral analysis vs. period-amplitude analysis of narrowband EEG activity: a comparison based on the sleep delta-frequency band. Sleep 1981; 4: 193-206.

Landolt HP, Finelli LA, Roth C, Buck A, Achermann P, Borbély AA. Zolpidem and sleep deprivation: different effect on EEG power spectra. J Sleep Res 2000; 9: 175-183.

Lopes da Silva FH, Storm van Leewen W, Rémond A. Handbook of electroencephalography and clinical neurophysiology: clinical applications of computer analysis of EEG and other neurophysical signals. Vol 2. Amsterdam: Elsevier, 1986.

Maquet P, Dive D, Salmon E, Sadzot B, Franco G, Poirrier R, et al. Cerebral glucose utilization during sleep-wake cycle in man determined by positron emission tomography and [18F]2-fluoro-2-D-glucose method. Brain Res 1990; 513: 136-143.

Maquet P, Dive D, Salmon E, Sadzot B, Franco G, Poirrier R, et al. Cerebral glucose utilization during stage 2 sleep in man. Brain Res 1992; 571: 149-153.

Maquet P, Degueldre C, Delfiore G, Aerts J, Péters JM, Luxen A, et al. Functional neuroanatomy of human slow wave sleep. J Neurosci 1997; 17: 2807-2812.

Maquet P, Phillips C. Functional brain imaging of human sleep. J Sleep Res 1998; 7 (Suppl 1): 42-47.

Maquet P. Functional neuroimaging of normal human sleep by positron emission tomography. J Sleep Res 2000; 9: 207-231.

Meier-Koll A, Bussmann B, Schmidt C, Neuschwander D. Walking through a maze alters the architecture of sleep. Percept Mot Skills 1999; 88: 1141-1159.

Mölle M, Marschall L, Gais S, Born J. Grouping of spindle activity during slow oscillations in human non-rapid eye movement sleep. J Neurosci 2002; 22: 10941-10947.

Muzur A, Pace-Schott EF, Hobson JA. The prefrontal cortex in sleep. Trends Cogn Sci 2002; 6: 475-481.

Niedermeyer E, Lopes da Silva FH. Electroencephalography: basic principles, clinical applications and related fields. Baltimore: Urban and Schwarzenberg, 1987.

Obal F, Krueger JM. Biochemical regulation of non-rapid-eye-movement sleep. Front Biosci 2003; 8: d520-d550.

Oleksenko AI, Mukhametov LM, Polyakova IG, Supin AY, Kovalzon VM. Unihemispheric sleep deprivation in bottlenose dolphins. J Sleep Res 1992; 1: 40-44.

Peigneux P, Laureys S, Delbeuck X, Maquet P. Sleeping brain, learning brain. The role of sleep for memory systems. NeuroReport 2001; 12: A111-A124.

Rechtschaffen A, Kales A. A manual of standardized terminology, techniques and scoring system for sleep stages of human subjects. Bethesda, MD: US Dept of Health, Education and Welfare, Public Health Service, 1968.

Reppert SM, Weaver DR. Coordination of circadian timing in mammals. Nature 2002; 418: 935-941.

Scheuler W, Kubicki S, Scholz G, Marquardt J. Two different activities in the sleep spindle frequency band-discrimination based on the topographical distribution of spectral power and coherence. In: Horne J, editor. Sleep '90. Bochum: Pontenagel Press, 1990: 13-16.

Schibler U, Sassone-Corsi P. A web of circadian Pacemakers. Cell 2002; 111: 919-922.

Schibler U, Ripperger J, Brown SA. Peripheral circadian oscillators in mammals: time and food. J Biol Rhythms 2003; 18: 250-260.

Schwartz S, Maquet P. Sleep imaging and the neuropsychological assessment of dreams. Trends Cogn Sci 2002; 6: 23-30.

Sejnowski TJ, Destexhe A. Why do we sleep? Brain Res 2000; 886: 208-223.

Siapas AG, Wilson MA. Coordinated interactions between hippocampal ripples and cortical spindles during slow-wave sleep. Neuron 1998; 21: 1123-1128.

Stanewsky R. Clock mechanisms in Drosophila. Cell Tissue Res 2002; 309: 11-26.

Stephan FK, Zucker I. Circadian rhythms in drinking behavior and locomotor activity of rats are eliminated by hypothalamic lesions. Proc Natl Acad Sci USA 1972; 69: 1583-1586.

Steriade M, Contreras D, Curró Dossi R, Nuñez A. The slow (< 1 Hz) oscillation in reticular thalamic and thalamocortical neurons: scenario of sleep rhythm generation in interacting thalamic and neocortical networks. J Neurosci 1993a; 13: 3284-3299.

Steriade M, McCormick DA, Sejnowski TJ. Thalamocortical oscillations in the sleeping and aroused brain. Science 1993b; 262: 679-685.

Steriade M, Contreras D, Amzica F. Synchronized sleep oscillations and their paroxysmal developments. Trends Neurosci 1994; 17: 199-208.

Strogatz SH, Kronauer RE, Czeisler CA. Circadian pacemaker interferes with sleep onset at specific times each day: role in insomnia. Am J Physiol Regulatory Integrative Comp Physiol 1987; 253: R172-R178.

Sutherland GR, Mc Naughton B. Memory trace reactivation in hippocampal and neocortical neuronal ensembles. Curr Opin Neurobiol 2000; 10: 180-186.

Tobler I, Borbély AA, Groos G. The effect of sleep deprivation on sleep in rats with suprachiasmatic lesions. Neurosci Lett 1983; 21: 49-54.

Tononi G, Cirelli C. Sleep and synaptic homeostasis: a hypothesis. Brain Res Bull 2003; 62: 143-150.

Trachsel L, Dijk DJ, Brunner DP, Klene C, Borbély AA. Effect of zopiclone and midazolam on sleep and EEG spectra in a phase-advanced sleep schedule. Neuropsychopharmacology 1990; 3: 11-18.

Van Esseveldt LE, Lehman MN, Boer GJ. The suprachiasmatic nucleus and the circadian time-keeping system revisited. Brain Res Rev 2000; 33: 34-77.

Vyazovskiy V, Borbély AA, Tobler I. Unilateral vibrissae stimulation during waking induces interhemispheric EEG asymmetry during subsequent sleep in the rat. J Sleep Res 2000; 9: 367-371.

Wei HG, Riel E, Czeisler CA, Dijk DJ. Attenuated amplitude of circadian and sleep-dependent modulation of electroencephalographic sleep spindle characteristics in elderly human subjects. Neurosci Lett 1999; 260: 29-32.

Weitzman ED, Nogeire C, Perlow M, Fukushima D, Sassin J, Mc Gregor P, et al. Effects of a prolonged 3-hour sleep-wake cycle on sleep stages, plasma cortisol, growth hormone and body temperature in man. J Clin Endocrinol Metab 1974; 38: 1018-1030.

Weitzman ED, Czeisler CA, Zimmermann JC, Ronda JM. Timing of REM and stages 3+4 sleep during temporal isolation in man. Sleep 1980; 2: 391-407.

Werth E, Achermann P, Borbély AA. Brain topography of the human sleep EEG: Antero-posterior shifts of spectral power. NeuroReport 1996a; 8: 123-127.

Werth E, Dijk DJ, Achermann P, Borbély AA. Dynamics of the sleep EEG after an early evening nap: experimental data and simulations. Am J Physiol Regulatory Integrative Comp Physiol 1996b; 271: 501-510.

Werth E, Achermann P, Borbely AA. Fronto-occipital EEG power gradients in human sleep. J Sleep Res 1997a; 6: 102-112.

Werth E, Achermann P, Dijk DJ, Borbély AA. Spindle frequency activity in the sleep EEG: individual differences and topographic distribution. Electroencephalogr Clin Neurophysiol 1997b; 103: 535-542.

Wilson MA, Mc Naughton B. Reactivation of hippocampal ensemble memories during sleep. Science 1994; 265: 676-679.

Zeitlhofer J, Gruber G, Anderer P, Asenbaum S, Schimicek P, Saletu B. Topographic distribution of sleep spindles in young healthy subjects. J Sleep Res 1997; 6: 149-155.

Chapter 2

Homeostatic control of slow wave- and spindle frequency activity during human sleep: effect of differential sleep pressure and brain topography

Vera Knoblauch, Kurt Kräuchi, Claudia Renz, Anna Wirz-Justice and Christian Cajochen

Centre for Chronobiology, Psychiatric University Clinic, Basel, Switzerland

Published in: Cerebral Cortex (2002), 12: 1092-1100

Abstract

The impact of a 40-h sleep deprivation versus a 40-h multiple nap paradigm on topographic and temporal aspects of electroencephalographic (EEG) activity during the subsequent recovery sleep was investigated in 10 young volunteers in a controlled "constant posture" protocol. The accumulation of sleep pressure with extended wakefulness could be significantly attenuated by intermittent naps. The differential sleep pressure conditions induced frequency- and topographic-specific changes in the EEG slow wave range (0.5-5 Hz) and in the low- (LSFA, 12.25-13.25 Hz) and high- spindle frequency range (HSFA, 13.75-16.5 Hz) during nonREM sleep. The observed increase of EEG slow wave activity (SWA) after high sleep pressure was significantly more pronounced in the fronto-central (Fz, Cz) than in the parieto-occipital (Pz, Oz) derivations. Low sleep pressure after the nap paradigm decreased SWA without a frontal - but an occipital predominance. Spindle frequency activity showed a dissimilar homeostatic regulation: HSFA was significantly decreased after high sleep pressure and increased after low sleep pressure, exclusively in the centro-parietal brain region (Cz, Pz). LSFA was significantly enhanced after both manipulations. The data indicate that EEG activity, in particular frontal SWA and centro-parietal HSFA, are under a clear sleep-wake-dependent homeostatic control and imply a reciprocal relationship in the homeostatic regulation of SWA and HSFA, which however shows different spatio-temporal aspects.

Introduction

The electroencephalogram (EEG) during non-rapid eye movement sleep (NREMS) is generally characterized by low frequency oscillations (1-7 Hz) and transient oscillations in the spindle frequency range (SFA, 12-16 Hz). The dynamics of EEG slow-wave activity (SWA, EEG power density in the range of 0.75-4.5 Hz) and SFA have a clear mutual temporal relationship in the course of a nocturnal sleep episode (Uchida et al., 1991; Aeschbach and Borbély, 1993; Dijk et al., 1993). Both SWA and SFA are thought to be generated by a common thalamocortical mechanism, which depends on the degree of hyperpolarisation of thalamocortical neurons (Steriade et al., 1993; Mc Cormick and Bal, 1997). SWA and SFA during the human sleep cycle are modulated by an interaction of two processes: a circadian process generated in the suprachiasmatic nuclei (SCN) of the hypothalamus, and a sleep homeostatic process representing the sleep-wake-dependent pressure for sleep (Daan et al., 1984; Dijk and Czeisler, 1995). Forced desynchrony experiments and observations during spontaneous desynchronisation between the sleep-wake cycle and the circadian system have demonstrated that slow wave sleep (SWS) and SWA during NREMS decrease throughout the course of sleep at all circadian phases (Weitzman et al., 1980; Dijk and Czeisler, 1995). These data are in accordance with the hypothesis that these low frequency EEG components during sleep are an electrophysiological marker of the dissipation of homeostatic sleep pressure (Borbély et al., 1981). Sleep-deprivation and nap experiments had previously demonstrated a monotonic relationship between wake duration and SWA at the beginning of sleep (Borbély et al., 1981; Dijk et al., 1993; Werth et al., 1996). Lesions of the SCN in rodents do not abolish this increase of SWA in response to an extension of wakefulness (Tobler et al., 1983). Thus, SWA during sleep is a reliable marker of the sleep homeostatic process (Dijk et al., 1997).

The function of sleep spindles is to a large extent unknown. It has been speculated that they may serve to prevent arousing stimuli from reaching the cortex (Jankel and Niedermeyer, 1985; Steriade et al., 1993). A negative correlation between regional cerebral blood flow (rCBF) in the medial thalamus and EEG spindle activity during sleep has been reported and interpreted as reflecting the loss of consciousness and sensory awareness during sleep (Hofle et al., 1997). After

benzodiazepine intake, SWA is decreased, whereas the occurrence of sleep spindles and SFA is enhanced (Johnson et al., 1976; Borbély et al., 198; Trachsel et al., 1990; Brunner et al., 1991). This has led to the hypothesisthat the sleep-promoting action of benzodiazepines may be based on their ability to enhance SFA (Johnson et al., 1976), which in turn prevent sensory input signals being relayed to the cortex (Jankel and Niedermeyer, 1985; Steriade et al., 1993), However, current concepts of sleep-wake regulation still lack crucial understanding of the role of sleep spindles. There is a general consensus that SFA is under both circadian and homeostatic control (Dijk et al., 1997; Aeschbach et al., 1997). After sleep deprivation, SFA is reduced and shows an inverse relationship to SWA and thus to sleep pressure (Borbély et al., 1981; Dijk et al., 1993; Finelli et al., 2001). However, this reduction in SFA is limited to the upper frequency range (15Hz-bin, Borbély et al., 1981; 13.75-14Hz, Dijk et al., 1993), whereas low-frequency spindle activity is not affected. In a nap study, where the duration of prior wakefulness varied from 2 to 20 hours, a significant decrease of power density with increasing duration of prior wakefulness was observed in the 15 Hz-bin, but not in the lower SFA range (Dijk et al., 1987). These and other findings indicate that there may be a frequency-dependent homeostatic control of SFA. Most studies have used only one or two EEG derivations (C3, C4, or a fronto-occipital bipolar derivation) to describe the effects of different sleep pressure levels on SFA (Borbély et al., 1981; Dijk et al., 1987; Dijk et al., 1993; Dijk et al., 1997). However, sleep spindles may not be a homogenous group of EEG waves: their frequency-specific distribution over different brain locations was recognized as early as 1950 (Gibbs and Gibbs, 1950). This study reported that sleep spindles with a frequency around 12 Hz exhibit an anterior dominance, whereas spindles with a frequency around 14 Hz were most prominent in more posterior derivations. This frequency-specific topographical distribution was later confirmed by several authors (Zeitlhofer et al., 1997; Werth et al., 1997; Zygierewicz et al., 1999; Finelli et al., 2001). However, a dose-response relationship between the amount of prior wakefulness and its repercussions on frequency- and derivation-specific SFA during NREMS has, to our knowledge, not been reported.

In the present study, EEG spectra during recovery sleep after 40h of either total sleep deprivation or a 75/150-min sleep-wake (nap) schedule were compared. The build-up of sleep pressure during scheduled wakefulness could be significantly attenuated by intermittent naps (Knoblauch et al., 2001; Cajochen et al., 2001). We

aimed at assessing the effect of differential levels of sleep pressure on the dynamics of EEG power density along the antero-posterior axis, in particular in the slow wave- and spindle frequency range. We hypothesized that the reciprocal homeostatic regulation of SWA and SFA depends on brain location. We further hypothesized that the response to differential sleep pressure conditions in the spindle frequency range (12-16 Hz) is not uniform.

Methods

Subject Selection

Subjects were recruited via poster advertisements at the University of Basel. After successfully completing a brief telephone screening, they received detailed information on the study and 3 questionnaires: a morning-evening-type questionnaire (Torsvall and Åkerstedt, 1980), the Pittsburgh Sleep Quality Index (PSQI), and an extensive questionnaire covering sleep habits, sleep quality, life habits, physical health and medical history. Subjects with self-reported sleep complaints (PSQI score $\geq$5) as well as extreme morning or evening types (score $<$12 or $>$23) were excluded from participation. Other exclusion criteria were chronic or current major medical illness or injury, smoking, medication or drug consumption, shift work within three months or transmeridian travel within one month prior to the study, excessive caffeine consumption and excessive physical activity.

Subjects who did not fulfill any of the above exclusion criteria were invited to the laboratory and interviewed. They spent an adaptation night in the laboratory to test his or her ability to sleep in a new environment and to exclude primary sleep disorders (i.e. insomnia). A physical examination excluded medical disorders. All subjects gave signed informed consent, and the study protocol, screening questionnaires and consent form were approved by the Ethical Committee of the Cantons Basel-Stadt and Baselland.

Subjects

Ten healthy subjects (six male, four female, age range 24-32 years, mean: 27.1 $\pm$ 2.3 s.e.m.) were studied. Female subjects started the study on day 1 to 5 after the onset

of menstruation in order to complete the entire study block within their follicular phase. Three female subjects used oral contraceptives. During the week preceding the study (baseline week), subjects were instructed to maintain a regular sleep-wake schedule (bed- and wake times within ± 30 minutes of self-selected target time). The latter was verified by a wrist activity monitor (Cambridge Neurotechnologies , UK) and sleep logs. They were also instructed to refrain from excessive physical activity, caffeine and alcohol consumption. Drug-free status was verified upon admission via urine toxicologic analysis (Drug-Screen Card Multi-6 for amphetamines, benzodiazepines, cocaine, methadone, opiates and THC; von Minden Gmbh). All ten subjects completed the study without any complaints.

Design

Subjects underwent two study blocks in a balanced crossover design: a sleep-deprivation (SD) and a nap protocol (NP) (Figure 1). In either protocol, subjects reported to the laboratory in the evening for an 8-h sleep episode . The timing of their sleep-wake schedule was calculated in such a way that the sleep episode was centered at the midpoint of each subject's habitual sleep episode as assessed by actigraphy during the baseline week. On the next afternoon (Day 1) electrodes and thermosondes were attached. After a second 8-h sleep episode (baseline night) at their habitual bedtime, a 40-h sleep deprivation under constant routine (CR) conditions or a 40-h nap protocol under constant posture conditions (near recumbent during wakefulness and supine during scheduled sleep episodes) was carried out (for details of the CR method see (Cajochen et al., 1999b). In the NP, subjects completed 10 alternating cycles of 75 min of scheduled sleep and 150 min of scheduled wakefulness. The light levels were <8 lux (typically 3-5 lux at the angle of gaze) during scheduled wakefulness and 0 lux during scheduled sleep. The protocol ended with a 8-h recovery sleep episode starting again at habitual bedtime. After a 1-4 week interval, the subjects started their second study block.

Sleep recording and analysis

Sleep was recorded polysomnographically using the VITAPORT digital ambulatory sleep recorder (Vitaport-3 digital recorder, TEMEC Instruments B.V., Kerkrade, The Netherlands). Twelve EEGs, two electrooculograms (EOG), one submental electromyogram (EMG) and one electrocardiogram (ECG) signal were recorded. All

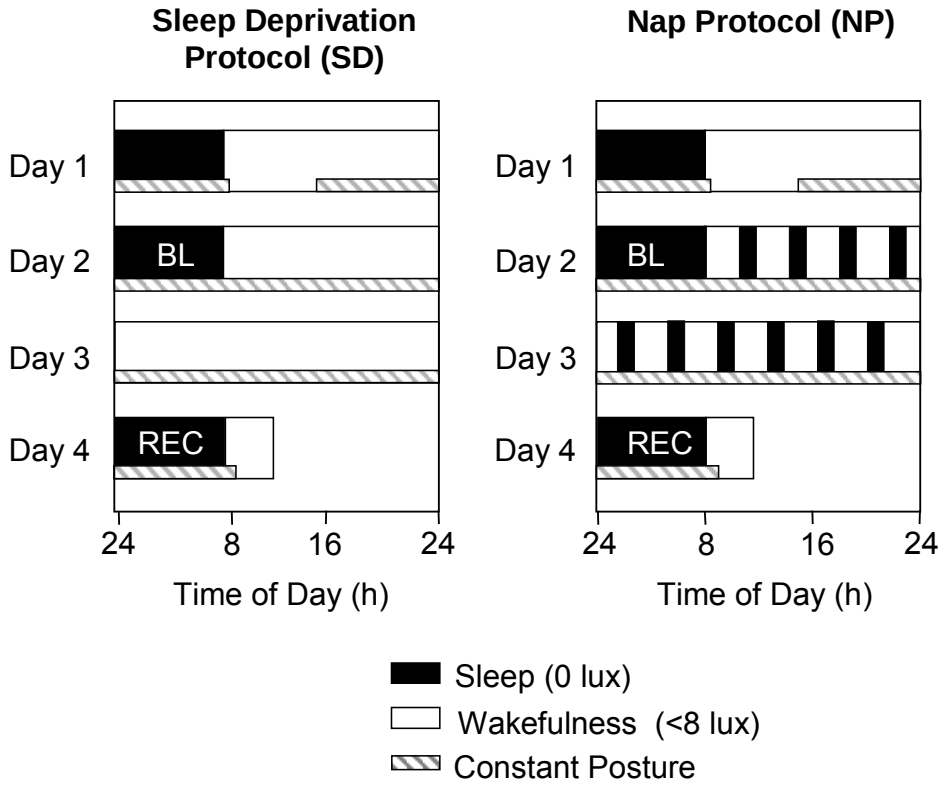

Figure 1. Overview of the protocol design. Subjects entered the lab for an 8-h nocturnal sleep episode followed by a day to adjust to the <8 lux experimental conditions. After the second 8-h night (baseline, BL), either a 40-h sleep deprivation or a 40-h multiple nap paradigm (ten 75/150-min sleep/wake cycles) under constant posture conditions was carried out, followed by an 8-h recovery night (REC). Black bars indicate scheduled sleep episodes (light levels: 0 lux), white bars indicate scheduled episodes of wakefulness (light levels: <8 lux), hatched bars indicate controlled posture (semi-recumbent during wakefulness and supine during scheduled sleep).

signals were on-line digitized (12 bit AD converter, 610 µV/bit; storage sampling rate at 128 Hz for the EEG) and digitally filtered at 30 Hz (4th order Bessel type anti-aliasing filters, total 24 dB/Oct.) using a time constant of 1.0 s. The raw signals were stored on-line on a Flash RAM Card (Viking, USA) and downloaded off-line to a PC hard drive. EEG artifacts were detected by an automated artifact detection algorithm. This algorithm was based on a instantaneous frequency analysis, which yields the amplitude-envelope and the frequency of 8 band-filtered components instantaneously at a rate of 8 per second. Low-frequency (as movement) artifacts, mid-frequency (as ECG interference) and high-frequency (as EMG) artifacts are detected individually if the respective instantaneous frequencies and amplitudes in the relevant frequency bands are not within preset ranges (CASA, 2000 Phy Vision B.V., Kerkrade, The Netherlands). The EEGs were off-line subjected to spectral analysis using a fast Fourier transform (FFT, 10% cosine 4-s window) resulting in a 0.25 Hz bin resolution. For data reduction, artifact-free 4-s epochs were averaged over 20-s epochs. Sleep stages were visually scored on a 20-s basis (Vitaport Paperless Sleep Scoring Software) according to standard criteria (Rechtschaffen and Kales, 1968). EEG power spectra were calculated during NREMS in the frequency range from 0.5 to 32 Hz. Here, we only report EEG data derived from the midline (Fz, Cz, Pz, Oz) referenced against linked mastoids (A1, A2) in the range of 0.5 - 25 Hz.

Statistics

The statistical packages SAS ® (SAS ® Institute Inc., Cary, NC, Version 6.12) and Statistica ® (StatSoft Inc.(1995). STATISTICA for Windows) were used. Statistical analyses did not reveal any significant difference between the two baseline nights, neither for sleep stage measures nor for EEG power density in any of the frequency bins. Therefore, for the sake of simplicity, the two baseline nights were pooled.

In order to analyze the time course of sleep stages and EEG power density in the course of the sleep episodes, the 8-h sleep episodes were subdivided into 2-h intervals after the first occurrence of stage two (i.e. sleep onset). This resulted in the fourth 2-h interval being shorter than 2 hours and of variable length for each subject and night. To correct for this, relative values for sleep stage variables (% of total sleep time) are reported. Values of each interval were compared to values of the corresponding intervals during the baseline night. In one case, artifacts considerably

disturbed EEG recordings in interval 3 and 4. This subject was excluded for the time course analysis of the visual scoring data.

In the topographical analysis of SWA, HSFA and LSFA, a first statistical analysis with the four separate EEG derivations (Fz, Cz, Pz, Oz) did not yield consistent significant interactions between cond * derivations. Therefore, derivations were pooled in order to obtain consistent significant interaction in the ANOVA. The frontal and central derivation (Fz+Cz) and the parietal and occipital derivation (Pz+Oz) were pooled for SWA and LSFA, the frontal and occipital derivation (Fz+Oz) and the central and parietal derivation (Cz+Pz) for HSFA.

One-, two- and three-way analyses of variance for repeated measures (rANOVA) were performed. All *p* values derived from rANOVAs were based on Huynh-Feldt's (H-F) corrected degrees of freedom, but the original degrees of freedom are reported. For *post-hoc* comparisons the Duncan's multiple range test and t-tests with correction for multiple comparisons (Curran-Everett, 2000) were used.

Results

Sleep measures derived from visual scoring

Sleep during naps:

In order to test whether the subjects were able to sleep sufficiently during the NP protocol, the amount of total sleep time (TST; NREM sleep + REM sleep + stage 1) and relative sleep stages (percent of TST) during the baseline night (BL), throughout the 40-h episode of the NP protocol and during the recovery night (REC) were calculated for each subject and then averaged over subjects. Across the total of 12.5 hours scheduled sleep episodes (10 naps each of 75-min duration), TST did not significantly differ from accumulated TST in the 8-h baseline sleep episode (459.27 ± 27.52 vs. 434.93 ± 8.98 min; $F_{2,18} = 1.34$, $p = 0.28$). However, the proportion of sleep stages was different. The percentage of SWS was significantly higher than during baseline (19.71 ± 1.73 *vs*. 15.99 ± 1.33 %, $p<0.05$), whereas REM sleep (REMS)

Table 1: Sleep measures derived from visual scoring of the average baseline night and the SD - and NP recovery night (mean ± s.e.m., n=10).

	Baseline	**SD rec**		**NP rec**	
TST (min)	433.10 ± 9.12	457.37± 4.3	*	417.73 ± 13.64	
SE (%)	90.28 ± 1.89	95.50 ± 0.90	*	87.03 ± 2.80	
% MT	2.82 ± 0.43	2.20 ± 0.32		3.96 ± 0.96	
% WALO	8.40 ± 2.10	2.86 ± 0.77	°	12.10 ± 3.72	
% arousal	11.23 ± 2.38	5.06 ± 1.05	*	16.06 ± 4.09	
% stage 1	13.53 ± 1.51	7.09 ± 1.03	*	13.99 ± 1.53	
% stage 2	49.31 ± 1.59	46.34 ± 1.61	*	52.22 ± 1.87	*
% stage 3	9.02 ± 0.48	13.18 ± 1.77	*	8.73± 0.73	
% stage 4	7.02 ± 1.68	13.86 ± 2.72	*	5.15 ± 1.44	
% SWS	16.04 ± 1.54	27.04 ± 1.66	*	13.87 ± 1.48	*
% NREMS	65.36 ± 1.37	73.38 ± 1.35	*	66.09 ± 1.30	
% REMS	21.12 ± 1.12	19.53 ± 1.63		19.92 ± 1.64	
SL1 (min)	9.63 ± 2.23	4.37 ± 0.90	*	19.37 ± 7.57	
SL2 (min)	14.15 ± 2.44	6.60 ± 1.17	*	27.47 ± 7.04	*
RL (min)	73.02 ± 4.69	64.00 ± 7.75		72.93 ± 9.26	

For sleep stages, relative values (percent of total sleep time) are shown. TST = total sleep time (stage 1-4 + REMS), SE = sleep efficiency [(TST/time in bed)*100], MT = movement time, WALO = wakefulness after lights off, arousal = WALO + MT, SL1 = latency to stage one (min), SL2 = latency to stage two (min), RL = latency to REMS (min). For SL1, SL2 and RL, statistics were applied on log transformed values. An asterisk indicates significant differences to the average baseline night (p<0.05), an open circle indicates a tendency (p<0.1, Duncan's multiple range test).

percentage was significantly reduced (15.70 ± 1.92 *vs*. 21.59 ± 1.37 %, $p<0.05$, Duncan's multiple range test).

Details about the changes in sleep structure throughout the NP protocol are summarized in (Knoblauch et al., 2001); spectral EEG changes will be reported elsewhere.

Recovery nights:

Table 1 summarizes all-night sleep measures (% of total sleep time) for the average baseline night and the SD - and NP recovery night. A one-way rANOVA with the factor *Condition* (BL, SD, NP) yielded a significant variation in all measures ($F_{2,18} > 6.0$, $p<0.03$) except for REMS, movement time (MT) and latency to REMS. Post-hoc comparisons revealed that TST, sleep efficiency (SE, [TST/time in bed]*100), NREMS, SWS, stage 3 and stage 4 were significantly enhanced in the recovery night following the SD protocol compared to the baseline night at the expense of stage 1 and 2 and the arousal index (WALO+MT) (for statistics see table 1). WALO (wakefulness after lights off) tended to be reduced ($p=0.06$). Sleep latency to stage 2 and to stage 1 was significantly reduced. SWS in the recovery night after the NP protocol. was significantly reduced whereas stage 2 was significantly enhanced, and the latency to stage 2 was significantly longer (see Table 1).

Although there was no significant variation in all-night REMS, the time course of REMS throughout the night was significantly different in the NP recovery night compared to baseline. This was analyzed by a two-way rANOVA with the factors *condition* (BL, SD, NP) and *interval* (2-h interval 1 – 4, see Methods section) which yielded a significant interaction of these two factors ($F_{6,48}=3.53$; $p<0.01$). Post-hoc comparisons showed that REMS was significantly increased in interval 1 ($p<0.05$) and tended to be decreased ($p=0.06$) in interval 4. REMS in the NP did not show the usual overall increase across the night ($p=0.48$ for interval 1 to 2 and $p=0.08$ for interval 1 to 4), as it did in BL ($p<0.01$).

EEG power spectra during NREM sleep: all-night absolute EEG power density (0.5-25 Hz)

All-night absolute EEG power density in each frequency bin between 0.5 - 25 Hz for the midline derivations (Fz, Cz, Pz, Oz) during NREMS is illustrated in Figure 2 for the average baseline night (BL) and the SD - and NP recovery night. A two-way

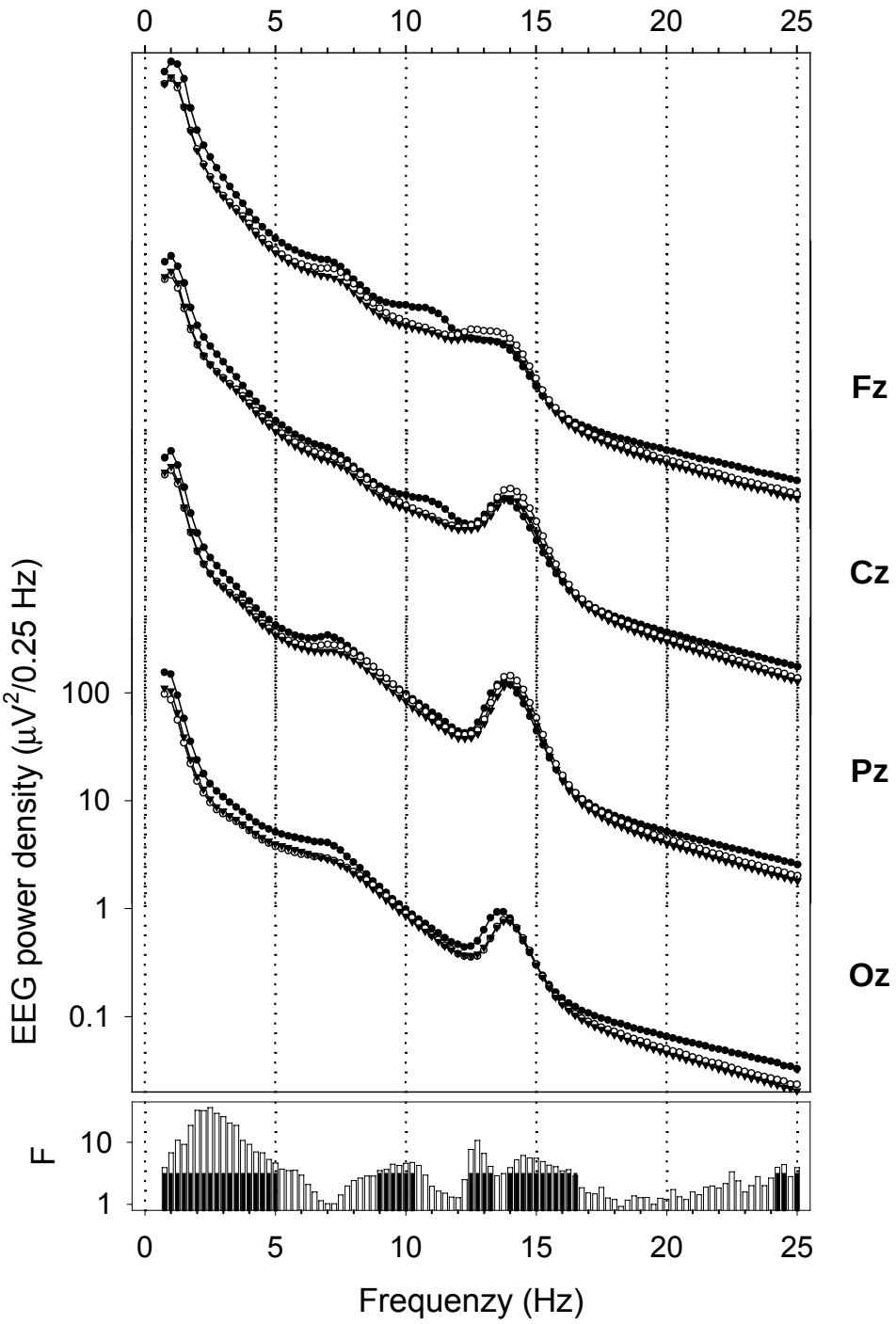

Figure 2. EEG power spectra during NREM sleep of the midline derivations (Fz, Cz, Pz, Oz) for the average baseline night (BL, ▼) and the SD (●) and NP (○) recovery night. Mean values (n=10) are shown for each 0.25 Hz-bin in the range of 0.5-25 Hz. The lowest panel shows F-values (gray bars) of a two-way rANOVA with the factors derivation (Fz, Cz, Pz, Oz) and condition (BL, SD, NP). Black bars near the abscissa represent frequency bins showing a significant interaction of these two factors (p<0.05).

rANOVA with the factors *derivation* (Fz, Cz, Pz, Oz) and *condition* (BL, SD, NP) revealed a significant interaction in the following frequency bins: 0.5 - 5 Hz, 8.75 - 10.25 Hz, 12.25 - 13.25 Hz, 13.75 - 16.5 Hz, 24 - 24.5 Hz, 24.75 - 25.5 Hz ($p < 0.05$ for each frequency bin, bottom panel of Figure 2). Visual inspection of the curves indicated a prominent spindle peak in the central, parietal and occipital derivation, whereas it was less pronounced in the frontal derivation.

All-night SWA, low- and high spindle frequency activity

EEG power density in the 0.5-5 Hz- (SWA), in the 12.25-13.25 Hz- (low spindle frequency activity, LSFA) and the 13.75-16.5 Hz-range (high spindle frequency activity, HSFA) were each collapsed into bands. The frequency ranges for these bands were chosen based on a significant interaction in the two-way rANOVA with the factors *derivation* and *condition* (see Figure 2). SWA, LSFA and HSFA are plotted for each derivation and night in Figure 3 (panel 1 to 3). A 2-way rANOVA with the factors *derivation* and *condition* was performed and showed a significant interaction of these 2 factors for SWA ($F_{6,54}$=16.22; p<0.01), LSFA ($F_{6,54}$=7.05; p<0.01) and HSFA ($F_{6,54}$=6.47; p<0.01). *SWA:* Post hoc comparisons indicated that SWA significantly decreased from Fz to Cz to Pz to Oz in BL, SD and NP (Figure 3, panel 1; p<0.01, Duncan's multiple range test). Compared to BL, SWA was significantly increased after SD (p<0.01, Duncan's multiple range test) and not significantly changed in NP (p>0.05) for all derivations.

LSFA:

LSFA was significantly enhanced after SD in all derivations (Figure 3, panel 2; p<0.01, Duncan's multiple range test) except for Fz (p=0.77). LSFA after NP showed a significant increase in the more frontal derivations Fz (p<0.01) and Cz (p<0.05), tended to be enhanced in Pz (p=0.09) and was not significantly changed in Oz (p=0.77).

HSFA:

The SD and NP condition elicited opposite effects on HSFA: There was a significant increase during the NP recovery night in Cz and Pz (p<0.01, Duncan's multiple range test) whereas in the SD recovery night HSFA was significantly decreased in Cz

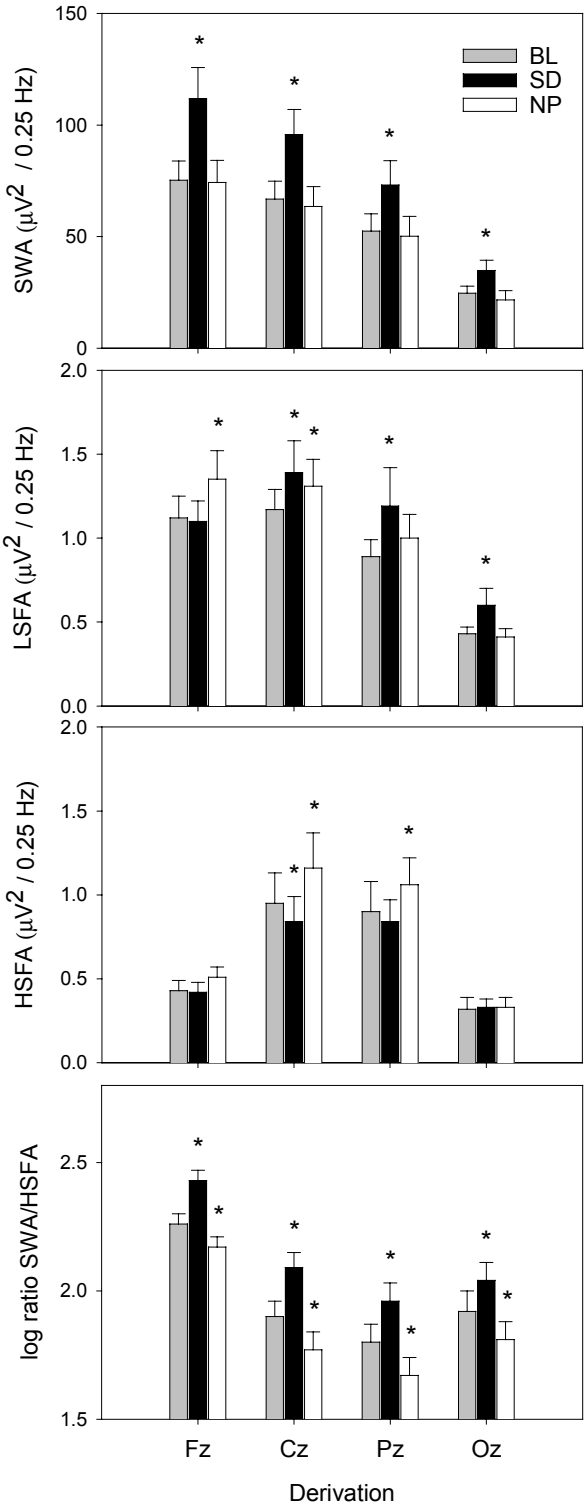

Figure 3. Topographical distribution and effects of SD and NP on selected EEG frequency bands (panel 1 to 4). Values of SWA (0.5-5 Hz), low spindle frequency activity (LSFA, 12.25-13.25 Hz), high spindle frequency activity (HSFA, 13.75-16.5 Hz) and the logarithmic SWA/HSFA ratio for the averaged baseline night (BL, gray bars), the SD- (black bars) and NP (white bars) recovery night are depicted for the midline derivations along the antero-posterior axis (mean ± s.e.m., n=10). Asterisks indicate significant differences to baseline values (p<0.05, Duncan's multiple range test).

(Figure 3, panel 3; $p<0.05$). HSFA in the frontal and occipital derivation was not significantly changed ($p>0.05$).

Topography of LSFA and HSFA:

For analyzing the different topographical distribution of LSFA and HSFA, values in the frontal and central derivation and in the parietal and occipital derivation were added together for LSFA ([Fz+Cz], [Pz+Oz]) and in the frontal and occipital derivation and in the central and parietal derivation for HSFA ([Fz+Oz], [Cz+Pz] (see Methods) HSFA exhibited a centro-parietal dominance in all conditions (Figure 3, panel 3, $p<0.05$, Duncan's multiple range test) and LFSA a fronto-central dominance (Figure 3, panel 2, $p<0.05$, Duncan's multiple range test).

SWA-HSFA Ratio:

The lowest panel in Figure 3 depicts the logarithmic ratio between SWA and HSFA. A 2-way rANOVA with the factors *derivation* and *condition* was performed and showed a significant interaction ($F_{6,54}=6.14$; $p<0.01$). Post-hoc comparisons to baseline showed that the ratio was enhanced in SD and reduced in NP in all derivations ($p<0.05$, Duncan's multiple range test). The ratio significantly decreased from Fz to Cz to Pz and was significantly higher in Oz than in Pz for all conditions.

Time course of relative EEG power density (0.5-25 Hz)

In a next step, EEG power density during NREMS for each frequency bin and derivation in the SD - and NP recovery night was expressed as a percentage of the corresponding value of the averaged baseline night for each 2-h interval (Figure 4). A two-way rANOVA with the factor *condition* (BL, SD, NP) x *time* (interval 1-4) and a paired *t*-test corrected for multiple comparisons (NP vs BL, SD vs BL) was performed for each derivation and frequency bin separately.

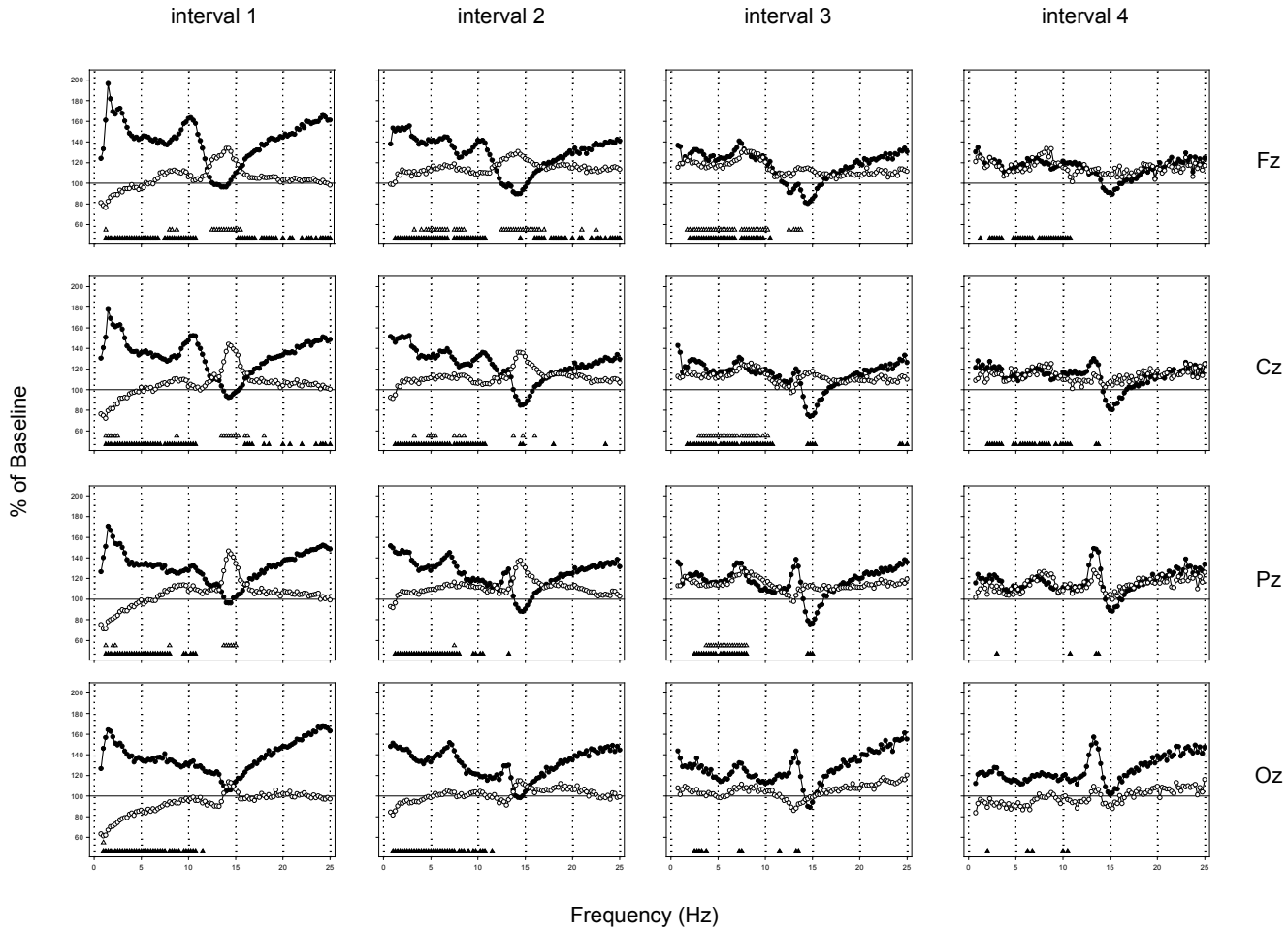

Figure 4. Relative EEG power spectra during NREM sleep in the midline derivations (Fz, Cz, Pz, Oz) for 2-h intervals after sleep onset (mean, n=10). For each frequency bin, values for the SD (●) and the NP (○) recovery night are expressed relative to corresponding values of the averaged baseline night (=100%). Triangles near the abscissa indicate frequency bins for which a significant difference to baseline was found in the SD- (▲) and the NP (Δ) protocol (p<0.05, paired t-test with correction for multiple comparisons)

SD recovery

Slow wave range (0.5-5 Hz):

There was a global increase in NREMS EEG power density over a broad frequency range. The largest increase in the slow wave range occurred in interval 1 (1-5 Hz in Fz, Cz and Pz, 0.75-5 Hz in Oz).

Theta range (5-8 Hz):

EEG power density in the theta range was significantly increased in most of the theta bins in interval 1 and 2 for all derivations, in interval 3 for Fz, Cz, Pz and in interval 4 for Fz and Cz. Some theta bins in interval 3 and 4 for Oz were also significantly increased.

Alpha range (8-12 Hz):

EEG power density was significantly increased in a broad part of the alpha frequency range for all derivations in interval 1 and 2 and in the frontal and central derivation in interval 3 and 4. A distinct peak in relative alpha activity appeared in the first 2 intervals in the frontal and central derivation.

Spindle frequency range (12-16 Hz):

A bimodal pattern emerged in the spindle frequency range. While spindle frequency activity (SFA) was unchanged in interval 1, EEG power density in the upper spindle frequency range was significantly decreased in interval 2 in Fz (14.25-14.5 Hz) and Cz (14.25-14.75 Hz) and in interval 3 in Cz (14.25-15.25 Hz) and Pz (14.25-15 Hz). A distinct peak in relative low spindle frequency activity emerged in Cz, Pz and Oz during intervals 2 - 4. This increase was significant in interval 2 for Pz (13-13.25 Hz), in interval 3 for Oz (13-13.5 Hz) and in interval 4 for Cz and Pz (13.25-13.75 Hz).

Beta range (>16 Hz):

EEG power density between 16.25 and 25 Hz was significantly increased at the beginning of the night in the fronto-central region (in interval 1 in Fz and Cz and in interval 2 in Fz).

NP recovery

Slow wave range (0.5-5 Hz):

EEG power density in the lower slow wave range (0.75 - 2.25 Hz) was significantly decreased in interval 1 in all derivations (Fz: 1-1.25 Hz, Cz: 1-2.5 Hz, Pz: 1-1.25 Hz and 1.75-2.25 Hz, Oz: 0.75-1 Hz). In the intervals 2 - 4, EEG power density in this frequency range was not significantly changed. EEG power density in the higher SW range (> 2.75 Hz) was significantly enhanced in interval 2 in Fz (3-3.25 Hz, 3.75-4 Hz, 4.25-5 Hz) and Cz (3-3.25 Hz, 4.5-5.5 Hz), and in interval 3 in Fz (1.5-5 Hz), Cz (2.75-5 Hz) and Pz (3.5-5 Hz).

Theta range (5-8 Hz):

There was a significant increase in some frequency bins in the theta range in interval 2 (Fz and Cz) and in interval 3 (Fz, Cz and Pz).

Alpha range (8-12 Hz):

EEG power density was significantly increased in some of the bins, particularly in the fronto-central region during interval 3.

Spindle frequency range (12-16 Hz):

EEG power density in the low- and high spindle frequency range showed similar patterns after the NP protocol – either enhanced or unaffected - and did not show the bimodal pattern observed after SD. The increase was significant in interval 1 for Fz (12.25-15.5 Hz), for Cz (13.25-15.25 Hz, 15.75-16.25 Hz) and

for Pz (13.5-15 Hz), in interval 2 for Fz (12.25-16.5 Hz) and Cz (13.5-13.75 Hz, 14.5-14.75 Hz, 15.75-16 Hz) and in interval 3 for Fz (12.25-12.5 Hz, 12.75-13.75 Hz).

Beta range (>16 Hz):

EEG power density above 16 Hz was not significantly affected by the NP for any of the derivations.

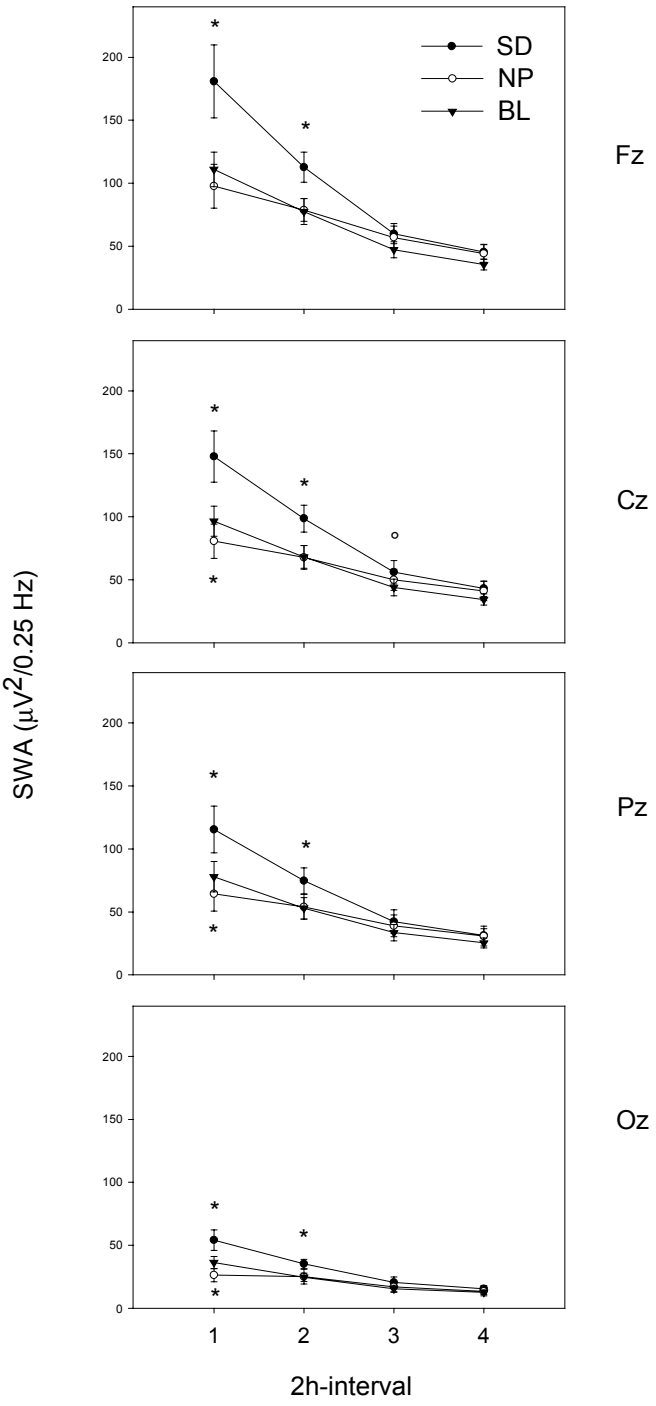

Figure 5. Time course of SWA (0.5-5 Hz) during the averaged baseline night (BL, ▼),the SD (●) and NP (○) recovery night in the midline derivations (Fz, Cz, Pz, Oz; mean ± s.e.m., n=10). Asterisks and open circles indicate differences to corresponding baseline values (*p<0.05, ° p<0.1, Duncan's multiple range test)

Time course of SWA

Figure 5 shows the time course of SWA (0.5-5 Hz) throughout the sleep episodes for each derivation. A 2-way rANOVA with the factors *condition* x *time* (2-h interval 1 – 4) yielded a significant interaction for all derivations (F_6>10; p<0.05). Post-hoc comparisons revealed that during recovery sleep after SD, SWA was significantly enhanced in the 2-h interval 1 and 2 in all derivations (p<0.05, Duncan's multiple range test). In the NP recovery night, SWA was significantly reduced in the first 2-h interval in all derivations except for Fz (Figure 5; p<0.05, Duncan's multiple range test). No significant change was observed in the remaining 2-h intervals.

Post-hoc comparisons indicated that the relative increase of SWA in interval 1 of the SD recovery night was more pronounced in the fronto-central than in the parieto-occipital derivations ([Fz+Cz] > [Pz+Oz]), p<0.05, Duncan's multiple range test), whereas the decrease in the NP recovery night showed a parieto-occipital dominance ([Fz+Cz]<, [Pz+Oz], p<0.05, Duncan's multiple range test).

Discussion

We could confirm that SWA in the range from 0.5 to 5 Hz, and SFA in the high frequency range (13.75-16.5 Hz) are oppositely affected by differential sleep pressure conditions. The homeostatic regulation of SWA and SFA strongly depended on brain location. After high sleep pressure (SD protocol), the rebound in SWA at the beginning of the night yielded a clear fronto-central predominance, whereas the decrease in SWA observed after low sleep pressure (NP protocol) showed a parieto-occipital predominance. Centro-parietal HSFA was enhanced after low sleep pressure and reduced after high sleep pressure. In contrast, low-frequency spindle activity (LSFA) was increased after both manipulations. Therefore, EEG power density within the range of SFA (12-16 Hz) exhibited a dissimilar homeostatic regulation.

Taken together, frontal low EEG activity and centro-parietal high spindle frequency activity were the bands with a clear homeostatic regulation, and therefore

represent two distinct indexes of sleep pressure during human sleep. The balance between these indexes (SWA/HSFA) represents a very sensitive marker of changes in sleep homeostatic pressure.

Slow Wave Activity

The observed increases in SWA after high sleep pressure are in good accordance with previous studies in which the effects of sleep deprivation on EEG power spectra have been quantified (Borbély et al., 1981; Dijk et al. 1993). Furthermore, we could confirm recent reports (Cajochen et al., 1999a; Finelli et al., 2001) that this increase in SWA varies along the antero-posterior axis and shows a fronto-central predominance. The reduction of SWA in the recovery night after the nap protocol, particularly at the beginning of the night, is likely to be a result of the low level of sleep pressure. The observed decrease in SWA, although smaller, is in good accordance with a study in which the duration of prior wakefulness was reduced by a single early evening nap (Werth et al., 1996). The observed changes in SWA confirmed the visually scored SWS findings. Interestingly, the SWA reduction after low sleep pressure did not display the corresponding frontal predominance. It may be that the degree of sleep satiation obtained in the NP protocol was not strong enough to elicit regional differences. However, the occipital predominance in the SWA response after low sleep pressure may not support this hypothesis. Another explanation may be that frontal cortical areas of the brain are particularly affected by sleep deprivation, whereas after sleep satiation, the negative rebound in SWA is not confined to frontal brain areas, and rather manifests itself in more occipital brain regions. In other words, challenging the sleep homeostat by an extension of wakefulness elicits ‘frontal deactivation’, whereas challenging the sleep homeostat by a reduction of wakefulness does not result in ‘frontal activation’. PET studies have demonstrated that the decline of regional cerebral blood flow (rCBF) during SWS is most prominent in frontal cortical areas (Maquet et al., 1997; Hofle et al., 1997), and rCBF in the anterior cingulate and orbitofrontal cortex are negatively correlated with EEG SWA during sleep (Hofle et al., 1997). Nevertheless, how the frontal rCBF decline during slow wave sleep is associated with the homeostatic regulation of SWS remains to be elucidated.

Spindle Frequency Activity

Previous studies have suggested that spindle frequency activity, particularly in the high frequency range, may be under homeostatic control (Borbély et al., 1981; Dijk et al., 1987; Aeschbach and Borbély, 1993; Dijk et al., 1993). Our present results are in accordance with this hypothesis. The reduction of high spindle frequency activity (HSFA) after sleep deprivation was rather small. However, the negative peak in the shape of the generally enhanced relative spectra was outstanding. Besides the differential qualitative response of SWA and HSFA to high sleep pressure, the time course was also different. The increase of power density in the SWA range was most salient in the first 2-h interval and dissipated thereafter. The reduction in the HSFA range, on the other hand, only became evident after the second 2-h interval. This delayed response to sleep deprivation in the high spindle frequency range has also previously been described (Borbély et al., 1981; Dijk et al., 1993).

After the nap protocol, when sleep pressure was low, HSFA increased markedly. This increase peaked in, but was not limited to the high-frequency range, as it was for the decrease after sleep deprivation, but also covered the lower sigma frequency range. There is evidence in the literature that homeostatic regulation may be weaker for LSFA than for HSFA. LSFA did not increase with time awake in a nap study, as did HSFA (Dijk et al., 1987; Dijk et al., 1993). The results of an increase limited to the high SF range (13.25-15 Hz) in the course of a nocturnal sleep episode (Aeschbach and Borbély, 1993) would fit the idea that the same underlying process is present within a sleep episode (Borbély et al., 1981). However, in a forced desynchrony study where sleep occurred at all circadian phases, low-, intermediate-, and high-frequency SFA all increased with the progression of sleep which would rather suggest homeostatic control of LSFA (Dijk et al., 1997). Here we report for the first time a dissimilar homeostatic regulation of LSFA and HSFA after sleep loss.

Furthermore, we could show that the effects of differential levels of sleep pressure on SFA depend on brain location. We found the previously reported centro-parietal dominance of HSFA (Jankel and Niedermeyer, 1985; Jobert et al., 1992; Zeitlhofer et al., 1997) and could show that here, HSFA was sensitive to different levels of sleep pressure, but not in the frontal and occipital derivation. Our data confirm analyses of scalp-recorded sleep spindles with topographically distinct slow- and fast-spindle waves (Gibbs and Gibbs, 1950; Scheuler et al., 1990; Jobert et al., 1992; Werth et al., 1997; Zeitlhofer et al., 1997; Zygierewicz et al., 1999).

Theta and alpha activity

EEG theta and alpha activity was significantly increased after the nap protocol, an effect usually seen after sleep deprivation, when sleep pressure is enhanced. The decrease of SWS and SWA at the beginning of the recovery night indicates that the subjects were indeed sleep satiated at the end of the nap schedule. The extent of this sleep satiation was, however, less pronounced than the extent of the 40-h sleep deprivation compared to baseline (note: TST was not significantly enhanced in the nap protocol compared to baseline conditions, and the reduced sleep pressure at the beginning of the recovery night may be due to the higher level of accumulated SWS and the short duration of wakefulness prior to sleep). When sleep pressure was considerably diminished by an evening nap, theta and alpha activity was reduced in the first two NREM sleep episodes during post-nap nocturnal sleep (Werth et al., 1996). This reduction in theta and alpha activity was not found after our NP protocol. However, the increase of EEG activity in these frequency bands was hardly present in the nonREM spectrum during the first 2-h interval, emerged slightly in interval 2 and more prominently in interval 3. This indicates that after an initial reduction of sleep pressure, there might have been an intra-night build-up of sleep pressure which led to a partial increase of EEG activity in the theta-, alpha- and slow wave range in the latter part of the night.

Conclusion

Topographic analyses of the sleep EEG along the antero-posterior axis on the effects of differential sleep pressure revealed brain locations which are highly responsive to the process of homeostatic sleep regulation in a frequency-specific manner. Frontal regions of the brain show strong homeostatic control in the SWA range of the EEG, central-parietal brain regions in the high spindle frequency range. These data further support the idea that some aspects of human sleep may be local in nature as was previously demonstrated in animals (Oleksenko et al., 1992; Pigarev et al., 1997). Studies both in humans (Kattler et al.,1994) and rats (Vyazovskiy et al., 2000) where local cortical activation during wakefulness resulted in a local response in the EEG power density in the corresponding area during subsequent NREM sleep imply that the human sleep EEG exhibits use dependent characteristics as hypothesized by Krueger and Obal (Krueger and Obal, 1993). Further studies are needed to firmly

establish whether the observed local differences in SWA and HSFA in response to differential sleep pressure are related to use-dependent phenomena.

Acknowledgments

We thank Giovanni Balestrieri and Marie-France Dattler for their help in data acquisition, Drs. Alexander Rösler and Tobias Müller for medical screening, and the subjects for participating. This research was supported by Swiss National Foundation Grants START # 3130-054991.98 and #3100-055385.98 to CC.

References

Aeschbach D, Borbély AA. All-night dynamics of the human sleep EEG. J Sleep Res 1993; 2: 70-81.

Aeschbach D, Dijk DJ, Borbély AA. Dynamics of EEG spindle frequency activity during extended sleep in humans: relationship to slow-wave activity and time of day. Brain Res 1997; 748: 131-136.

Borbély AA, Baumann F, Brandeis D, Strauch I, Lehmann D. Sleep deprivation: effect on sleep stages and EEG power density in man. Electroencephalogr Clin Neurophysiol 1981; 51: 483-495.

Borbély AA, Mattmann P, Loepfe M, Strauch I, Lehmann D. Effect of benzodiazepine hypnotics on all-night sleep EEG spectra. Human Neurobiol 1985; 4: 189-194.

Brunner DP, Dijk DJ, Münch M, Borbèly AA. Effect of zolpidem on sleep and sleep EEG spectra in healthy young men. Psychopharmacology 1991; 104: 1-5.

Cajochen C, Foy R, Dijk DJ. Frontal predominance of a relative increase in sleep delta and theta EEG activity after sleep loss in humans. Sleep Res Online 1999a; 2: 65-69.

Cajochen C, Khalsa SBS, Wyatt JK, Czeisler CA, Dijk DJ. EEG and ocular correlates of circadian melatonin phase and human performance decrements during sleep loss. Am J Physiol Regulatory Integrative Comp Physiol 1999b; 277: R640-R649.

Cajochen C, Knoblauch V, Kräuchi K, Renz C, Wirz-Justice A. Dynamics of frontal EEG activity, sleepiness and body temperature under high and low sleep pressure. NeuroReport 2001; 12: 2277-2281.

Curran-Everett D. Multiple comparisons: philosophies and illustrations. Am J Physiol Regul Integr Comp Physiol 2000; 279: R1-R8.

Daan S, Beersma DGM, Borbély AA. Timing of human sleep: recovery process gated by a circadian pacemaker. Am J Physiol Regulatory Integrative Comp Physiol 1984; 246: R161-R183.

Dijk DJ, Beersma DGM, Daan S. EEG power density during nap sleep: reflection of an hourglass measuring the duration of prior wakefulness. J Biol Rhythms 1987; 2: 207-219.

Dijk DJ, Czeisler CA. Contribution of the circadian pacemaker and the sleep homeostat to sleep propensity, sleep structure, electroencephalographic slow waves, and sleep spindle activity in humans. J Neurosci 1995; 15: 3526-3538.

Dijk DJ, Hayes B, Czeisler CA. Dynamics of electroencephalographic sleep spindles and slow wave activity in men: effect of sleep deprivation. Brain Res 1993; 626: 190-199.

Dijk DJ, Shanahan TL, Duffy JF, Ronda JM, Czeisler CA. Variation of electroencephalographic activity during non-rapid eye movement and rapid eye movement sleep with phase of circadian melatonin rhythm in humans. J Physiol 1997; 505: 851-858.

Finelli LA, Borbély AA, Achermann P. Functional topography of the human nonREM sleep electroencephalogram. Eur J Neurosci 2001; 13: 2282-2290.

Gibbs FA, Gibbs EL. Atlas of Electroencephalography. Cambridge: Addison-Wesley Press, 1950.

Hofle N, Paus T, Reutens D, Fiset P, Gotman J, Evans AC, et al. Regional cerebral blood flow changes as a function of delta and spindle activity during slow wave sleep in humans. J Neurosci 1997; 17: 4800-4808.

Jankel WR, Niedermeyer E. Sleep spindles. J Clin Neurophysiol 1985; 2: 1-35.

Jobert M, Poiseau E, Jähnig P, Schulz H, Kubicki S. Topographical analysis of sleep spindle activity. Neuropsychobiology 1992; 26: 210-217.

Johnson LC, Hanson K, Bickford RG. Effect of flurazepam on sleep spindles and K-complexes. Electroencephalogr Clin Neurophysiol 1976; 40: 67-77.

Knoblauch V, Kräuchi K, Renz C, Müller T, Wirz-Justice A, Cajochen C. Effect of a 75/150 minute sleep-wake schedule on the accumulation of slow-wave sleep and wakefulness after lights off. Sleep 2001; 24: A194.

Krueger JM, Obal F. A neuronal group theory of sleep function. J Sleep Res 1993; 2: 63-69.

Maquet P, Degueldre C, Delfiore G, Aerts J, Péters JM, Luxen A, et al. Functional neuroanatomy of human slow wave sleep. J Neurosci 1997; 17: 2807-2812.

Mc Cormick D, Bal T. Sleep and arousal: thalamocortical mechanisms. Annu Rev Neurosci 1997; 20: 185-215.

Oleksenko AI, Mukhametov LM, Polyakova IG, Supin AY, Kovalzon VM. Unihemispheric sleep deprivation in bottlenose dolphins. J Sleep Res 1992; 1: 40-44.

Pigarev IN, Nothdurft HC, Kastner S. Evidence for asynchronous development of sleep in cortical areas. Neuro Report 1997; 8: 2557-2560.

Rechtschaffen A, Kales A. A manual of standardized terminology, techniques and scoring system for sleep stages of human subjects. Bethesda, MD: US Dept of Health, Education and Welfare, Public Health Service, 1968.

Scheuler W, Kubicki S, Scholz G, Marquardt J. Two different activities in the sleep spindle frequency band-discrimination based on the topographical distribution

of spectral power and coherence. In: Horne J (Ed), Sleep '90. Pontenagel Press, Bochum, 1990: 13-16.

Steriade M, McCormick DA, Sejnowski TJ. Thalamocortical oscillations in the sleeping and aroused brain. Science 1993; 262: 679-685.

Tobler I, Borbély AA, Groos G. The effect of sleep deprivation on sleep in rats with suprachiasmatic lesions. Neurosci Lett 1983; 21: 49-54.

Torsvall L, Åkerstedt T. A diurnal type scale. Construction, consistency and validation in shift work. Scand J Work Environ Health 1980; 6: 283-290.

Trachsel L, Dijk DJ, Brunner DP, Klene C, Borbély AA. Effect of zopiclone and midazolam on sleep and EEG spectra in a phase-advanced sleep schedule. Neuropsychopharmacology 1990; 3: 11-18.

Uchida S, Maloney T, March JD, Azari R, Feinberg I. Sigma (12-15 Hz) and delta (0.3-3Hz) EEG oscillate reciprocally within NREM sleep. Brain Res Bull 1991; 27: 93-96.

Vyazovskiy V, Borbély AA, Tobler I. Unilateral vibrissae stimulation during waking induces interhemispheric EEG asymmetry during subsequent sleep in the rat. J Sleep Res 2000; 9: 367-371.

Weitzman ED, Czeisler CA, Zimmermann JC, Ronda JM. Timing of REM and stages 3+4 sleep during temporal isolation in man. Sleep 1980; 2: 391-407.

Werth E, Achermann P, Dijk DJ, Borbély AA. Spindle frequency activity in the sleep EEG: individual differences and topographic distribution. Electroencephalogr Clin Neurophysiol 1997; 103: 535-542.

Werth E, Dijk DJ, Achermann P, Borbély AA. Dynamics of the sleep EEG after an early evening nap: experimental data and simulations. Am J Physiol Regulatory Integrative Comp Physiol 1996; 271: 501-510.

Zeitlhofer J, Gruber G, Anderer P, Asenbaum S, Schimicek P, Saletu B. Topographic distribution of sleep spindles in young healthy subjects. J Sleep Res 1997; 6: 149-155.

Zygierewicz J, Blinowska KJ, Durka PJ, Szelenberger W, Niemcewicz S, Androsiuk W. High resolution study of sleep spindles. Clin Neurophysiol 1999; 110: 2136-2147.

Chapter 3

Human sleep spindle characteristics after sleep deprivation

Vera Knoblauch[1], Wim L. J. Martens[2], Anna Wirz-Justice[1] and Christian Cajochen[1]

[1] Centre for Chronobiology, Psychiatric University Clinic, Basel, Switzerland

[2] TEMEC Instruments B.V., KERKRADE, The Netherlands

Published in: Clinical Neurophysiology (2003), 114:2258-67.

Abstract

Sleep spindles (12-15 Hz oscillations) are one of the hallmarks of the electroencephalogram (EEG) during human non-rapid eye movement (non-REM) sleep. The effect of a 40-h sleep deprivation (SD) on spindle characteristics along the antero-posterior axis was investigated. EEGs during non-REM sleep in healthy young volunteers were analyzed with a new method for instantaneous spectral analysis, based on the Fast Time Frequency Transform (FTFT), which yields high-resolution spindle parameters in the combined time and frequency domain. FTFT revealed that after SD, mean spindle amplitude was enhanced, while spindle density was reduced. The reduction in spindle density was most prominent in the frontal derivation (Fz), while spindle amplitude was increased in all derivations except in Fz. Mean spindle frequency and its variability within a spindle were reduced after SD. When analyzed per 0.25-Hz frequency bin, amplitude was increased in the lower spindle frequency range (12-13.75 Hz), whereas density was reduced in the high spindle frequency range (13.5-14.75 Hz). The observed reduction in spindle density after SD confirms the inverse homeostatic relationship between sleep spindles and slow waves whereas the increase in spindle amplitude and the reduction in intra-spindle frequency variability support the hypothesis of a higher level of synchronization in thalamocortical cells when homeostatic sleep pressure is enhanced.

Introduction

Sleep spindles (transient EEG oscillations in the 12-15 Hz range) are, besides slow waves, the hallmarks of the human EEG during non-REM sleep. The mechanism underlying these oscillations depends on the degree of hyperpolarization of thalamocortical cells. At the transition from wakefulness to sleep, the membrane potential of thalamocortical cells undergoes a progressive hyperpolarization, whereby synaptic responsiveness is reduced**,** and the transfer of sensory information is interrupted. When a certain hyperpolarization level is achieved, rhythmic bursts in the frequency range of sleep spindles begin to appear in neurons of the nucleus reticularis of the thalamus. These oscillations are transferred to other nuclei within the thalamus and, via thalamocortical projections, to cortical cells. Further hyperpolarization of the membrane potentials leads to oscillations in the frequency range of slow waves. The sum of these oscillations at the cortical surface is represented as sleep spindles and slow waves in the macroscopic EEG (for a review see Steriade et al., 1993; Amzica and Steriade, 1998).

Spectral analysis of the non-REM sleep EEG by means of Fast Fourier Transform (FFT) revealed frequency-specific modulation of spindle frequency activity depending on circadian phase (Dijk et al., 1997; Knoblauch et al., 2003), homeostatic sleep pressure (Borbély et al., 1981; Dijk et al., 1987; Dijk et al., 1993; Knoblauch et al., 2002), pharmacological intervention (Borbély et al., 1985; Trachsel et al., 1990; Brunner et al., 1991), and the scalp location of EEG leads (Scheuler et al., 1990; Werth et al., 1997). Here, we focus on the effect of enhanced homeostatic sleep pressure after sleep deprivation (SD) on spindle frequency activity and characteristics along the antero-posterior axis. In previous reports, spindle frequency activity was reduced in the recovery night after SD (Borbély et al., 1981; Dijk et al., 1993; Knoblauch et al., 2002) and exhibited an increasing trend across non-REM sleep episodes in the course of a night (Dijk et al., 1993; Aeschbach and Borbély, 1993; Werth et al., 1997). These results indicate an inverse homeostatic regulation of slow wave- and spindle activity. The reduction of spindle frequency activity after SD was limited to the higher spindle frequency range, whereas power density in the lower spindle frequency range was not significantly affected (Borbély et al., 1981; Dijk et al., 1993) or enhanced (Knoblauch et al., 2002). It is not known whether this

frequency-specific effect in the power spectra is caused by a general slowing in the spindle frequency range, which would shift the spindle frequency peak towards lower frequencies, or if it represents a frequency-specific change in the amplitude, i.e. an increase in the amplitude of low-frequency spindles and a decrease in the amplitude of high-frequency spindles. These questions cannot be fully answered by spectral analysis since spectral components over the considered time-window are averaged and therefore, the mean amplitude and the number of waves within the time-window cannot be segregated. Moreover, spectral analysis does not separate synchronized spindle activity from background activity in the same frequency band.

To answer these questions, data from a 40-h sleep deprivation experiment, from which FFT results from the first 10 subjects have previously been reported (Knoblauch et al., 2002), were re-analyzed with a new method, the Fast Time Frequency Transform (FTFT). This method discriminates synchronized activity from background noise and calculates amplitude and incidence of synchronized spindle frequency activity with a high frequency (0.25 Hz)- and temporal (0.125 s)-resolution, as well as yielding a series of other spindle parameters. The aim of the present analysis was to separate and quantify the relative contribution of spindle amplitude, frequency, incidence and duration to the change in EEG power spectra after SD.

The impact of SD on sleep spindles has been studied before using methods other than spectral analysis. Spindle density, detected visually (De Gennaro et al., 2000a) or by transient pattern recognition (Dijk et al., 1993), was reduced after SD. The latter method calculated a number of other spindle parameters and revealed no significant change in spindle amplitude and frequency after sleep deprivation. In contrast to these studies, we report regional differences in spindle incidence and amplitude after SD on a high frequency (0.25 Hz)- and time (0.125 s)-resolution.

Methods

Study participants

Sixteen healthy volunteers (8 female, 8 male, age range 20-31 years, mean: 25.3 ± 0.9 s.e.m.) participated in the study. All participants were non-smokers, free from medical, psychiatric and sleep disorders as assessed by screening questionnaires, a

physical examination and a polysomnographically recorded screening night. Drug-free status was verified via urinary toxicologic analysis. Female participants were studied during the follicular phase of their menstrual cycle; four of them used oral contraceptives. All participants gave signed informed consent. The study protocol, screening questionnaires and consent form were approved by the local Ethical Committee, and all procedures conformed with the Declaration of Helsinki.

Study design

The entire study comprised two protocol blocks, a sleep-deprivation (SD) and a nap block, in a balanced crossover design with an off-protocol episode of 2-4 weeks in between. Here, we report data from the SD block; data from the nap block have been published elsewhere (Knoblauch et al., 2002; Knoblauch et al., 2003). Volunteers reported to the laboratory in the evening and spent an 8-h night at their habitual bedtime. The timing of their sleep-wake schedule was calculated such that the 8-h sleep episode was centered at the midpoint of each volunteer's habitual sleep episode as assessed by actigraphy during the baseline week. After a second 8-h sleep episode (baseline night) at their habitual bedtime, either a 40-h sleep deprivation (under constant routine conditions) or a 40-h multiple nap protocol was carried out (for details see Cajochen et al., 2001). Each study block ended with an 8-h recovery sleep episode starting again at habitual bedtime.

Sleep recordings and analysis

Sleep was recorded polysomnographically using the VITAPORT digital ambulatory sleep recorder (Vitaport-3 digital recorder, TEMEC Instruments B.V., Kerkrade, The Netherlands). Twelve EEGs, two electrooculograms (EOG), one submental electromyogram (EMG) and one electrocardiogram (ECG) signal were recorded. All signals were filtered at 30 Hz (4th order Bessel type anti-aliasing low-pass filter, total 24 dB/Oct.), and a time constant of 1.0 s was used prior to on-line digitization (range 610 μV, 12 bit AD converter, 0.15 μV/bit; sampling rate at 128 Hz for the EEG). The raw signals were stored on-line on a Flash RAM Card (Viking, USA) and downloaded off-line to a PC hard drive. Sleep stages were visually scored on a 20-s basis (Vitaport Paperless Sleep Scoring Software) from the C3 derivation according to standard criteria (Rechtschaffen and Kales, 1968).

EEG spectral analysis

EEGs were subjected to spectral analysis using a fast Fourier transform (FFT, 10% cosine 4-s window) resulting in a 0.25 Hz bin resolution. EEG artifacts were detected by an automated artifact detection algorithm. This algorithm was based on a instantaneous frequency analysis, which yields the amplitude-envelope and the frequency of 8 band-filtered components instantaneously at a rate of 8 per second. Low-frequency (as movement) artifacts, mid-frequency (as ECG interference) and high-frequency (as EMG) artifacts are detected individually if the respective instantaneous frequencies and amplitudes in the relevant frequency bands are not within preset ranges(CASA, 2000 Phy Vision B.V., Kerkrade, The Netherlands). For final data reduction, the artifact-free 4-s epochs were averaged over 20-s epochs.

EEG power spectra were calculated during non-REM sleep in the frequency range between 0.5 and 32 Hz from the midline derivations (Fz, Cz, Pz, Oz) referenced against linked mastoids (A1, A2). Over the range of 0.5-25 Hz, mean EEG spectra averaged over the entire group of 16 participants were very similar to those of the first 10 participants previously published (Knoblauch et al., 2002).

Instantaneous spectral analysis of the EEG

The same digitized EEGs were subjected to instantaneous spectral analysis using the Fast Time Frequency Transform (FTFT; Martens, 1992). For the EEG, the FTFT calculates instantaneous amplitude, frequency and bandwidth in 8 frequency bands from 0–4 Hz, 4–8 Hz, …. 28–32 Hz. Instantaneous bandwidth is computed from the instantaneous frequency as the rectified first derivative with respect to time. Therefore, the higher the frequency variability, the higher the bandwidth. Based on the 4 Hz range of the filters, the temporal resolution of the above parameters is 0.125 s. Over a moving template of 1-s duration, thresholds are applied to amplitude, frequency and bandwidth parameters to differentiate synchronized activity from ongoing noise as well as to remove artifacts (Martens, 1999). The thresholds were determined empirically on a learning-set of EEG recordings to yield the closest possible agreement with visual scores. Incorporating the instantaneous bandwidth helped to achieve a closer agreement than using only an amplitude threshold. Finally, the optimized settings from the learning set were applied to this data set, focusing on detected synchronized spindle activity. Spindles were detected from the outcome of the 8 - 12 Hz and 12 - 16 Hz frequency band, but the frequency and

bandwidth threshold for spindle detection was limited to the range of 11 - 16 Hz. These thresholds again were determined empirically and compared with visual scores. Furthermore, a duration limit (≥ 0.5 s and ≤ 2s) was applied to detected spindles. As a result, we obtained the amplitude and frequency of each individual spindle at a time-resolution of 0.125 s and a frequency resolution of 0.25 Hz. In other words, for each 0.25 Hz frequency bin between 11 and 16 Hz, the time incidence (corresponds to the number of 0.125-s epochs within the given frequency bin) and the amplitude in these 0.125-s epochs was calculated. A further parameter was spindle density (number of sleep spindles / 20-s epoch). Finally, for each individual spindle, the following parameters were computed: duration, mean frequency, mean amplitude, and standard deviation of frequency.

Statistics

The statistical packages SAS ® (SAS® Institute Inc., Cary, North Carolina, USA, Version 6.12) and Statistica® (StatSoft Inc. 2000. STATISTICA for Windows, Tulsa, Oklahoma, USA) were used. One-, two- and three-way analysis of variance for repeated measures (rANOVA) were performed between the factors 'derivation' (Fz, Cz, Pz, Oz), 'night' (baseline, recovery), 'frequency bin' (12-15.5 Hz), and 'non-REM sleep episode' (non-REM sleep episode 1 to 4). All *p* values derived from rANOVAs were based on Huynh-Feldt's (H-F) corrected degrees of freedom, but the original degrees of freedom are reported. For *post-hoc* comparisons, the Duncan's multiple range test was used.

One subject was excluded from time course analysis because EEG recordings during non-REM sleep episode 3 and 4 contained considerable artifacts.

For EEG power density, spindle amplitude per 0.25 Hz and time incidence per 0.25 Hz in the range between 11-16 Hz (Figure 1), a three-way rANOVA with the factors 'derivation', 'night' and 'frequency bin' was performed and yielded a significant interaction between these three factors for EEG power density and time incidence, but not for amplitude. The non-significant interaction for spindle amplitude was presumably due to the prominent peak around 11.25-11.5 Hz. Because of the relatively broad frequency range for spindle detection (11-16 Hz) in the present analysis, this peak probably came about by short alpha intrusions. The rANOVA was therefore limited to a more restricted frequency range, between 12-15.5 Hz.

Table 1. Sleep variables derived from visual scoring for the baseline and recovery night (mean ± s.e.m., n=16).

Baseline	**Recovery**		
TST (min)	438.13 ± 7.17	458.79 ± 3.38	**
SE (%)	91.31 ± 1.50	95.72 ± 0.69	**
% MT	3.04 ± 0.39	2.53 ± 0.42	**
% WALO	6.94 ± 1.68	2.19 ± 0.54	**
% stage 1	12.55 ± 1.41	6.50 ± 0.77	**
% stage 2	50.25 ± 1.33	46.53 ± 1.19	**
% stage 3	10.34 ± 0.65	13.66 ±1.24	*
% stage 4	6.88 ± 1.46	14.27 ± 2.04	**
% SWS	17.22 ± 1.65	27.93 ± 1.59	**
% non-REM sleep	67.48 ± 1.50	74.45 ± 1.09	**
% REM sleep	19.97 ± 1.03	19.06 ± 1.22	
SL1 (min)	10.23 ± 2.25	3.94 ± 0.59	**
SL2 (min)	15.19 ± 2.33	6.33 ± 0.75	**
RL (min)	78.88 ± 5.95	73.60 ± 8.69	

Sleep stages are expressed as percent of total sleep time. TST = total sleep time (stage 1-4 + REM sleep), SE = sleep efficiency [(TST/time in bed)*100], MT = movement time, WALO = wakefulness after lights off, SL1 = latency to stage one (min), SL2 = latency to stage two (min), RL = latency to REM sleep (min). For SL1, SL2 and RL, statistics were applied on log-transformed values. Asterisks indicate significant differences between the baseline and recovery night (*p<0.05, ** p<0.01, one-way rANOVA).

Table 2. Three-way rANOVA with the factors derivation (D), night (N) and frequency bin (FB) for EEG power density, spindle amplitude and time incidence per 0.25 Hz frequency bin from 12-15.5 Hz (F; *p*).

		FFT power spectra		FTFT amplitude		FTFT time incidence	
Derivation	$F_{3,45}$	70.0;	<0.001	67.8;	<0.001	35.6;	<0.001
Night	$F_{1,15}$	8.5;	<0.05	7.3;	<0.05	28.9;	<0.001
Frequency bin	$F_{13,195}$	42.4	<0.001	42.9;	<0.001	23.3;	<0.001
D x N	$F_{3,45}$	6.6;	<0.01	6.1;	<0.01	3.4;	<0.05
D x FB	$F_{39,585}$	38.7;	<0.001	32.6;	<0.001	15.8;	<0.001
N x FB	$F_{13,195}$	2.1;	0.15	1.7;	0.20	2.6;	0.11
D x N x FB	$F_{39,585}$	7.7;	<0.001	1.9;	<0.05	3.0;	<0.05

For EEG power density and spindle amplitude, statistics were performed on log transformed values.

Results

Visual scoring

Table 1 summarizes sleep variables derived from visual scoring for the baseline night and the recovery night after SD. All variables differed significantly between the baseline and recovery night, except for REM sleep duration (percent of total sleep time) and latency to REM sleep (log-transformed; for statistics see Table 1).

EEG power density, spindle amplitude and time incidence per 0.25 Hz bin

In Figure 1, EEG power density derived from spectral analysis (top panels) is illustrated along with the results from the FTFT, i.e. spindle amplitude and time incidence per 0.25 Hz bin (middle and bottom panels, respectively), from the midline

derivations during baseline and recovery sleep. Values are depicted from 11 to 16 Hz, statistics was performed on the 12-15.5 Hz range (see Methods). A three-way rANOVA with the factors 'derivation', 'night' and 'frequency bin' yielded a significant interaction between these three factors for EEG power density, amplitude, and time incidence (for statistics see Table 2).

Spectral analysis (FFT): EEG power density

EEG power density was significantly increased after SD in the lower spindle frequency range in Cz (12-12.25 Hz, 12.5–13.75 Hz), Pz (12.25-13.75 Hz), and Oz (12-13.75 Hz; Figure 1, top panels; $p<0.05$, Duncan's multiple range test on log-transformed values), whereas for Fz no such difference in the 12-15.5 Hz range was found (Figure 1, top left hand panel).

Instantaneous frequency analysis (FTFT):

Amplitude per 0.25 Hz frequency bin

Similar to EEG power density, the amplitude of synchronized spindle frequency activity per 0.25 Hz bin was increased in the low- and middle spindle frequency range after SD in Cz, Pz and Oz, but not in Fz (Figure 1, middle panels). The increase was significant between 12.75 and 13.75 Hz in Cz, between 12 and 13.5 Hz in Pz and between 12.25 and 13 Hz and 13.25 and 13.75 Hz in Oz ($p<0.05$, Duncan's multiple range test on log-transformed values). In addition, there was another prominent peak in the very low frequency range, between 11.25 and 11.5 Hz.

Time incidence per 0.25 Hz frequency bin

In contrast to EEG power density and spindle amplitude, time incidence per 0.25 Hz bin in Cz, Pz and Oz was significantly reduced in the higher spindle frequency range after SD, and not significantly changed in the lower spindle frequency range (Figure 1, bottom panels). The reduction was significant between 13.5 and 14.75 Hz in Cz, between 13.75 and 14.5 Hz in Pz, and between 13.5 and 14.25 Hz in Oz ($p<0.05$, Duncan's multiple range test). Time incidence in the lower and middle frequency range (up to 13.5 Hz) was not significantly changed in these derivations. In Fz, time incidence was reduced over a broader frequency range (significant between 12.5 and 14.75 Hz).

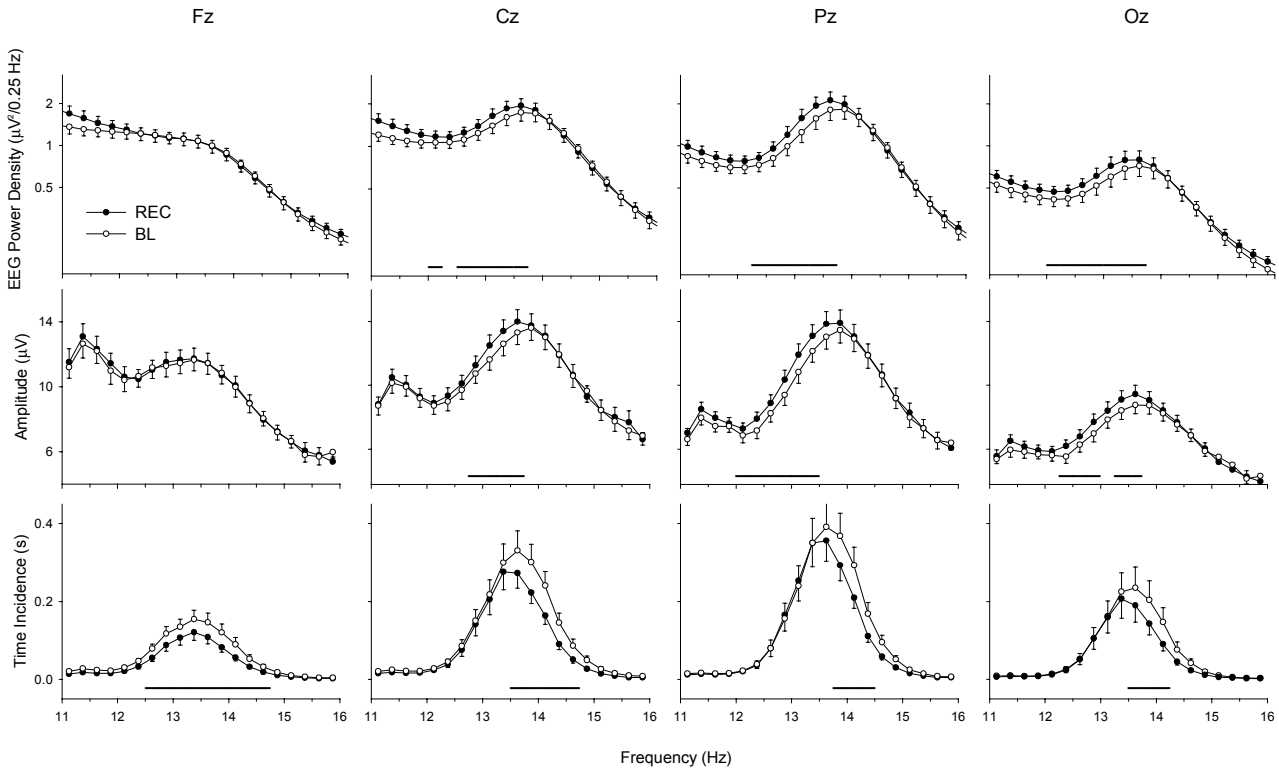

Figure 1. EEG power density (from FFT, top panels), amplitude (from FTFT, middle panels) and frequency incidence (from FTFT, bottom panels) per 0.25-Hz bin between 11 and 16 Hz for the midline derivations (Fz, Cz, Pz, Oz) during baseline night (BL, ○) and recovery night after SD (REC, ●) (mean ± s.e.m.; n=16). Horizontal lines near the abscissa indicate frequency bins for which a significant difference between BL and REC was found (p<0.05, Duncan's multiple test).

Spindle parameters

In a next step, spindle density (number per 20-s epoch), amplitude, frequency, duration, and intra-spindle frequency variability (standard deviation of intra-spindle frequency) were calculated (Figure 2). A two-way rANOVA with the factors 'derivation' and 'night' was performed and revealed a significant effect of 'derivation' for all parameters, and a significant effect of 'night' for all parameters except for spindle duration (p=0.07). The interaction between 'derivation' and 'night' was significant for spindle density, amplitude, frequency, and intra-spindle frequency variability (p<0.05; two-way rANOVA). For those parameters with a significant interaction, *post hoc* comparison between baseline and recovery night revealed that in the recovery night, spindle density, spindle frequency, and intra-spindle frequency variability were significantly reduced in all four derivations, whereas spindle amplitude was significantly increased in all derivations except in Fz (p<0.05; Duncan's multiple range test). In both nights, spindle density and amplitude were highest in Cz and Pz. Additionally, spindle density was significantly higher in Pz than in Cz in both nights, and spindle amplitude was significantly higher in Pz than in Cz in the recovery night, but not in the baseline night. In both nights, spindle frequency significantly increased from Fz to Cz to Pz and significantly decreased to Oz, and intra-spindle frequency variability significantly decreased from Fz to Cz to Pz, and significantly increased from Pz to Oz (p<0.05; Duncan's multiple range test).

For spindle duration, the interaction between the factors 'derivation' and 'night' was not significant. When averaged across derivations, a one-way rANOVA with the factor 'night' revealed that spindle duration tended to be longer in the recovery night than in the baseline night (p=0.07, one-way rANOVA).

Dynamics of spindle parameters across non-REM sleep episodes

The same spindle parameters were calculated per non-REM sleep episodes (Figure 3). A three-way rANOVA with the factor 'derivation', 'night' and 'non-REM sleep episode' revealed no significant interaction between these three factors except for spindle density ($F[9,126]=3.54$; p=0.002). For sake of clarity, only data from Fz and Pz are reported in the following.

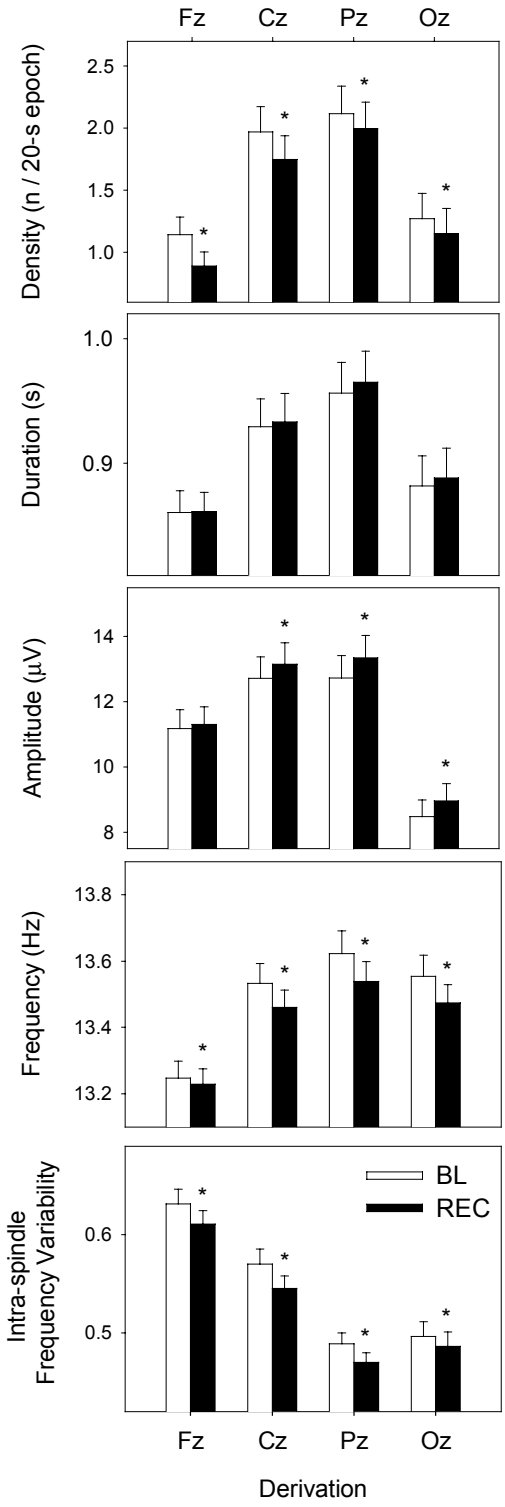

Figure 2. Mean density (number of sleep spindles per 20-s epoch), frequency, duration, amplitude, and intra-spindle frequency variability (standard deviation of intra-spindle frequency) of sleep spindles along the midline during baseline night (BL, white bars) and recovery night after SD (REC, black bars) (mean ± s.e.m.; n=16). Asterisks indicate a significant difference between BL and REC (p<0.05; one-way rANOVA).

Baseline night:

A one-way rANOVA with the factor 'non-REM sleep episode' was performed on these parameters during the baseline night for Fz and Pz separately. All parameters derived from Pz varied significantly across non-REM sleep episodes (F[3,42] at least .>9; *p* at least <0.001). In Pz, spindle density and duration progressively rose over consecutive sleep episodes ($p<0.05$; Duncan's multiple range test), and also spindle amplitude exhibited an increasing trend. An orthogonal-polynomial rANOVA yielded a significant linear component for the above parameters (*p* at least <0.0001). This linear increase was significant between non-REM sleep episode 1 and 2 and between non-REM sleep episode 2 and 4. Spindle frequency showed a U-shaped time course, which was corroborated by a significant quadratic component in the rANOVA ($F[1,14]=40.5$, $p<0.0001$). It significantly decreased from a highest level in non-REM episode 1 to non-REM episode 2 and increased from non-REM episode 3 to 4. Intra-spindle frequency variability was highest at the beginning of the night and significantly declined from episode 1 to 2 ($p<0.05$, Duncan's multiple range test), and both a significant linear and quadratic component were present (*p* at least < 0.001). In contrast to Pz, spindle amplitude and spindle frequency in Fz remained fairly stable and did not show a significant variation across non-REM sleep episodes (*p* at least > 0.16). The other spindle parameters such as spindle density, duration and intra-spindle frequency variability showed similar time courses in Fz as for Pz, but on different absolute levels (compare left and right-hand side panels in figure 3).

Effect of SD:

To assess whether the time course of spindle parameters in Fz and Pz were changed after SD, a two-way rANOVA with the factors 'non-REM sleep episode' and 'night' was performed for Fz and Pz separately. For Pz, the factor 'non-REM sleep episode' was significant for all parameters ($p<0.05$). The interaction between factors 'non-REM sleep episode' and 'night' was significant for spindle density ($p<0.05$) and tended to be significant for intra-spindle frequency variability ($p<0.06$, two-way rANOVA; Figure 3), indicating that SD affected the time course of these parameters. Post hoc comparison revealed that compared to the baseline night, spindle density in the recovery night was significantly reduced in episode 1 and 2 ($p<0.05$) and tended to be reduced in episode 3 ($p=0.06$; Duncan's multiple range test). There was no significant interaction between 'night' and 'non-REM sleep episode' for the other

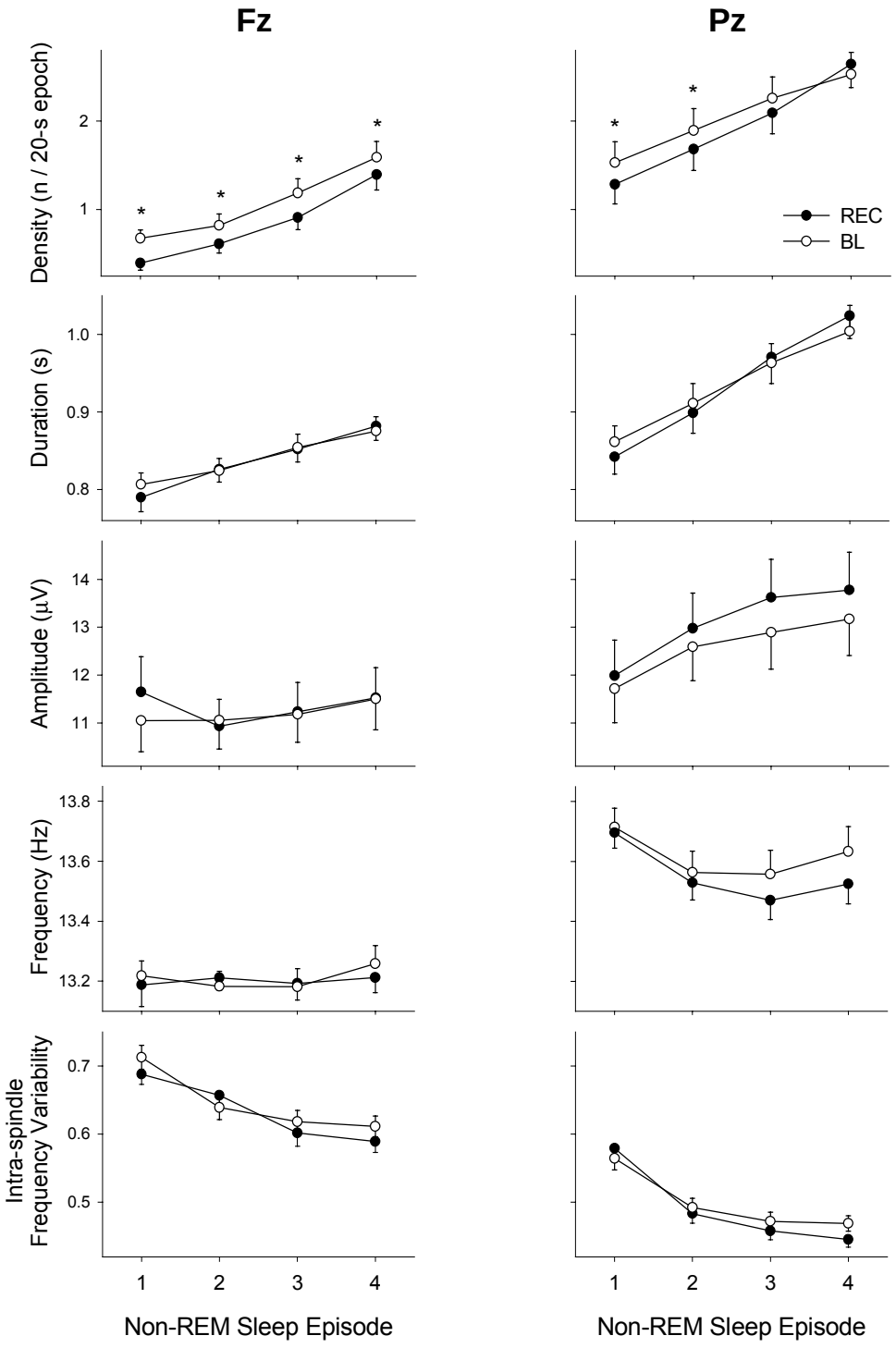

Figure 3. Mean spindle density (number of sleep spindles per 20-s epoch), frequency, duration, amplitude, and intra-spindle frequency variability (standard deviation of intra-spindle frequency) in Fz and Pz during non-REM sleep episodes of the baseline (BL, ○) and recovery night (REC, ●) (mean ± s.e.m.; n=15). Asterisks indicate significant differences to corresponding baseline values (p<0.05, Duncan's multiple range test).

parameters. The factor ‘non-REM sleep episode’ yielded a significant main effect on all spindle parameters derived from Pz. For none of the parameters derived from Fz a significant interaction between the factors ‘non-REM sleep episode’ and ‘night’ was found (p at least >0.1). This indicates that, in contrast to Pz, the time course of spindle parameters derived from Fz was not significantly affected by SD. There was only a significant main effect of the factor ‘night’ for sleep spindle density, and a significant main effect of the factor ‘non-REM episode’ for spindle density, spindle duration and intra-spindle variability.

Discussion

The present data confirm and further extend that sleep spindle characteristics are significantly affected by the sleep homeostat. High resolution analysis of spindle amplitude per 0.25 Hz bin revealed that the amplitude of sleep spindles was enhanced in the lower spindle frequency range and not affected in the high frequency range in the recovery night after SD. In contrast, the incidence of sleep spindle activity per 0.25 Hz was reduced in the high spindle frequency range, and unchanged in the lower spindle frequency range. Our results confirm previous reports of reduced sleep spindle density after SD (Dijk et al., 1993; De Gennaro et al., 2000a). In contrast to a previous report which found no change in spindle frequency after SD using an other methodology (Dijk et al., 1993), here spindle frequency was significantly reduced after SD. Within a spindle, frequency variability was reduced after SD, indicating that spindles were more homogenous and stable. The topographical analysis showed that intra-spindle frequency variability was highest in Fz and decreased from Fz to Pz. Since alpha activity exhibits a frontal predominance during non-REM sleep (Finelli et al., 2001b; for a review see Pivik and Harman, 1995), and the relatively broad frequency range for spindle detection (11-16 Hz) in the present analysis partly overlaps with the alpha band, the high frequency variability in Fz was probably due to short alpha intrusions into sleep spindles. The peak between 11.25 and 11.5 Hz in spindle amplitude in Figure 1 (middle panels, spindle amplitude per 0.25 Hz), which was most prominent in Fz, supports this hypothesis.

Also the extent of the SD effect varied between derivations, as indicated by the significant interaction between 'derivation' and 'night' for spindle density, amplitude, frequency, and intra-spindle frequency variability. In particular, the reduction in spindle density was most prominent in Fz, while spindle amplitude was increased in all derivations except in Fz. In view of the mutual exclusivity of spindle and slow wave oscillations on the level of single neurons (Nuñez et al., 1992) and on the level of the EEG (De Gennaro et al., 2000b; Uchida et al., 1991), this finding fits with the frontal predominance of the slow wave activity (SWA, EEG power density in the 0.75-4.5 Hz range) increase after SD (Cajochen et al., 1999).

It has been shown before that frontal spindles have a lower frequency (around 12 Hz) than parietal spindles (around 14 Hz), and these findings were interpreted as indication for the existence of two separate sleep spindles types (Gibbs and Gibbs, 1950; Zeitlhofer et al., 1997; Werth et al., 1997; Zygierewicz et al., 1999; Anderer et al., 2001). Our data do not corroborate such a concept that frontally and parietally scalp-recorded sleep spindles originate from two functionally distinct thalamic sources. We think that differences between frontally and parietally scalp-recorded sleep spindles rather represent a topography-dependent modulation of one single type of spindle oscillations, whose origin can be traced back to the thalamic reticular nucleus from where it disseminates to distant sites within the thalamus.

The reduction in spindle density, most pronounced in the first part of the night, confirms the expected and previously described inverse relationship to slow waves (Borbély et al., 1981; Dijk et al., 1993; Finelli et al., 2001b). This reciprocity between slow waves and sleep spindles is based on their generating mechanism at the cellular level. After sleep onset, the progressive hyperpolarization in thalamic and cortical neurons leads to oscillations in the membrane potential in the frequency range of spindles, and, with further hyperpolarization, in the frequency range of delta waves (for a review see Amzica and Steriade, 1998). When sleep pressure is high, this hyperpolarization seems to proceed faster. The more rapid rise of both spindle and slow wave activity in the first minutes of recovery sleep after SD (Dijk et al., 1993) supports this hypothesis. Since the degree of hyperpolarization is enhanced after SD, more neurons would fire in the delta instead of the spindle mode. This would explain the reduction of spindle density after SD.

The reduction in spindle density is not contradictory to the enhanced spindle amplitude seen after sleep deprivation. The above described oscillations in thalamic

and cortical neurons are only reflected in the scalp-recorded EEG when a large number of neurons synchronously oscillate in these frequency modes. With sleep deepening, larger numbers of neurons are recruited to oscillate in the spindle or delta mode, and their firing activity becomes more synchronized. Thus, while wakefulness is characterized by low-amplitude oscillations of relatively low spatio-temporal coherence, oscillations during sleep exhibit high temporal and spatial correlation across wide regions of the cortex (Sejnowski and Destexhe, 2000). The size of the neuronal population that oscillates in synchrony with a given frequency, is, on the level of the macroscopic EEG, reflected in the amplitude of the wave with this frequency (Amzica and Steriade, 1998). Both the increase of SWA (Borbély et al., 1981; Dijk et al., 1993; Finelli et al., 2001b; Knoblauch et al., 2002) and the here reported increase in spindle amplitude indicate that the recruitment of large neuronal populations and their synchronization is reinforced after SD. The reduction in intra-spindle frequency variability also supports this hypothesis of a higher level of synchronization of thalamic and cortical oscillations under high sleep pressure.

Mean spindle frequency was reduced after SD. Our data indicate that a specific reduction in the incidence of fast spindle components, rather than a uniform slowing of spindles, underlies the frequency reduction. The reduction in the incidence of high-frequency spindle elements calculated by the FTFT was not manifested in the FFT power spectrum. This suggests that the power spectrum mainly represents changes in spindle amplitude, while changes in spindle frequency and incidence are poorly reflected. Additionally, the fact that FFT power spectra include background activity within the spindle frequency range, while spindle FTFT discriminates synchronized spindle activity from background noise, may also contribute to the discrepancy between the results from the two methods.

Taken together, non-REM sleep EEGs from the recovery night after a 40-h sleep deprivation were analyzed with two methods, the classical spectral analysis by means of FFT, and the new instantaneous spectral analysis by means of FTFT. Whereas the effect of SD on EEG power density in the spindle frequency range has been described before (Borbély et al., 1981; Dijk et al., 1993; Finelli et al., 2001a; Knoblauch et al., 2002), the present results from the FTFT provide additional, more detailed information about the changes sleep spindles undergo when homeostatic sleep pressure is enhanced, and thereby contribute to a more comprehensive understanding of the homeostatic regulation of sleep spindles. The increase in

spindle amplitude and the decrease in intra-spindle frequency variability support the hypothesis of a higher degree of synchronization of oscillations in cortico-thalamic circuitries under enhanced sleep pressure.

Acknowledgments

We thank Claudia Renz, Giovanni Balestrieri and Marie-France Dattler for their help in data acquisition, Drs. Alexander Rösler and Tobias Müller for medical screenings, and the subjects for participating. This research was supported by Swiss National Foundation Grants START # 3130-054991.98 and #3100-055385.98 to CC.

References

Aeschbach D, Borbély AA. All-night dynamics of the human sleep EEG. J Sleep Res 1993; 2: 70-81.

Amzica F, Steriade M. Electrophysiological correlates of sleep delta waves. Electroencephalogr Clin Neurophysiol 1998; 107: 69-83.

Anderer P, Klösch G, Gruber G, Trenker E, Pascual-Marqui RD, Zeitlhofer J, et al. Low-resolution brain electromagnetic tomography revealed simultaneously active frontal and parietal sleep spindle sources in the human cortex. Neuroscience 2001; 103: 581-592.

Borbély AA, Baumann F, Brandeis D, Strauch I, Lehmann D. Sleep deprivation: effect on sleep stages and EEG power density in man. Electroencephalogr Clin Neurophysiol 1981; 51: 483-495.

Borbély AA, Mattmann P, Loepfe M, Strauch I, Lehmann D. Effect of benzodiazepine hypnotics on all-night sleep EEG spectra. Human Neurobiol 1985; 4: 189-194.

Brunner DP, Dijk DJ, Münch M, Borbèly AA. Effect of zolpidem on sleep and sleep EEG spectra in healthy young men. Psychopharmacology 1991; 104: 1-5.

Cajochen C, Foy R, Dijk DJ. Frontal predominance of a relative increase in sleep delta and theta EEG activity after sleep loss in humans. Sleep Res Online 1999; 2: 65-69.

Cajochen C, Knoblauch V, Kräuchi K, Renz C, Wirz-Justice A. Dynamics of frontal EEG activity, sleepiness and body temperature under high and low sleep pressure. NeuroReport 2001; 12: 2277-2281.

De Gennaro L, Ferrara M, Bertini M. Effect of slow-wave sleep deprivation on topographical distribution of spindles. Behav Brain Res 2000a; 116: 55-59.

De Gennaro L, Ferrara M, Bertini M. Topographical distribution of spindles: variations between and within NREM sleep cycles. Sleep Res Online 2000b; 3: 155-160.

Dijk DJ, Beersma DGM, Daan S. EEG power density during nap sleep: reflection of an hourglass measuring the duration of prior wakefulness. J Biol Rhythms 1987; 2: 207-219.

Dijk DJ, Hayes B, Czeisler CA. Dynamics of electroencephalographic sleep spindles and slow wave activity in men: effect of sleep deprivation. Brain Res 1993; 626: 190-199.

Dijk DJ, Shanahan TL, Duffy JF, Ronda JM, Czeisler CA. Variation of electroencephalographic activity during non-rapid eye movement and rapid eye movement sleep with phase of circadian melatonin rhythm in humans. J Physiol 1997; 505: 851-858.

Finelli LA, Achermann P, Borbély AA. Individual ' fingerprints ' in human sleep EEG topography. Neuropsychopharmacology 2001a; 25: S57-S62.

Finelli LA, Borbély AA, Achermann P. Functional topography of the human nonREM sleep electroencephalogram. Eur J Neurosci 2001b; 13: 2282-2290.

Gibbs FA, Gibbs EL. Atlas of Electroencephalography. Cambridge: Addison-Wesley Press, 1950.

Knoblauch V, Kräuchi K, Renz C, Wirz-Justice A, Cajochen C. Homeostatic control of slow-wave and spindle frequency activity during human sleep: effect of differential sleep pressure and brain topography. Cereb Cortex 2002; 12: 1092-1100.

Knoblauch V, Martens W, Wirz-Justice A, Kräuchi K, Cajochen C. Regional differences in the circadian modulation of human sleep spindle characteristics. Eur J Neurosci 2003; 18: 155-163.

Martens WLJ. The fast time frequency transform (F.T.F.T.): a novel on-line approach to the instantaneous spectrum. 14th International Conference of the IEEE Engineering in Medicine and Biology Society, Paris 1992.

Martens WLJ. Segmentation of 'rhythmic' and 'noisy' components of sleep EEG, Heart Rate and Respiratory signals based on instantaneous amplitude, frequency, bandwidth and phase. 1st joint BMES / EMBS IEEE Conference, Atlanta 1999.

Nuñez A, Curro Dossi R, Contreras D, Steriade M. Intracellular evidence for incompatibility between spindle and delta oscillations in thalamocortical neurons of cat. Neuroscience 1992; 48: 75-85.

Pivik RT, Harman K. A reconceptualization of EEG alpha activity as an index of arousal during sleep: all alpha activity is not equal. J Sleep Res 1995; 4: 131-137.

Rechtschaffen A, Kales A. A manual of standardized terminology, techniques and scoring system for sleep stages of human subjects. Bethesda, MD: US Dept of Health, Education and Welfare, Public Health Service, 1968.

Scheuler W, Kubicki S, Scholz G, Marquardt J. Two different activities in the sleep spindle frequency band-discrimination based on the topographical distribution of spectral power and coherence. In: Horne J (Ed), Sleep '90. Pontenagel Press, Bochum 1990: 13-16.

Sejnowski TJ, Destexhe A. Why do we sleep? Brain Res 2000; 886: 208-223.

Steriade M, McCormick DA, Sejnowski TJ. Thalamocortical oscillations in the sleeping and aroused brain. Science 1993; 262: 679-685.

Trachsel L, Dijk DJ, Brunner DP, Klene C, Borbély AA. Effect of zopiclone and midazolam on sleep and EEG spectra in a phase-advanced sleep schedule. Neuropsychopharmacology 1990; 3: 11-18.

Uchida S, Maloney T, March JD, Azari R, Feinberg I. Sigma (12-15 Hz) and delta (0.3-3Hz) EEG oscillate reciprocally within NREM sleep. Brain Res Bull 1991; 27: 93-96.

Werth E, Achermann P, Dijk DJ, Borbély AA. Spindle frequency activity in the sleep EEG: individual differences and topographic distribution. Electroencephalogr Clin Neurophysiol 1997; 103: 535-542.

Zeitlhofer J, Gruber G, Anderer P, Asenbaum S, Schimicek P, Saletu B. Topographic distribution of sleep spindles in young healthy subjects. J Sleep Res 1997; 6: 149-155.

Zygierewicz J, Blinowska KJ, Durka PJ, Szelenberger W, Niemcewicz S, Androsiuk W. High resolution study of sleep spindles. Clin Neurophysiol 1999; 110: 2136-2147.

Chapter 4

Regional differences in the circadian modulation of human sleep spindle characteristics

Vera Knoblauch[1], Wim L. J. Martens[2], Anna Wirz-Justice[1], Kurt Kräuchi[1] and Christian Cajochen[1]

[1] Centre for Chronobiology, Psychiatric University Clinic, Basel, Switzerland

[2] TEMEC Instruments B.V., KERKRADE, The Netherlands

Published in: European Journal of Neuroscience (2003), 18: 155-163.

Abstract

Electroencephalographic oscillations in the sleep spindle frequency range (11-16 Hz) are a key element of human non-rapid eye movement sleep. In the present study, sleep spindle characteristics along the anterior-posterior axis were analyzed during and outside the circadian phase of melatonin secretion. Sleep electroencephalograms were recorded during naps distributed over the entire circadian cycle and analyzed with two different methodological approaches, the classical Fast Fourier Transform in the frequency-domain and a new method for instantaneous spectral analysis, the Fast Time Frequency Transform that yields high-resolution parameters in the combined time-frequency-domain. During the phase of melatonin secretion, spindle density was generally increased and intra-spindle frequency variation reduced. Furthermore, lower spindle frequencies were promoted: peak frequencies shifted towards the lower end of the spindle frequency range, and spindle amplitude was enhanced in the low-frequency range (up to ~14.25 Hz) and reduced in the high-frequency range (~ 14.5-16 Hz). The circadian variation showed a clear dependence on brain topography such that it was maximal in the parietal and minimal in the frontal derivation. Our data provide evidence that the circadian pacemaker actively promotes low frequency sleep spindles during the biological night with a parietal predominance.

Introduction

Timing and structure of human sleep are regulated by the endogenous circadian pacemaker located in the suprachiasmatic nuclei (SCN) of the hypothalamus (Dijk and Czeisler, 1995b; Dijk et al., 1997). The strength of this circadian control is very different for the two main electroencephalographic (EEG) oscillations during non-rapid eye movement (NREM) sleep - slow waves and sleep spindles. Slow-wave activity (SWA, EEG power density in the 0.75-4.5 Hz range) does not exhibit substantial circadian modulation, while activity in the spindle frequency range (SFA, EEG power density in the 11-16 Hz range) shows a clear circadian rhythm (Dijk and Czeisler, 1995b; Dijk et al., 1997). This circadian rhythm is frequency-specific, such that SFA in the 12.25-13 Hz range coincides with the peak, and SFA in the 14.25-15.5 Hz range with the nadir of the endogenous rhythm of melatonin secretion (Dijk et al., 1997). This inverse circadian phase relationship in low and high SFA has two possible explanations. The frequency *per se* of sleep spindles could be modulated (i.e. a general slowing of spindle frequencies during the night), or their amplitude and/or duration may exhibit frequency-specific modulation. Indeed, a recent study has demonstrated that frequency, amplitude as well as the duration of sleep spindles during NREM sleep all varied significantly across the circadian cycle (Wei et al., 1999).

The role of sleep spindles is to a large extent unknown. Spindle oscillations originate in the thalamus, which is the major gateway for information flow to the cortex (Steriade et al., 1993). Sleep spindles may reduce this sensory transmission and thereby protect the cortex from arousing stimuli (Steriade et al., 1993). There is also increasing evidence for an involvement of sleep spindles in synaptic plasticity and memory processes (Siapas and Wilson, 1998; Gais et al., 2002; for a review see Sejnowski and Destexhe, 2000).

Spectral analysis of the EEG, the method of choice in sleep research, averages spectral components over the considered time-window and does not discriminate synchronized spindle activity from de-synchronized activity in the same frequency band. Therefore, it does not segregate the contribution of changes in frequency from amplitude, nor can it yield time-incidence and time-duration in sleep spindle frequency activity.

It is not yet known whether a frequency-specific circadian modulation of spindle amplitude exists, nor is it known whether circadian modulation of SFA characteristics varies across brain locations. We hypothesized that EEG power density, as well as spindle density (number per time epoch), amplitude and duration show a frequency-specific circadian variation. Furthermore, we hypothesized that the circadian variation of these spindle characteristics depends on brain topography along the antero-posterior axis.

In order to test these hypotheses, we have applied two methodological approaches to quantify the contribution of spindle amplitude, frequency and density to the circadian as well as topographic modulation of SFA: classical spectral analysis in the frequency-domain (by means of the Fast Fourier Transform, FFT) and a new method for so-called joint time-frequency domain or instantaneous spectral analysis (by means of the Fast Time Frequency Transform, FTFT).

Methods

Study participants

Seventeen healthy volunteers (9 female, 8 male, age range 20-31 years, mean: 25 ± 0.9 s.e.m.) participated in the study. All subjects were non-smokers, free from medical, psychiatric and sleep disorders as assessed by screening questionnaires, a physical examination and a polysomnographically recorded screening night. Drug-free status was verified via urinary toxicologic analysis. Female subjects were studied during the follicular phase of their menstrual cycle, five of them using oral contraceptives. All participants gave signed informed consent, and the study protocol, screening questionnaires and consent form were approved by the local Ethical Committee.

Protocol

During the week preceding the study (baseline week), subjects were instructed to refrain from excessive physical activity, caffeine and alcohol consumption and to maintain a regular sleep-wake schedule (bed- and wake times within ± 30 minutes of self-selected target time). The latter was verified by a wrist activity monitor (Cambridge Neurotechnologies , UK) and sleep logs. The timing of their sleep-wake

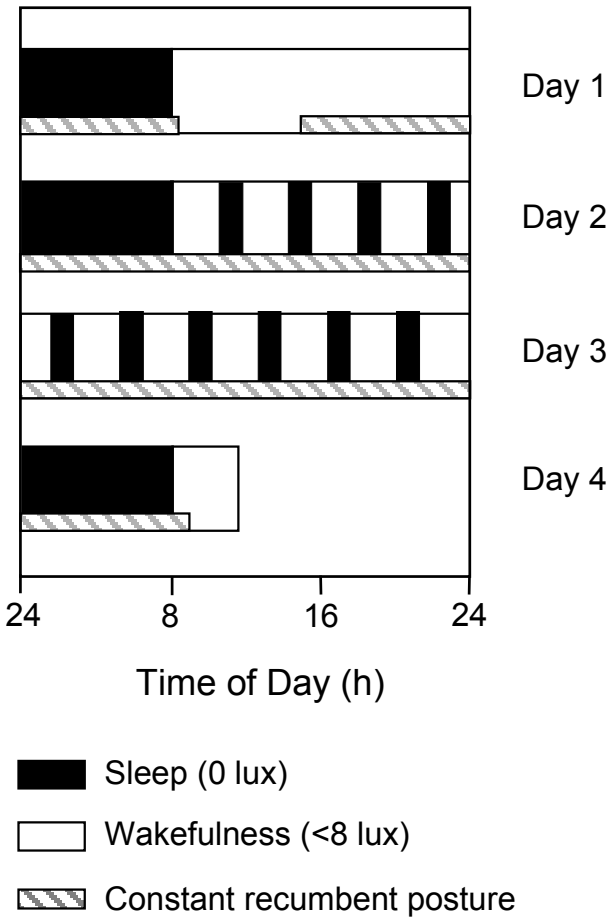

Figure 1. Overview of the protocol design. After two nights and a day in the laboratory to adapt, a 40-h short sleep-wake cycle paradigm (75/150-min) under constant posture was carried out, followed by an 8-h recovery night. Black bars indicate scheduled sleep episodes (light levels: 0 lux), white bars indicate scheduled episodes of wakefulness (light levels: <8 lux), hatched bars indicate controlled posture (semi-recumbent during wakefulness and supine during scheduled sleep).

schedule was calculated in such a way that the 8-h sleep episode was centered at the midpoint of each subject's habitual sleep episode as assessed by actigraphy and sleep logs during the baseline week. After the baseline week, subjects reported to the laboratory in the evening and spent an 8-h sleep episode, followed by 16 hours of scheduled wakefulness to adjust to the <8 lux experimental conditions (Day 1; Figure 1). After a second 8-h sleep episode (baseline night), subjects underwent a 40-h short sleep-wake cycle paradigm under constant posture conditions (near recumbent during wakefulness and supine during scheduled sleep episodes) during which they completed 10 alternating cycles of 75 min of scheduled sleep (light levels: 0 lux) and 150 min of scheduled wakefulness. The wake episodes were spent under constant routine conditions (constant dim light levels <8 lux, constant posture, food and liquid intake at regular intervals, no time cues; for details of the CR method see (Cajochen et al., 1999). The protocol ended with a 8-h recovery sleep episode. Results from the baseline and recovery night have been reported elsewhere (Knoblauch et al., 2002).

Sleep recordings and analysis

Sleep was recorded polysomnographically using the VITAPORT digital ambulatory sleep recorder (Vitaport-3 digital recorder, TEMEC Instruments B.V., Kerkrade, The Netherlands). Twelve EEGs, two electrooculograms, one submental electromyogram and one electrocardiogram signal were recorded. All signals were filtered at 30 Hz (4th order Bessel type anti-aliasing low-pass filter, total 24 dB/Oct.) and a time constant of 1.0 s. was used prior to on-line digitization (range 610 μV, 12 bit AD converter, 0.15 μV/bit; sampling rate at 128 Hz for the EEG). The raw signals were stored on-line on a Flash RAM Card (Viking, USA) and downloaded off-line to a PC hard drive. Sleep stages were visually scored on a 20-s basis (Vitaport Paperless Sleep Scoring Software) according to standard criteria (Rechtschaffen and Kales, 1968) and all further quantitative spindle analyses were limited to sleep stage two.

EEG spectral analysis

All EEGs were subjected to spectral analysis using a fast Fourier transform (FFT, 10% cosine 4-s window) resulting in a 0.25 Hz bin resolution. In parallel, EEG artifacts were detected by an automated artifact detection algorithm (CASA, 2000 PhyVision B.V., Gemert, The Netherlands). For final data reduction, the artifact-free 4-s epochs were averaged over 20-s epochs.

EEG power spectra were calculated during stage two in the frequency range from 0.5 to 32 Hz. Here, we report EEG data derived from the midline (Fz, Cz, Pz, Oz) referenced against linked mastoids (A1, A2) in the range of 0.5 - 25 Hz.

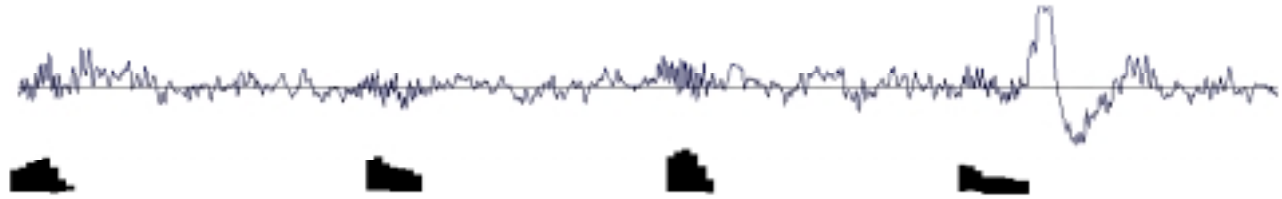

Figure 2. Raw EEG signal (above) and the output of the Fast Time Frequency Transform (FTFT, below) derived from Pz during a 20-s epoch of stage two sleep. The FTFT depicts synchronized spindle activity, subdivides each spindle into 0.125-s epochs (each represented by a black horizontal bar) and computes frequency and amplitude for each 0.125-s epoch separately. The height of a horizontal bar reflects the mean amplitude (μV), the position relative to the horizontal lines reflects the mean frequency within a 0.125-s epoch. The upper horizontal line is at 12 Hz, the lower at 16 Hz.

EEG instantaneous spectral analysis

The same digitized EEGs were subjected to instantaneous spectral analysis using the Fast Time Frequency Transform (FTFT) (Martens, 1992). For the EEG, the FTFT calculates instantaneous amplitude, frequency and bandwidth in 8 frequency bands from 0–4 Hz, 4–8 Hz, …. 28–32 Hz. Instantaneous bandwidth is computed from the instantaneous frequency as the rectified first derivative with respect to time. Therefore, the higher the frequency variability, the higher the bandwidth. Based on the 4 Hz range of the filters, the resolution in time of the above parameters is 0.125 s.

Over a moving template of 1-second duration, thresholds are applied to amplitude, frequency and bandwidth parameters to differentiate synchronized activity from ongoing noise as well as to remove artifacts (Martens, 1999). The thresholds were determined empirically on a learning-set of EEG recordings to yield the closest possible agreement with visual scores. Incorporating the instantaneous bandwidth helped to achieve a closer agreement in comparison with using only an amplitude threshold. Finally, the optimized settings from the learning set were applied to the data set of this study. Here, we focus on detected synchronized spindle activity. Spindles were detected from the outcome of the 8 - 12 Hz and 12 - 16 Hz frequency band, but the frequency and bandwidth threshold for spindle detection were limited to the range of 11 -16 Hz. These thresholds again were determined empirically and compared with the visual score. Furthermore, a duration limit (≥ 0.5 s and ≤ 2s) was applied for detected spindles. As a result, we obtained the amplitude and frequency of each individual spindle at a time-resolution of 0.125 seconds. The frequency resolution was 0.25 Hz. In other words, for each 0.25 Hz frequency bin between 11 and 16 Hz, the time incidence (corresponds to the number of 0.125-s epochs within the given frequency bin) and the amplitude in these 0.125-s epochs was calculated. Figure 2 depicts a raw EEG curve together with the output of the spindle FTFT. For each 20-s epoch of stage two sleep, the mean time incidence and amplitude of synchronized spindle frequency activity were computed per 0.25-Hz frequency bin between 11 to 16 Hz. Furthermore, spindle density (number of sleep spindles / 20-s epoch) was calculated. Finally, for each individual spindle, the following parameters were computed: duration, mean frequency, mean amplitude, standard deviation of frequency, frequency at onset and offset.

To compare spindle detection of this method with other spindle detection techniques, spindle density in Cz was calculated during the baseline night of this protocol. The value obtained (2.0176 n/20 s ± 0.23) was very similar to spindle density in central derivations (C3, C4 or Cz) reported in other studies using automated (Dijk et al., 1993; Wei et al., 1999) or visual (De Gennaro et al., 2000) spindle detection algorithms. Furthermore, detected synchronized spindle activity (Figure 2) was visually verified by one rater (V.K.). Since we have used a relatively low amplitude threshold (3-5 μVolt template) and a relatively broad frequency range (11-16 Hz), the algorithm detected a spindle density slightly higher than if visually scored. The thresholds for spindle detection were deliberately set such that the

algorithm yielded more spindles than when visually scored; this is particularly important in the presence of delta waves where the human eye often misses superimposed sleep spindles.

Salivary melatonin

Saliva was collected at ~30-min intervals during scheduled wakefulness. Saliva samples were assayed for melatonin using a direct double-antibody radio-immunoassay validated by gas chromatography-mass spectroscopy with an analytical least detectable dose of 0.15 pg/ml and a functional least detectable dose of 0.65 pg/ml (Bühlmann Laboratories, Schönenbuch, Switzerland; Weber et al., 1997).

Classification of naps

Naps comprising a total stage two duration of less than 5 minutes were excluded from the analysis. The first 75 minutes after lights off in the recovery night were considered as an additional nap. For time course analyses, nap 4 and 10 were excluded because too few subjects fulfilled these criteria of a stage two duration of at least 5 min (5 and 3 subjects, respectively), whereas a total of nine subjects fulfilled these criteria in the remaining naps.

The top left hand panel in Figure 3 illustrates the timing of the scheduled naps across the protocol in relation to endogenous melatonin secretion. Naps were classified into night naps and day naps depending on their occurrence during or outside melatonin secretory phase. This was defined as follows: the 24-hour mean melatonin concentration (between hours 5 and 29 of the 40-hour nap protocol) was calculated for each subject as an individual threshold level. The mean overall threshold was 9.1 $\pm$ 1.4 pg/ml (mean ± s.e.m.; n=17) and is indicated as a horizontal line in the top left hand panel in Figure 3. A nap was rated as a night nap if the melatonin concentration of the last saliva sample before the nap was above the threshold, otherwise, it was rated as a day nap. There were on average 5.76 $\pm$ 0.39 day naps and 2.94 $\pm$ 0.2 night naps per subject. The duration of stage two sleep did not significantly differ between day and night naps ($F[1,16]=0.2$; $p=0.7$).

Statistics

The statistical packages SAS® (SAS® Institute Inc., Cary, North Carolina, USA, Version 6.12) and Statistica® (StatSoft Inc. 2000. STATISTICA for Windows, Tulsa, Oklahoma, USA) were used. For day-night comparisons, averaged values across daytime naps were compared with averaged values across nighttime naps. For time course analyses, data derived from the spectral analysis were subjected to two-way analyses of variance for repeated measures (rANOVA) with the factors Derivation and Nap. For day-night comparisons, two-way rANOVAs with the factors Derivation and Condition or three-way rANOVAs with the factors Condition, Derivation and Frequency bin (for the time incidence and amplitude per 0.25 Hz bin) were used. All *p* values derived from rANOVAs were based on Huynh-Feldt's (H-F) corrected degrees of freedom, but the original degrees of freedom are reported. For *post-hoc* comparisons the Duncan's multiple range test and t-tests with correction for multiple comparisons (Curran-Everett, 2000) were used.

Results

Spectral analysis (FFT)

Time course

Figure 3 illustrates the timing of the scheduled naps across the protocol in relation to endogenous melatonin secretion (top left hand panel) and the dynamics of EEG power density across naps (relative stage two spectra of each nap, expressed as a percentage of the mean of all naps) in the range of 0.5-25 Hz in Pz. In the insets, the corresponding absolute spectra between 11 and 16 Hz are shown (spectra of the individual nap together with the mean spectra of all naps). Successive naps (without nap 4 and 10, see Methods) are plotted one below another in two columns, whereby naps occurring at similar circadian times are placed next to each other. Visual inspection reveals a prominent time-dependent modulation in the spindle frequency range. A one-way rANOVA with the factor Nap was performed and revealed that power density in most frequency bins between 9 and 21.75 Hz varied significantly across naps (see symbols above the top right hand panel of Figure 3). On the other hand, power density between 0.5 to 9 Hz, thus in the delta, theta and lower alpha

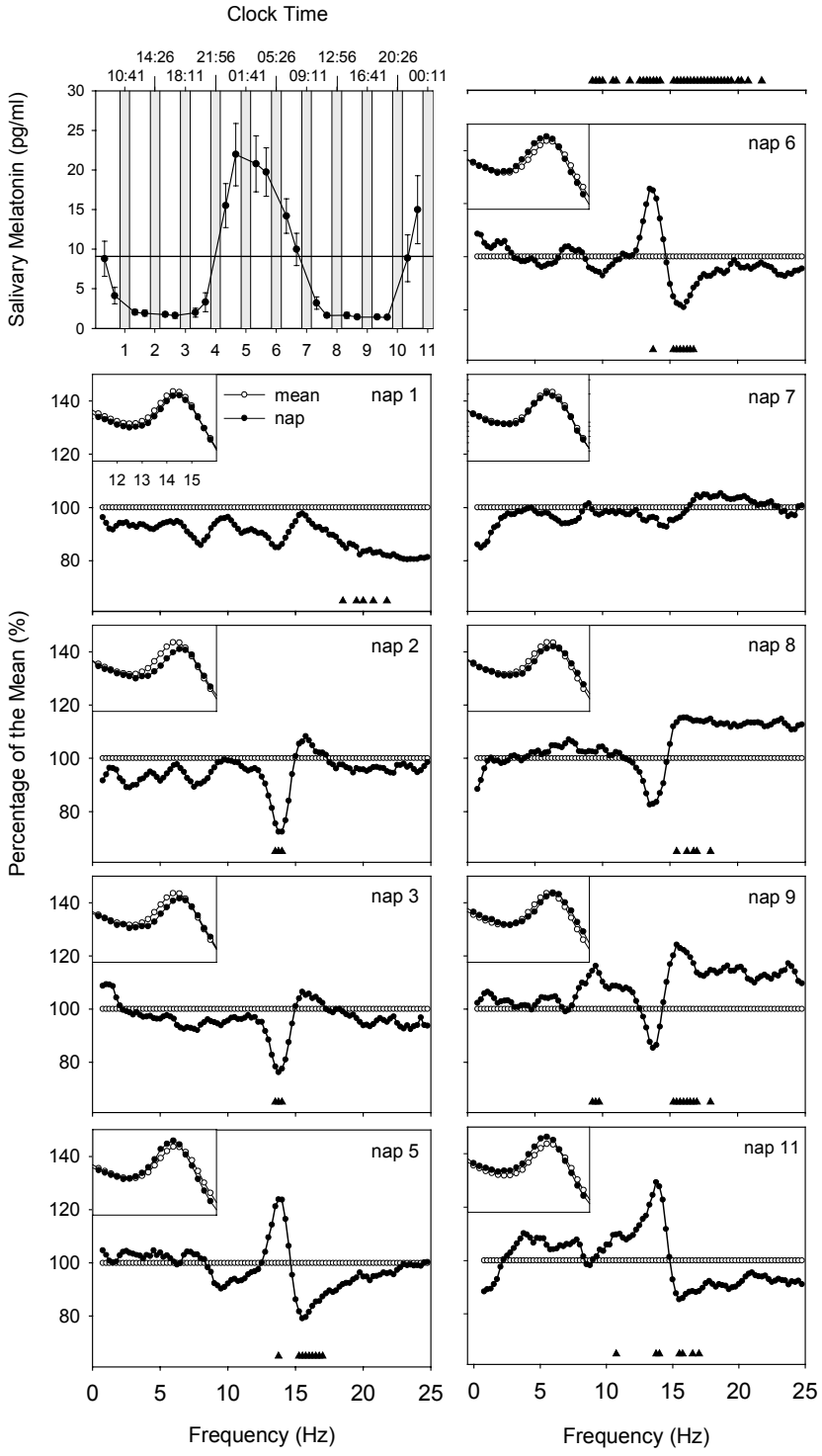

Figure 3. Melatonin secretion, timing of the naps, and the time course of EEG power density in the naps (nap 1-3, 5-9 and 11). *Top left hand panel*: Black symbols represent the mean curve of melatonin secretion (mean ± s.e.m.; n=17). The horizontal line marks the mean threshold (calculated as the 24-hour mean melatonin concentration). Vertical gray bars represent nap 1 to 11. Average times, when the midpoint of the naps occurred, are indicated on the top horizontal axis (mean times, n=17). *Other panels*: EEG power density in the range from 0.5 to 25 Hz in nap 1 to 11 (without nap 4 and 10) expressed as a percentage of the mean of all naps (except nap 4 and 10) for Pz (mean ± s.e.m.; n=9). Symbols above the top right hand panel (nap 6) indicate frequency bins for which the factor Nap was significant (p<0.05; one-way rANOVA on log transformed absolute values). Triangles near the abscissa indicate a significant difference between the value for the respective nap and the mean of all naps in these frequency bins (p<0.05; Duncan's multiple range test on log transformed absolute values). *Insets:* original absolute spectra between 11 and 16 Hz (spectra of the individual nap (●) ; mean spectra of all naps (○); mean, n=9).

range, as well as above 21.75 Hz did not exhibit a significant modulation over time. For frequency bins with a significant rANOVA, *post hoc* comparisons between the value for the individual nap and the mean of all naps were performed (Duncan's multiple range test on log transformed absolute values). In general, power density was reduced in the lower spindle frequency range and enhanced in the higher frequency range in naps 2, 3, 8 and 9, i. e. in naps occurring when melatonin was not secreted. In naps occurring when melatonin was secreted (i.e. naps 5, 6 and 11), power density was enhanced in the lower spindle frequency range and reduced in the higher frequency range (see Figure 3 for frequency bins with a significant difference from the mean). The absolute spectra in the insets help to illustrate that the opposite day- and nighttime peaks in the low- and high frequency range come about by a shift in the absolute power spectra towards lower frequencies during the night.

Day-night difference

In a next step, the spectra of naps occurring during melatonin secretion (night naps) were compared to the spectra of naps occurring outside melatonin secretion (day naps; see Methods section). The left hand panel in Figure 4 shows mean absolute EEG power density between 8 - 18 Hz during night and day naps. Visual inspection reveals more power in the spindle peak during the night than during the day, and the curves are shifted towards lower frequencies relative to the day spectra. For better visualization of this day-night difference, the spectra of the night naps are expressed as a percentage of the day nap spectra in the range from 0.5-25 Hz (Figure 4, right hand panels). The interaction between Derivation (Fz, Cz, Pz, Oz) and Condition (day, night) was significant in the following frequency ranges: 5.5-14.75 Hz, 16.5-17.75 Hz and 18.5-19 Hz (p at least < 0.05; rANOVA).

There was a pronounced and significant nocturnal increase of EEG power density in Cz, Pz and Oz in the following frequency ranges: between 11.25-14.25 Hz in Cz, between 12.25-14.25 Hz in Pz, and between 13-14.25 Hz in Oz (p<0.05, day *vs.* night; paired t-test corrected for multiple comparisons). In Fz, the increase (significant between 11-12.75 and 13.25 -13.75 Hz) was less distinct and also spanned to adjacent lower frequency ranges , i.e. the alpha and theta range (see Figure 4). The increase was maximal in the 13.5-13.75 Hz bin and was significantly higher in Pz than in Cz, Oz and Fz, as well as significantly lower in Fz than in the

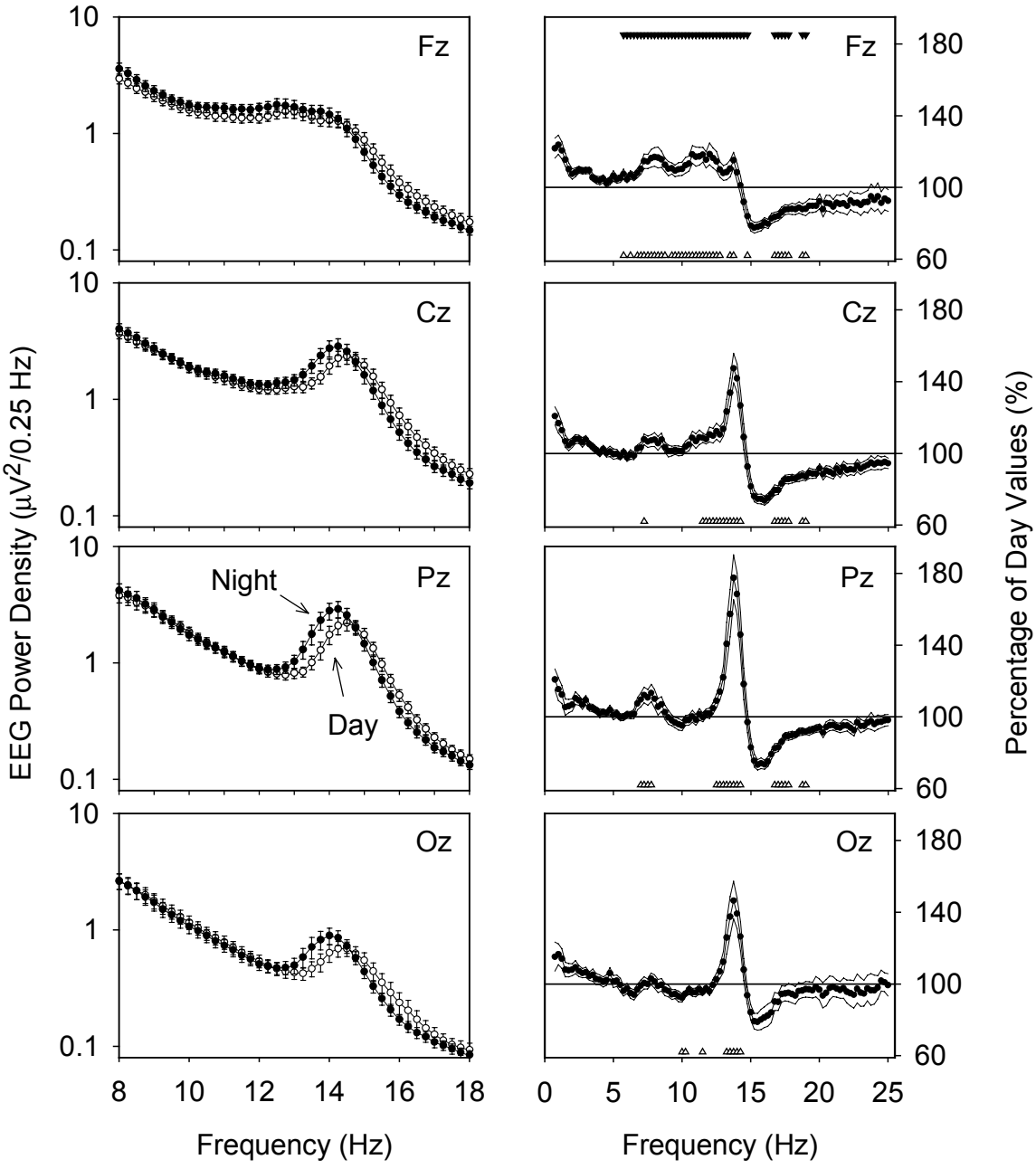

Figure 4. EEG power density per 0.25-Hz bin for the midline derivations (Fz, Cz, Pz, Oz) during stage two (mean ± s.e.m.; n=17). *Left hand panels*: absolute EEG power density between 8 - 18 Hz for the night naps (●) and the day naps (○). *Right hand panels*: relative night spectra (expressed as percentage of day values) between 0.5-25 Hz. Symbols at the top of the top panel indicate frequency bins for which the interaction between Derivation and Condition was significant ($p<0.05$; rANOVA on log transformed absolute values). Triangles near the abscissa indicate a significant difference between day and night in these frequency bins ($p<0.05$; paired *t*-test corrected for multiple comparisons).

other three derivations (Derivation, F[3,48]=42.3, p<0.01, rANOVA; Duncan's multiple range test, p<0.0001). The nocturnal reduction of EEG power density in the higher spindle frequency range (>14.75 Hz) did not depend on derivation (no significant interaction between Derivation and Condition in the 14.75-16.5 Hz range).

Instantaneous frequency analysis (FTFT)

Spindle density and spindle parameters

Spindle density (number of spindles / 20-s epoch), duration, frequency, amplitude, standard deviation of frequency (SD Frequency), frequency at onset, frequency at offset, and the difference between frequency at onset and frequency at offset (Δ Frequency) were calculated (Figure 5). A two-way rANOVA with the factors Condition and Derivation was performed for each of these variables (Table 1). The interaction between these two factors yielded significance for spindle density, frequency and duration. *Post-hoc* comparison revealed that spindle density was significantly higher during the night than during the day in Pz (p<0.001, Duncan's multiple range test), whereas in Fz, no significant day-night difference was observed. Spindle frequency was significantly lower during the night than during the day in both Fz and Pz (Figure 5, p<0.05, Duncan's multiple range test). Spindle duration was shorter during the night in Fz, and higher during the night than during the day in Pz (Figure 5, p<0.05, Duncan's multiple range test). The main factor Derivation was significant for all variables, the main factor Condition for all variables except for spindle duration. Spindle amplitude was significantly higher during the night than during the day and significantly higher in Pz than in Fz. SD Frequency, a measure for intra-spindle frequency variability, was significantly higher during the day than during the night and significantly higher in Fz than in Pz (Figure 5). In both derivations and during both conditions (day, night), onset frequency was significantly higher than offset frequency (Variable x Derivation, F[1,16]=12.9, p<0.01, rANOVA; Variable x Condition, F[1,6]=6.3, p<0.05, rANOVA; Duncan's multiple range test, p<0.001, data not shown), i.e. frequency within a spindle generally slowed down. The extent of this frequency reduction (expressed as Δ Frequency, the difference between onset and offset frequency) was however significantly higher in Fz than in Pz and significantly higher during the day than during the night (Figure 5). The smaller intra-spindle downward frequency modulation during the night than during the day implies an

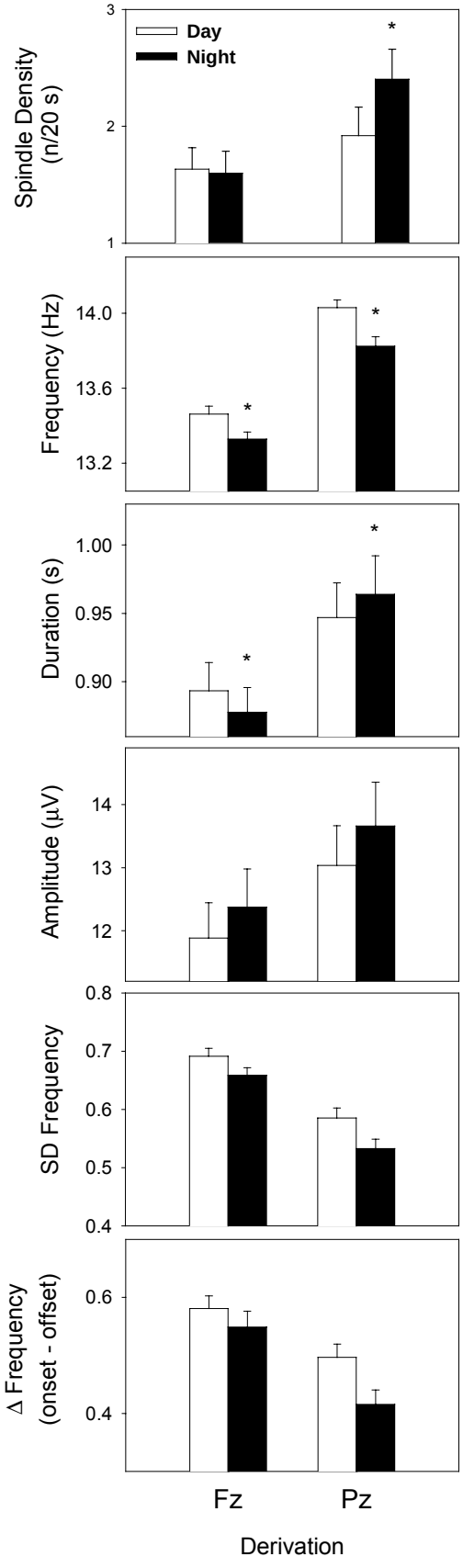

Figure 5. Mean density (number of sleep spindles per 20-s epoch of stage two), frequency, duration, amplitude, standard deviation of frequency (SD Frequency, intra-spindle frequency variability), and difference between onset and offset frequency (Δ Frequency) of sleep spindles during night naps (black bars) and day naps (white bars) for the frontal (Fz) and parietal (Pz) derivation (mean ± s.e.m.; n=17). Asterisks indicate a significant difference between day and night (p<0.05; Duncan's multiple range test).

unequal reduction of onset and offset frequency during the night. To test this, onset and offset frequency at night were expressed as a percentage of onset and offset frequency during the day (relative onset and offset frequency). In Fz, there was no significant difference between the relative onset and offset frequency, whereas in Pz, the onset frequency during the night was significantly more reduced than the offset frequency ($F[1, 16]=11.6$, $p<0.005$, rANOVA).

Table 1. Two-way rANOVA with the factors Condition and Derivation for spindle density (n/20 s), duration, frequency, amplitude, standard deviation of frequency (SD Frequency), onset frequency, offset frequency, and difference between onset and offset frequency (Δ Frequency) of sleep spindles.

	Condition		Derivation		Condition x Derivation	
Variable	$F_{1,16}$	(*p*)	$F_{1,16}$	(*p*)	$F_{1,16}$	(*p*)
Density	20.56	(<0.001)*	16.93	(<0.001) *	111.83	(<0.0001) *
Duration	0.01	(0.939)	25.12	(<0.001) *	12.29	(<0.01) *
Mean Frequency	81.76	(<0.001)*	132.92	(<0.001) *	5.38	(<0.034) *
Mean Amplitude	19.05	(<0.001) *	11.25	(<0.01) *	1.13	(0.303)
SD Frequency	30.39	(<0.001)*	72.12	(<0.001) *	3.16	(0.1)
Onset frequency	57.52	(<0.001)*	100.39	(<0.001) *	3.72	(0.072)
Offset frequency	54.18	(<0.001)*	135.27	(<0.001) *	0.36	(0.556)
Δ Frequency	6.26	(<0.05) *	12.92	(<0.01) *	2.26	(0.15)

p-values <0.05 were considered significant.

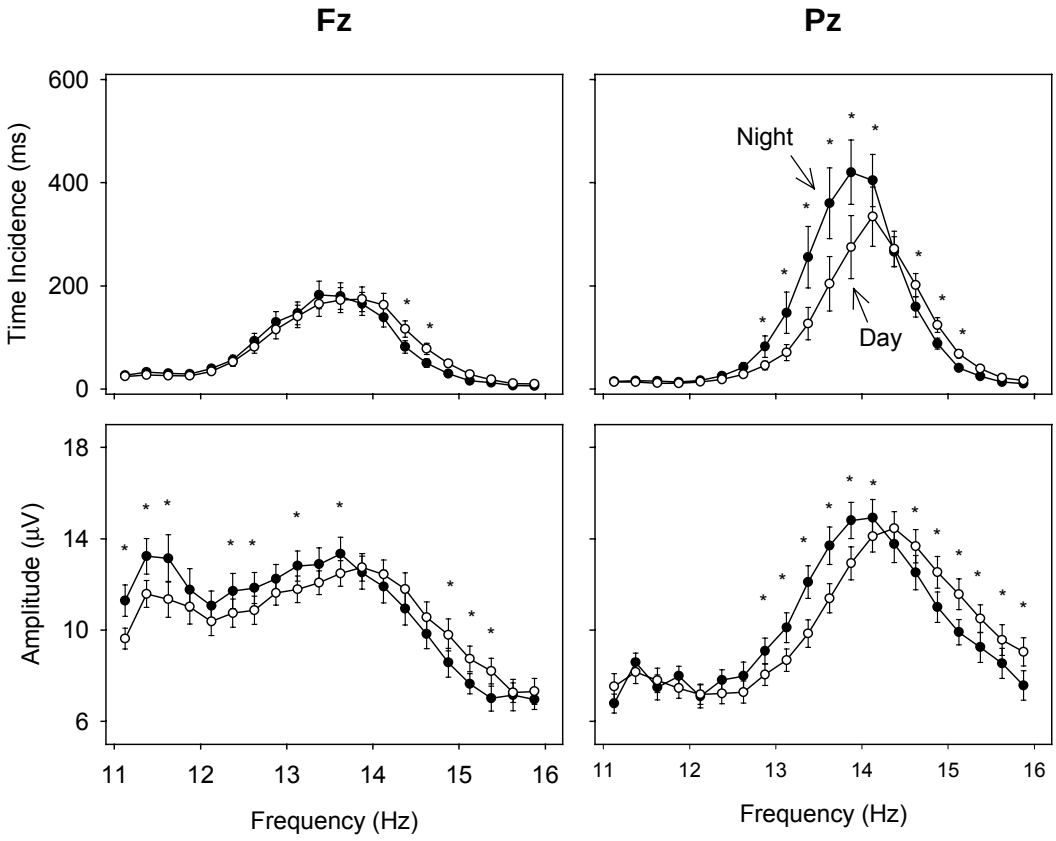

Figure 6. Time incidence (per 20-s epoch stage two, above) and amplitude (below) per 0.25 Hz bin from 11 – 16 Hz during night naps (●) and day naps (○); mean ± s.e.m.; n=17. Asterisks indicate significant day-night differences (p<0.05; Duncan's multiple range test).

Time incidence per 0.25 Hz frequency bin

The upper panels of Figure 6 depict the time incidence per 0.25 Hz bin in the 11-16 Hz range. A three-way rANOVA Derivation x Condition x Frequency bin revealed a significant interaction between these factors ($F[19, 304]=11.7$; $p<0.0001$). There was a pronounced day-night difference in time incidence in Pz. The curve was shifted towards lower frequencies during the night, resulting in a significant increase in the low and middle spindle frequency range and significant reduction in the upper frequency range ($p<0.05$, Duncan's multiple range test; see Figure 6 for exact frequency ranges). In Fz, there was not such a shift between the curves, and they did not differ significantly up to 14 Hz. A significant reduction, however, was found in the upper frequency range (between 14-14.75 Hz) during the night ($p<0.05$, Duncan's multiple range test).

Amplitude per 0.25 Hz frequency bin

The amplitude per 0.25 Hz bin in the 11-16 Hz range is illustrated in the bottom panels of Figure 6. The interaction between Derivation, Condition and Frequency bin was significant ($F[19,304]=5.1$; $p<0.0001$, rANOVA). In both derivations, the night curve was shifted towards lower frequencies relative to the day curve. The amplitude at night was increased in the low frequency range and reduced in the higher frequency range (for statistics see Figure 6). The peak amplitude, in the range between 13.5 and 14.5 Hz, was less distinct in Fz, where a second peak in the very low frequency range (between 11 and 12 Hz) occurred.

Discussion

The new combined high-time and high-frequency resolution spindle analysis showed that density, frequency and amplitude of sleep spindles vary with the circadian phase of endogenous melatonin secretion and revealed a shift of sleep spindles to lower frequencies concomitant with a higher amplitude in this frequency range during the night. Circadian modulation of sleep spindle characteristics was not uniform along the antero-posterior axis, but showed a parietal maximum.

Furthermore, we show that during the biological night, sleep spindles were more stable in terms of reduced intra-spindle frequency variability. We found a general downward trend in frequency within sleep spindles: spindle frequency at the end of the spindle was always lower than at the beginning, but this intra-spindle downward frequency modulation was reduced during the night.

The shift towards lower frequencies during the subjective night (when melatonin is secreted) comprised both time incidence and amplitude. This confirms and extends previous data which demonstrated a tight temporal association between the endogenous melatonin rhythm and the circadian profile of sleep spindle activity in the low frequency range (12.25-13 Hz; Dijk et al., 1997). It is known that administration of both a classical hypnotic such as a benzodiazepine or (to a lesser extent) daytime melatonin both enhance spindle frequency activity particularly in the low frequency range (12.25-14 Hz; Johnson et al., 1976; Borbély et al., 1985; Trachsel et al., 1990; Brunner et al., 1991; Dijk et al., 1995). This has led to the hypothesis that the frequency-specific circadian modulation of SFA is a mechanism to reduce sensory sensitivity and thus favor sleep at the phase of normal sleep time (Dijk and Czeisler, 1995a; Dijk et al., 1997). As yet, there are no experimental data demonstrating a decrease in sensory throughput associated with reduced spindle frequency which might support this hypothesis

We have evidence that the variation of sleep pressure across naps was only moderate. SWA, a measure for the level of homeostatic sleep pressure during sleep, did not show a substantial or significant variation over time (Figure 3). In addition, frontal low EEG activity during wakefulness, a marker of the homeostatic buildup of sleep pressure during wake, exhibited only small changes in the time course of this protocol (Cajochen et al., 2001). These data demonstrates that we were successful in keeping sleep pressure generally low during the 40 hours and supports the assumption that, although the influence of homeostatic sleep pressure can not be excluded completely, the effects reported here mainly reflect the influence of circadian phase. Thus, our data further quantify the sleep spindle promoting action of the circadian pacemaker. It is still unknown whether the spindle generating thalamo-cortical network is directly influenced by the SCN via neuronal pathways, or rather indirect, via other output variables of the circadian system. Direct projections from the SCN to the thalamus (the paraventricular thalamic nucleus) have recently been reported in rats (Novak et al., 2000). The SCN has indirect projections to the

ventrolateral preoptic nucleus (VLPO) via the dorsomedial hypothalamus (Chou et al., 2002). The VLPO is crucial for NREM sleep promotion (Sherin et al., 1996) and has reciprocal inhibitory connections with wake-promoting neurons in the basal forebrain and brainstem nuclei (reviewed by Saper et al., 2001 and Pace-Schott and Hobson, 2002). Among these, the pedunculopontine and laterodorsal tegmental nucei (PPT-LDT) send direct cholinergic projections to the reticular thalamic nucleus (Berendse and Groenewegen, 1990; Berendse and Groenewegen, 1991), which is thought to play a key role in the regulation of thalamocortical transmission and to be the initial site in the sleep spindle generating network (Steriade et al., 1993). This could be one possible neuronal pathway for the circadian signal from the SCN to the sleep spindle generating system in the thalamus. Alternatively, the circadian modulation of sleep spindles may be mediated indirectly, via other output variables of the circadian pacemaker, such as melatonin. There is, however, a debate on whether the changes in the EEG power spectra that occur across the circadian cycle are based on the concomitant changes in body (and brain) temperature, reflecting a non-specific effect of temperature, rather than a sleep- regulatory mechanism under circadian control (Deboer and Tobler, 1995; Deboer and Tobler, 1998). EEG frequencies slow down with a temperature coefficient (Q_{10}) of approximately 2.5 (Deboer and Tobler, 1995), thus low brain temperature at night could be responsible for the shift of SFA in the power spectra towards lower frequencies. To test this hypothesis, Dijk (1999) compared the EEG power spectra from two time points during a forced desynchrony protocol, one in the morning and one in the evening, where body temperature was nearly identical. Low spindle frequency activity was markedly enhanced in the evening, after the evening increase of plasma melatonin levels, as compared to the morning, where plasma melatonin levels were low. Consequently, the circadian variation of EEG spindle frequency activity is unlikely to be caused by changes in body temperature.

Our data demonstrate for the first time that the circadian modulation of sleep spindle characteristics varies with brain location. The most marked difference in the extent of circadian modulation is between frontal and parietal SFA. Frequency differences in frontal and parietal spindles during nocturnal sleep have been demonstrated before (Gibbs and Gibbs, 1950; Zeitlhofer et al., 1997; Werth et al., 1997; Zygierewicz et al., 1999; Anderer et al., 2001; Finelli et al., 2001). Frontal spindles were found to have a lower frequency (around 12 Hz) than parietal spindles

(around 14 Hz) and these findings were interpreted as indication for the existence of two separate types of sleep spindles. It is however still not known whether frontally and parietally scalp-recorded sleep spindles originate from two functionally distinct thalamic sources. Spindle oscillations presumably originate in the nucleus reticularis of the thalamus, and are transferred via inhibitory GABAergic projections to thalamocortical neurons in other thalamic nuclei (Steriade et al., 1993). As a result, sleep spindles can be recorded from distant sites in the dorsal thalamus (Contreras et al., 1997). Since the spindle generating network includes various reciprocal connections between the thalamus and the cortex, the cortical distribution of sleep spindles may probably reflect activities of corresponding nuclei within the dorsal thalamus. Thus, differences, e.g. in frequency or in circadian regulation, between frontally and parietally scalp-recorded sleep spindles, do not necessarily imply two distinct spindle generators, but may represent a topography-dependent modulation of one single type of spindle oscillations, whose origin can be traced back to the thalamic reticular nucleus from where is dispersed to distant sites within the thalamus. It remains to be elucidated whether this topography-dependent modulation is related to distinct functional roles - such as memory consolidation and sleep protection - of sleep spindles in these brain regions.

We have recently reported frequency-specific topographical changes within the spindle frequency range after manipulation of sleep pressure (Knoblauch et al., 2002). Thus, both circadian and homeostatic processes affect specific frequencies within the spindle frequency range and this in turn depends on brain region. These results emphasize the highly local and frequency-specific nature of sleep spindle regulation.

Conclusions

The present data show that the close temporal association between the melatonin secretory phase (“biological night”) and sleep spindle characteristics clearly depends on brain topography. They provide further evidence for a brain-region-specific modulation of sleep spindles, which is regulated by the endogenous circadian pacemaker, and strengthens the potential role of sleep spindles as a mechanism by which the SCN facilitates sleep consolidation.

Acknowledgments

We thank Claudia Renz, Giovanni Balestrieri and Marie-France Dattler for their help in data acquisition, Drs. Alexander Rösler and Tobias Müller for medical screenings, and the subjects for participating. This research was supported by Swiss National Foundation Grants START # 3130-054991.98 and #3100-055385.98 to CC.

References

Anderer P, Klösch G, Gruber G, Trenker E, Pascual-Marqui RD, Zeitlhofer J, et al. Low-resolution brain electromagnetic tomography revealed simultaneously active frontal and parietal sleep spindle sources in the human cortex. Neuroscience 2001; 103: 581-592.

Berendse HW, Groenewegen HJ. Organization of the thalamostriatal projections in the rat, with special emphasis on the ventral striatum. J Comp Neurol 1990; 299: 187-228.

Berendse HW, Groenewegen HJ. Restricted cortical termination fields of the midline and intralaminar thalamic nuclei in the rat. Neuroscience 1991; 42: 73-102.

Borbély AA, Mattmann P, Loepfe M, Strauch I, Lehmann D. Effect of benzodiazepine hypnotics on all-night sleep EEG spectra. Human Neurobiol 1985; 4: 189-194.

Brunner DP, Dijk DJ, Münch M, Borbèly AA. Effect of zolpidem on sleep and sleep EEG spectra in healthy young men. Psychopharmacology 1991; 104: 1-5.

Cajochen C, Khalsa SBS, Wyatt JK, Czeisler CA, Dijk DJ. EEG and ocular correlates of circadian melatonin phase and human performance decrements during sleep loss. Am J Physiol Regulatory Integrative Comp Physiol 1999; 277: R640-R649.

Cajochen C, Knoblauch V, Kräuchi K, Renz C, Wirz-Justice A. Dynamics of frontal EEG activity, sleepiness and body temperature under high and low sleep pressure. NeuroReport 2001; 12: 2277-2281.

Chou TC, Bjorkum AA, Gaus SE, Lu J, Scammell TE, Saper CB. Afferents to the ventrolateral preoptic nucleus. J Neurosci 2002; 22: 977-990.

Contreras D, Destexhe A, Sejnowski TJ, Steriade M. Spatiotemporal patterns of spindle oscillations in cortex and thalamus. J Neurosci 1997; 17: 1179-1196.

Curran-Everett D. Multiple comparisons: philosophies and illustrations. Am J Physiol Regul Integr Comp Physiol 2000; 279: R1-R8.

De Gennaro L, Ferrara M, Bertini M. Effect of slow-wave sleep deprivation on topographical distribution of spindles. Behav Brain Res 2000; 116: 55-59.

Deboer T, Tobler I. Temperature dependence of EEG frequencies during natural hypothermia. Brain Res 1995; 670: 153-156.

Deboer T, Tobler I. The effects of moderate body temperature changes on the sleep EEG. Sleep 1998; 21 (Suppl): 40.

Dijk DJ, Czeisler CA. Circadian control of the EEG in non REM sleep. Sleep Res 1995a; 24: 518.

Dijk DJ, Czeisler CA. Contribution of the circadian pacemaker and the sleep homeostat to sleep propensity, sleep structure, electroencephalographic slow waves, and sleep spindle activity in humans. J Neurosci 1995b; 15: 3526-3538.

Dijk DJ, Hayes B, Czeisler CA. Dynamics of electroencephalographic sleep spindles and slow wave activity in men: effect of sleep deprivation. Brain Res 1993; 626: 190-199.

Dijk DJ, Roth C, Landolt HP, Werth E, Aeppli M, Achermann P, et al. Melatonin effect on daytime sleep in men: suppression of EEG low frequency activity and enhancement of spindle frequency activity. Neurosci Lett 1995; 201: 13-16.

Dijk DJ, Shanahan TL, Duffy JF, Ronda JM, Czeisler CA. Variation of electroencephalographic activity during non-rapid eye movement and rapid

eye movement sleep with phase of circadian melatonin rhythm in humans. J Physiol 1997; 505: 851-858.

Finelli LA, Borbély AA, Achermann P. Functional topography of the human nonREM sleep electroencephalogram. Eur J Neurosci 2001; 13: 2282-2290.

Gais S, Mölle M, Helms K, Born J. Learning-dependent increases in sleep spindle density. J Neurosci 2002; 22: 6830-6834.

Gibbs FA, Gibbs EL. Atlas of Electroencephalography. Cambridge: Addison-Wesley Press, 1950.

Johnson LC, Hanson K, Bickford RG. Effect of flurazepam on sleep spindles and K-complexes. Electroencephalogr Clin Neurophysiol 1976; 40: 67-77.

Knoblauch V, Kräuchi K, Renz C, Wirz-Justice A, Cajochen C. Homeostatic control of slow-wave and spindle frequency activity during human sleep: effect of differential sleep pressure and brain topography. Cereb Cortex 2002; 12: 1092-1100.

Martens WLJ. The fast time frequency transform (F.T.F.T.): a novel on-line approach to the instantaneous spectrum. 14th International Conference of the IEEE Engineering in Medicine and Biology Society, Paris 1992.

Martens WLJ. Segmentation of 'rhythmic' and 'noisy' components of sleep EEG, Heart Rate and Respiratory signals based on instantaneous amplitude, frequency, bandwidth and phase. 1st joint BMES / EMBS IEEE Conference, Atlanta 1999.

Novak CM, Harris JA, Smale L, Nunez AA. Suprachiasmatic nucleus projections to the paraventricular thalamic nucleus in nocturnal rats (Rattus norvegicus) and diurnal nile grass rats (Arviacanthis niloticus). Brain Res 2000; 874: 147-157.

Pace-Schott EF, Hobson JA. The neurobiology of sleep: genetics, cellular physiology and subcortical networks. Nature Rev - Neurosci 2002; 3: 591-605.

Rechtschaffen A, Kales A. A manual of standardized terminology, techniques and scoring system for sleep stages of human subjects. Bethesda, MD: US Dept of Health, Education and Welfare, Public Health Service, 1968.

Saper CB, Chou TC, Scammell TE. The sleep switch: hypothalamic control of sleep and wakefulness. Trends Neurosci 2001; 24: 726-731.

Sejnowski TJ, Destexhe A. Why do we sleep? Brain Res 2000; 886: 208-223.

Sherin JE, Shiromani P, Mc Carley RW, Saper CB. Activation of ventrolateral preoptic neurons during sleep. Science 1996; 271: 216-219.

Siapas AG, Wilson MA. Coordinated interactions between hippocampal ripples and cortical spindles during slow-wave sleep. Neuron 1998; 21: 1123-1128.

Steriade M, McCormick DA, Sejnowski TJ. Thalamocortical oscillations in the sleeping and aroused brain. Science 1993; 262: 679-685.

Trachsel L, Dijk DJ, Brunner DP, Klene C, Borbély AA. Effect of zopiclone and midazolam on sleep and EEG spectra in a phase-advanced sleep schedule. Neuropsychopharmacology 1990; 3: 11-18.

Weber JM, Schwander JC, Unger I, Meier D. A direct ultrasensitive RIA for the determination of melatonin in human saliva: comparison with serum levels. J Sleep Res 1997; 26: 757.

Wei HG, Riel E, Czeisler CA, Dijk DJ. Attenuated amplitude of circadian and sleep-dependent modulation of electroencephalographic sleep spindle characteristics in elderly human subjects. Neurosci Lett 1999; 260: 29-32.

Werth E, Achermann P, Dijk DJ, Borbély AA. Spindle frequency activity in the sleep EEG: individual differences and topographic distribution. Electroencephalogr Clin Neurophysiol 1997; 103: 535-542.

Zeitlhofer J, Gruber G, Anderer P, Asenbaum S, Schimicek P, Saletu B. Topographic distribution of sleep spindles in young healthy subjects. J Sleep Res 1997; 6: 149-155.

Zygierewicz J, Blinowska KJ, Durka PJ, Szelenberger W, Niemcewicz S, Androsiuk W. High resolution study of sleep spindles. Clin Neurophysiol 1999; 110: 2136-2147.

Chapter 5

Concluding Remarks

In this thesis, spindle activity and spindle characteristics were studied in a recovery night after sleep deprivation, and in naps occurring either during the biological night (the period of melatonin secretion) or -day. Whereas the night following sleep deprivation represents a condition of high homeostatic sleep pressure, the biological night can be considered as a state of high circadian pressure for sleep. Both conditions substantially affect EEG spindle activity (Figure 1). By separately analyzing distinct spindle parameters, our data provide more detailed insight into the regulation of sleep spindles than can be obtained by spectral analysis alone.

Spindle density was reduced after SD, and enhanced during the biological night compared to the day. The reduction of spindle density after SD confirms the concept of an inverse homeostatic relationship of sleep spindles and slow waves (Borbély et al., 1981; Dijk et al., 1993; Finelli et al., 2001a). This relationship is probably based on the dependence on different levels of membrane potentials, which implies an incompatibility of these two types of oscillations at the level of single neurons (Nuñez et al., 1992; Steriade et al., 1991). Our data indicate that under high homeostatic sleep pressure, the level of hyperpolarization in neuronal populations in the thalamus and cortex is enhanced. A higher number of neurons is hyperpolarized enough to fire in the slow wave-, instead of the spindle mode. Thus, the ratio between sleep spindles and slow waves is a sensitive marker for homeostatic sleep pressure (see also Figure 3 of Chapter 2).

Spindle amplitude was enhanced, and frequency variability within a spindle reduced after SD and during the biological night. The amplitude of a wave with a given frequency in the EEG reflects the size of the neuronal population that oscillates in synchrony with this frequency (Amzica and Steriade, 1998). The increase in spindle amplitude, together with the reduction in intra-spindle frequency variability, indicates a higher level of synchronization under high sleep pressure both after sleep deprivation and at the circadian phase for sleep.

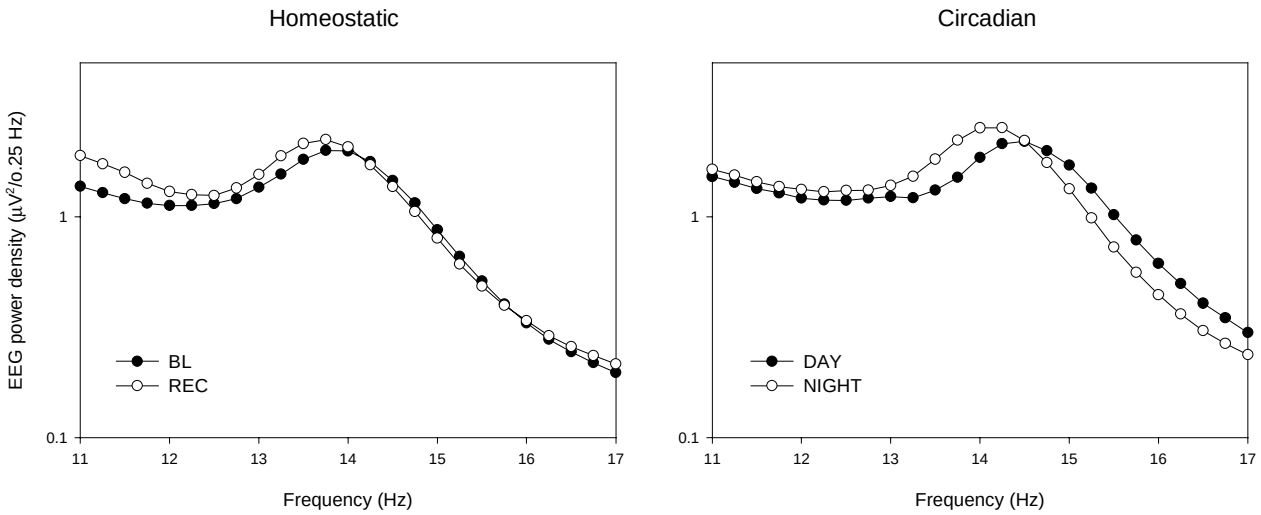

Figure 1. Homeostatic and circadian modulation of spindle frequency activity. EEG power density between 11 and 17 Hz during NREM sleep (stage 2-4) for the midline central derivation (Cz) during the baseline (white symbols) and recovery (black symbols) night after SD (left), and for daytime naps (white symbols) and nighttime naps (black symbols, right). Mean values, n=16.

The circadian modulation of sleep spindles is such that spindle density is high during the biological night. One proposed function of sleep spindles is to gate sensory transmission through the thalamus to the cortex during sleep (Steriade et al., 1993). The circadian modulation of sleep spindles with high spindle density during the biological night may represent a mechanism by which the circadian pacemaker reduces sensitivity to sensory input, and thus enhances sleep consolidation during the normal sleep phase (Dijk et al., 1997). Slow wave activity, in contrast, is only slightly affected by circadian phase (Dijk and Czeisler, 1995; Dijk et al., 1997). While the sleep homeostat modulates SWA to adjust sleep depth to different levels of homeostatic need, the circadian system seems to modulate sleep spindles to consolidate sleep at the appropriate circadian time.

A common feature of homeostatic and circadian spindle modulation is the reduction of spindle frequency both after sleep deprivation and during the biological

night. The significance of this phenomenon is unclear. It remains to be elucidated whether low-frequency spindles are particularly effective in gating sensory throughput to the cortex, and thereby in increasing sleep consolidation. The finding that both benzodiazepines and daytime administration of melatonin enhance low-frequency spindle activity in particular (Borbély et al., 1985; Brunner et al., 1991; Dijk et al., 1995; Trachsel et al., 1990) would corroborate such a hypothesis.

Regional differences

The present thesis demonstrates that both homeostatic and circadian processes affect spindle activity in different brain regions with different strength. After SD, the reduction in spindle density was most pronounced in the frontal derivation. The increase of SWA after SD also exhibits a frontal predominance (Cajochen et al., 1999; Finelli et al., 2001b). This local accentuation of the inverse relationship between slow waves and sleep spindles further supports the hypothesis that frontal brain areas are particularly sensitive to sleep loss (see Introduction) and that also locally, high sleep pressure is accompanied with a higher degree of hyperpolarization.

The circadian modulation of sleep spindles was most pronounced in the parietal, and less pronounced in the frontal derivation. Frontal and parietal sleep spindles also differ in their frequency (Anderer et al., 2001; Gibbs and Gibbs, 1950; Jobert et al., 1992; Scheuler et al., 1990; Werth et al., 1997; Zeitlhofer et al., 1997; see Introduction). It remains unclear whether these differences between frontally and parietally recorded spindles indicate different functional significance. The finding that the increase in spindle density after a declarative learning task was most pronounced in the frontal derivation (Gais et al., 2002) suggests that local features of sleep spindle distribution could be related to activity in specific brain regions during the preceding waking period, and/or that sleep spindles in frontal brain areas might be particularly involved memory consolidation.

Taken together, the studies presented in this thesis demonstrate that both homeostatic and circadian processes affect spindle activity in different brain regions with different strength. This indicates that specific brain areas are sensitive to sleep loss or to alterations in the phase relationships between the sleep-wake cycle and

the circadian pacemaker, and emphasizes the local nature of sleep regulation. An interesting goal for further studies would be to reveal if such state-dependent regional aspects represent use-dependent processes and if they can be related to the proposed functional relevance of sleep spindles, that is memory consolidation and sleep protection.

References

Amzica F, Steriade M. Electrophysiological correlates of sleep delta waves. Electroencephalogr Clin Neurophysiol 1998; 107: 69-83.

Anderer P, Klösch G, Gruber G, Trenker E, Pascual-Marqui RD, Zeitlhofer J, et al. Low-resolution brain electromagnetic tomography revealed simultaneously active frontal and parietal sleep spindle sources in the human cortex. Neuroscience 2001; 103: 581-592.

Borbély AA, Baumann F, Brandeis D, Strauch I, Lehmann D. Sleep deprivation: effect on sleep stages and EEG power density in man. Electroencephalogr Clin Neurophysiol 1981; 51: 483-495.

Borbély AA, Mattmann P, Loepfe M, Strauch I, Lehmann D. Effect of benzodiazepine hypnotics on all-night sleep EEG spectra. Human Neurobiol 1985; 4: 189-194.

Brunner DP, Dijk DJ, Münch M, Borbèly AA. Effect of zolpidem on sleep and sleep EEG spectra in healthy young men. Psychopharmacology 1991; 104: 1-5.

Cajochen C, Foy R, Dijk DJ. Frontal predominance of a relative increase in sleep delta and theta EEG activity after sleep loss in humans. Sleep Res Online 1999; 2: 65-69.

Dijk DJ, Hayes B, Czeisler CA. Dynamics of electroencephalographic sleep spindles and slow wave activity in men: effect of sleep deprivation. Brain Res 1993; 626: 190-199.

Dijk DJ, Czeisler CA. Contribution of the circadian pacemaker and the sleep homeostat to sleep propensity, sleep structure, electroencephalographic slow waves, and sleep spindle activity in humans. J Neurosci 1995; 15: 3526-3538.

Dijk DJ, Roth C, Landolt HP, Werth E, Aeppli M, Achermann P, et al. Melatonin effect on daytime sleep in men: suppression of EEG low frequency activity and enhancement of spindle frequency activity. Neurosci Lett 1995; 201: 13-16.

Dijk DJ, Shanahan TL, Duffy JF, Ronda JM, Czeisler CA. Variation of electroencephalographic activity during non-rapid eye movement and rapid eye movement sleep with phase of circadian melatonin rhythm in humans. J Physiol 1997; 505: 851-858.

Finelli LA, Achermann P, Borbély AA. Individual ' fingerprints ' in human sleep EEG topography. Neuropsychopharmacology 2001a; 25: S57-S62.

Finelli LA, Borbély AA, Achermann P. Functional topography of the human nonREM sleep electroencephalogram. Eur J Neurosci 2001b; 13: 2282-2290.

Gais S, Mölle M, Helms K, Born J. Learning-dependent increases in sleep spindle density. J Neurosci 2002; 22: 6830-6834.

Gibbs FA, Gibbs EL. Atlas of Electroencephalography. Cambridge: Addison-Wesley Press, 1950.

Jobert M, Poiseau E, Jähnig P, Schulz H, Kubicki S. Topographical analysis of sleep spindle activity. Neuropsychobiology 1992; 26: 210-217.

Nuñez A, Curro Dossi R, Contreras D, Steriade M. Intracellular evidence for incompatibility between spindle and delta oscillations in thalamocortical neurons of cat. Neuroscience 1992; 48: 75-85.

Scheuler W, Kubicki S, Scholz G, Marquardt J. Two different activities in the sleep spindle frequency band-discrimination based on the topographical distribution of spectral power and coherence. In: Horne J, editor. Sleep '90. Bochum: Pontenagel Press, 1990: 13-16.

Steriade M, Dossi RC, Nuñez A. Network modulation of a slow intrinsic oscillation of cat thalamocortical neurons implicated in sleep delta waves: cortically induced synchronization and brainstem cholinergic suppression. J Neurosci 1991; 11: 3200-3217.

Steriade M, McCormick DA, Sejnowski TJ. Thalamocortical oscillations in the sleeping and aroused brain. Science 1993; 262: 679-685.

Trachsel L, Dijk DJ, Brunner DP, Klene C, Borbély AA. Effect of zopiclone and midazolam on sleep and EEG spectra in a phase-advanced sleep schedule. Neuropsychopharmacology 1990; 3: 11-18.

Werth E, Achermann P, Dijk DJ, Borbély AA. Spindle frequency activity in the sleep EEG: individual differences and topographic distribution. Electroencephalogr Clin Neurophysiol 1997; 103: 535-542.

Zeitlhofer J, Gruber G, Anderer P, Asenbaum S, Schimicek P, Saletu B. Topographic distribution of sleep spindles in young healthy subjects. J Sleep Res 1997; 6: 149-155.

Curriculum vitae

NAME	Vera Knoblauch
BORN	March 8, 1974, in Binningen (BL), Switzerland

EDUCATION

1980-1986	Primary school, Chur (GR)
1986-1993	Gymnasium, Bündner Kantonsschule Chur (GR)
1993	Matura, Type D
1994 - 1999	Undergraduate studies in Biology, University of Basel, Switzerland
1999-2000	Diploma thesis in Neurobiology at the Centre for Chronobiology, Psychiatric University Clinic, Basel, under the direction of Prof. Dr. Anna Wirz-Justice (representative of the Faculty of Science: Prof. Dr. Heinrich Reichert)
2000	Diploma in Biology, University of Basel
2000-2004	Ph.D. student at the Centre for Chronobiology, Psychiatric University Clinic, Basel, under the supervision of Prof. Dr. Anna Wirz-Justice and Dr. Christian Cajochen (representative of the Faculty of Science: Prof. Dr. Heinrich Reichert)

List of Publications

Papers

Wirz-Justice, A., Werth, E., Savaskan, E., **Knoblauch, V.**, Fontana Gasio, P., Müller-Spahn, F. (2000) Haloperidol disrupts, clozapine reinstates the circadian rest-activity cycle in a patient with early-onset Alzheimer's disease. Alzheimer Disease and Associated Disorders, 14: 212-215.

Cajochen, C., **Knoblauch, V**., Kräuchi, K., Renz, C., Wirz-Justice, A. (2001) Dynamics of frontal EEG activity, sleepiness and body temperature under high and low sleep pressure. Neuroreport 12: 2277-2281.

Werth, E., Savaskan, E., **Knoblauch, V**., Fontana Gasio, P., Van Someren, E.J.W., Hock, C., Wirz-Justice, A. (2002) Decline in long-term circadian rest-activity cycle organisation in a demented patient. Journal of Geriatric Psychiatry and Neurology, 15: 55-59.

Knoblauch, V., Kräuchi, K., Renz, C., Wirz-Justice, A., Cajochen, C. (2002) Homeostatic control of slow wave- and spindle frequency activity during human sleep: effect of differential sleep pressure and brain topography. Cerebral Cortex, 12: 1092-100.

Knoblauch, V., Martens, M., Wirz-Justice, A., Kräuchi, K., Cajochen, C. (2003) Regional differences in the circadian modulation of human sleep spindle characteristics. European Journal of Neuroscience, 18: 155-63.

Knoblauch, V., Martens, W.J.L., Wirz-Justice, A. & Cajochen, C. (2003) Human sleep spindle characteristics after sleep deprivation. Clinical Neurophysiology, 114: 2258-2267.

Graw, P., Kräuchi, K., **Knoblauch, V**., Renz, C., Wirz-Justice, A. & Cajochen, C. (2004) Circadian and wake-dependent modulation of fastest and slowest reaction times of the Psychomotor Vigilance Task (PVT). Physiology & Behavior, 80: 695-701.

Cajochen, C., **Knoblauch, V**., Wirz-Justice, A., Kräuchi, K., Graw, P. & Wallach, D. (2004) Circadian modulation of sequence learning under high and low sleep pressure conditions. Behavioural Brain Research, in press.

Abstracts

Knoblauch, V., Werth, E., Savaskan, E., Fontana Gasio, P., Wirz-Justice, A. Haloperidol disrupts, clozapine reinstates the circadian rest-activity cycle in a patient with early-onset Alzheimer's disease. Joint Annual Meeting, Swiss Society for Neuroscience and Swiss Society for Sleep Research, Sleep Medicine and Chronobiology, Basel, January 2000, Abstract 1.8.

Werth, E., **Knoblauch, V.**, Savaskan, E., Fontana Gasio, P., Wirz-Justice, A., Hock, B., Müller-Spahn, F. Long-term changes in circadian rest-activity cycle organisation in two patients with Alzheimer's disease. APSS Meeting, Las Vegas NE, June 2000; Sleep 23 (Supplement #2): A217.

Fontana Gasio, P., Werth, E., **Knoblauch, V.**, Amrhein, I., Cajochen, C., Kräuchi, K., Savaskan, E., Wirz-Justice, A. Dawn-dusk simulation in Alzheimer's Disease patients with disturbed circadian rest-activity cycles. 13th Annual Meeting, Society for Light Treatment and Biological Rhythms, Stockholm, June 2001.

Knoblauch, V., Kräuchi, K., Renz, C., Müller, T., Wirz-Justice, A., Cajochen, C. Effect of a 75/150 minute sleep -wake schedule on the accumulation of slow-wave

sleep and wakefulness after lights off. APSS Meeting, Chicago IL, June 2001; Sleep 24 (Supplement #2):A194.

Cajochen, C., Kräuchi, K., **Knoblauch, V.**, Renz, C., Rösler, A., Balestrieri, G., Dattler, M.-F., Graw, P., Wirz-Justice, A. Dynamics of frontal low EEG-activity and subjective sleepiness under high and low sleep pressure. APSS Meeting, Chicago IL, June 2001; Sleep 24 (Supplement #2): A77.

Knoblauch, V., Kräuchi, K., Wirz-Justice, A., Müller, T., Renz, C., Cajochen, C. Homeostatic control of slow wave- and spindle frequency activity during human sleep: effect of differential sleep pressure. Joint Annual Meeting, Swiss Society for Neuroscience and Swiss Society for Sleep Research, Sleep Medicine and Chronobiology, Geneva, January 2002.

Cajochen, C., **Knoblauch, V.**, Kräuchi, K., Renz, C., Wirz-Justice, A., Wallach, D. Visuomotor sequence learning depends on sleep, the level of sleep pressure and circadian phase. Joint Annual Meeting, Swiss Society for Neuroscience and Swiss Society for Sleep Research, Sleep Medicine and Chronobiology, Geneva, January 2002.

Knoblauch, V., Kräuchi, K., Renz, C., Müller, T., Wirz-Justice, A., Cajochen, C. Regional differences in spindle frequency activity during and outside melatonin secretory phase. 16th Congress of the European Sleep Research Society (ESRS), Reykjavik, Iceland, June 2002; J Sleep Res 11 (Supplement #1): A 246.

Cajochen, C., **Knoblauch, V.**, Kräuchi, K., Renz, C., Wirz-Justice, A., Wallach, D. Sequence learning depends on sleep, the level of sleep pressure and circadian phase. 16th Congress of the European Sleep Research Society (ESRS), Reykjavik, Iceland, June 2002; J Sleep Res 11 (Supplement #1): A 59.

Kräuchi, K., **Knoblauch, V.**, Renz, C., Müller, T., Wirz-Justice, A., Cajochen, C. Thermoregulatory changes at lights off depend on circadian phase but not on sleep pressure or sleep. 16th Congress of the European Sleep Research Society (ESRS), Reykjavik, Iceland, June 2002; J Sleep Res 11 (Supplement #1): A 256.

Knoblauch, V., Martens, M., Kräuchi, K., Wirz-Justice, A., Cajochen, C. Regional differences in the circadian modulation of human sleep spindle characteristics. Joint Meeting Swiss Society for Neuroscience (SSN) and Swiss Society of Psychiatry and Psychotherapy (SSPP), Fribourg, January 2003.

Cajochen, C., Schröder, C., **Knoblauch, V.**, Kräuchi, K., Marti, A., Wirz-Justice, A. Homeostatic regulation of human rapid eye movement density: a comparison with EEG slow-wave activity. Joint Meeting Swiss Society for Neuroscience (SSN) and Swiss Society of Psychiatry and Psychotherapy (SSPP), Fribourg, January 2003.

Kräuchi, K., Cajochen, C., **Knoblauch, V**., Renz, C., Wirz-Justice, A. Disappearance of sleep inertia is correlated with distal vasoconstriction. Joint Meeting Swiss Society for Neuroscience (SSN) and Swiss Society of Psychiatry and Psychotherapy (SSPP), Fribourg, January 2003.

Graw, P., Kräuchi, K., **Knoblauch, V.**, Renz, C., Wirz-Justice, A., Cajochen, C. Circadian and wake-dependent modulation of fastest and slowest reaction times in a psychomotor vigilance task (PVT). Joint Meeting Swiss Society for Neuroscience (SSN) and Swiss Society of Psychiatry and Psychotherapy (SSPP), Fribourg, January 2003

Knoblauch, V., Martens, W., Kräuchi, K., Wirz-Justice, A., Cajochen, C. A new method for sleep spindle analysis: circadian and topographic aspects, 54. Mosbacher Kolloquium der Gesellschaft für Biochemie und Molecularbiologie (GBM), Mosbach, Germany, March 2003.

Knoblauch, V., Martens, W.J.L., Wirz-Justice, A., Kräuchi, K., Graw, P., Cajochen, C. Regional differences in the circadian modulation of human sleep spindle characteristics. APSS Meeting, Chicago IL, June 2003.

Cajochen, C., **Knoblauch, V.**, Kräuchi, K., Schröder, C., Wirz-Justice, A. Circadian modulation and EEG correlates of dream recall during a 75:150-min sleep-wake cycle paradigm. APSS Meeting, Chicago IL, June 2003.

Schröder, C., **Knoblauch, V.**, Renz, C., Kräuchi, K., Wirz-Justice, A., Christian, C. Circadian modulation of mood under differential sleep pressure conditions. APSS Meeting, Chicago IL, June 2003.

Cajochen, C., Schröder, C., **Knoblauch, V**., Kräuchi, K., Marti, A., Wirz-Justice, A. Homeostatic regulation of human rapid eye movement density: a comparison with EEG slow-wave activity. APSS Meeting, Chicago IL, June 2003.

Kräuchi, K., Cajochen, C., **Knoblauch, V.**, Renz, C., Wirz-Justice, A. Disappearance of sleep inertia is associated with distal vasoconstriction. APSS Meeting, Chicago IL, June 2003.

Graw, P., Kräuchi, K., **Knoblauch, V.**, Renz, C., Wirz-Justice, A., Cajochen, C. Circadian and wake-dependent modulation of fastest and slowest reaction times in the psychomotor vigilance task (PVT). APSS Meeting, Chicago IL, June 2003.

Knoblauch, V., Martens, M., Wirz-Justice, A., Kräuchi, K., Cajochen, C. Human sleep spindle characteristics after sleep deprivation. Joint Annual Meeting Swiss Society of Sleep Research, Sleep Medicine and Chronobiology & Swiss Neurologic Society, Zürich, November, 2003.

Münch, M., **Knoblauch, V**., Blatter, K., Kräuchi, K., Schröder, C., Renz, C., Wirz-Justice, A., Cajochen, C. Age related attenuation of the circadian arousal signal in the late evening. Joint Annual Meeting Swiss Society of Sleep Research, Sleep Medicine and Chronobiology & Swiss Neurologic Society, Zürich, November, 2003.

Acknowledgements

The present thesis was carried out in the Chronobiology Laboratory of the Psychiatric University Clinic Basel under the supervision of Prof. Dr. Anna Wirz-Justice and Dr. Christian Cajochen and represented in the Faculty of Science by Prof. Dr. Heinrich Reichert from the Department of Integrative Biology.

First I would like to express my sincere thanks to Prof. Dr. Anna Wirz-Justice for her dedication and constant strong support throughout my entire thesis project.
I am especially grateful to Dr. Christian Cajochen, whose great support was invaluable for my thesis. He introduced me to the sleep EEG, guided me through all steps of my work and instructed me in crucial skills, ranging from data collection techniques, various methods for sleep analysis and statistics to writing a paper at the end.
The new method for spindle analysis based on the FTFT was developped by Dr. Wim Martens, TEMEK, the Netherlands. I would like to thank Dr. Martens for his patient and persistent help whenever a change had to be implemented until the program attained its final version.
I thank Kurt Kräuchi for his scientific inputs, comments on manuscripts and for his expert advice on statistical problems.
Many thanks go to Claudia Renz for her crucial administrational and technikal work without which the study could not have been carried out, and Giovanni Balestrieri and Marie-France Dattler for their help with data collection.
I greatly appreciate that PD Dr. Hanspeter Landolt rendered his expert opinion as a co-referee.
My thanks go to all present and previous members of the Chronobiology group for the good collaboration and working atmosphere, and the Psychiatric University Clinic (Director: Fritz Jenni, Medical Director: Prof. Dr. Franz Müller-Spahn) for providing the infrastructure and facilities.

The studies carried out and analysed in this thesis were supported by the Swiss National Foundation (Grants START # 3130-054991.98 and #3100-055385.98 to CC).